TRANSPORTATION RESEARCH
CIRCULAR
Number E-C234 August 2018

Relationships of Laboratory Mixture Aging to Asphalt Mixture Performance

The National Academies of
SCIENCES • ENGINEERING • MEDICINE
TRB
TRANSPORTATION RESEARCH BOARD

TRANSPORTATION RESEARCH CIRCULAR E-C234

Relationships of Laboratory Mixture Aging to Asphalt Mixture Performance

Prepared by
Jo Sias Daniel, Fan Yin, Amy Epps Martin, Edith Arámbula-Mercado,
David Newcomb, Jean Pascal Planche, Adam Pauli, Mike Farrar,
Shin-Chi Huang, Gerald Reinke, and Andrew Hanz

With Contributions from
Frank Fee, Steve Engber, Doug Herlitzka, and Mary Ryan

For the
Standing Committee on Critical Issues and Emerging Technologies in Asphalt

August 2018

Transportation Research Board
500 Fifth Street, NW
Washington, D.C.
www.TRB.org

TRANSPORTATION RESEARCH CIRCULAR E-C234
ISSN 0097-8515

The **Transportation Research Board** is one of seven programs of the National Academies of Sciences, Engineering, and Medicine. The mission of the Transportation Research Board is to provide leadership in transportation innovation and progress through research and information exchange, conducted within a setting that is objective, interdisciplinary, and multimodal.

The **Transportation Research Board** is distributing this E-Circular to make the information contained herein available for use by individual practitioners in state and local transportation agencies, researchers in academic institutions, and other members of the transportation research community. The information in this circular was taken directly from the submission of the authors. This document is not a report of the National Academies of Sciences, Engineering, and Medicine.

Transportation Research Board
500 Fifth Street, NW
Washington, D.C.
www.TRB.org

Foreword

This E-Circular captures the results from TRB Session 462: Relationship of Laboratory Mix Aging to Asphalt Mixture Performance, which was held during the 95th Annual Meeting of the Transportation Research Board in 2016.

Numerous new or improved asphalt mixture testing and procedures are currently being evaluated to try to show relationships to mix field performance. One critical aspect of this work, that needs to be developed, is a lab aging method that will accurately reflect the mix aging in the field. This circular provides four papers on different aspects of addressing this issue. These range from handling the mix at the production facility, to varying the lab mix conditioning, toward capturing real world situations. It also includes the comparison of mix and binder properties from two field projects which shows the relationship to changes with aging of the pavement.

ACKNOWLEDGMENTS

The committee recognizes former members who contributed while serving during the workshop and development of this E-Circular: Harold "Skip" Paul, Timothy Aschenbrener, Dean Maurer, Rebecca McDaniel, Louay Mohammad, Marshall Shackelford, and Fred Hejl (TRB).

Contents

How Mixture, Fabrication, and Plant Production Parameters Affect Mixture Properties

JO SIAS DANIEL
University of New Hampshire

INTRODUCTION

As agencies move towards performance-based and performance-related methodologies for the design and acceptance of asphalt mixtures, it is important to understand the impact that the specimen fabrication method has on the properties that are measured and how potential changes influence the predicted performance. The mixture design stage is typically done several months ahead of production in the laboratory. Mixtures are produced in small quantities and production parameters such as gradation, asphalt content, and temperatures can be very tightly controlled. Standard procedures and protocols are used to simulate the aging that the materials would experience in the plant and in the field. In contrast, during production mixtures are produced in large quantities at the plant and it is not possible to have the same control over mixture parameters. There are many different factors that affect production that cannot be controlled, e.g., ambient temperature and moisture. Also, many different things can change during the course of a project, or could be different from those during the mix design stage, that affect the production and the properties of the asphalt mixture that is ultimately placed on the roadway. This paper specifically compares results of laboratory versus plant-produced materials, the impact of reheating plant mixture, and silo storage time in a plant.

MATERIALS AND METHODS

Materials

The results from three recently completed projects in the Northeast United States are presented here to illustrate potential impacts from various mixture, fabrication, and plant production parameters on measured properties. The projects include

- New Hampshire Department of Transportation (DOT) 15680R: Correlation Between Laboratory and Plant Produced High RAP/RAS (recycled asphalt pavement/recycled asphalt shingles) Mixtures;
- TPF 5(230): Evaluation of Plant-Produced High-Percentage RAP Mixtures in the Northeast; and
- New Hampshire DOT 15680B: Performance of High RAP Pavement Sections in New Hampshire.

Additional information and results from these projects can be found in published reports and papers (*1–10*).

These projects included testing of over 40 mixtures that incorporate four virgin binder grades [performance grade (PG) 52-34, PG 58-28, PG 64-22, and PG 64-28], six different binder

suppliers, RAP contents up to 40%, and mixtures with combined RAP and RAS, and three different nominal maximum aggregate size (NMAS) gradations (9.5, 12.5, and 19 mm). The mixtures were produced in batch and drum plants in three different states. Four of the most common methods used to prepare asphalt mixture test specimens were evaluated.

- Laboratory mixed, laboratory compacted (LMLC). The specimens are mixed and compacted in the laboratory using conditioning methods that are intended to simulate what happens in the plant and are generally used for mix design purposes. Materials in this study were short-term oven aged in the laboratory for 2 h at compaction temperature.
- Plant mixed, laboratory compacted (PMLC). The specimens are fabricated in the laboratory by reheating and compacting the loose mix produced at the plant.
- Plant mixed, plant compacted (PMPC). The specimens are compacted in a laboratory at the plant immediately following production without reheating of the loose mixture.
- Field cores. The specimens are taken from the asphalt pavement and are the best representation of in-place mixture conditions but may be limited to use in tests that use certain geometries due to available lift thickness.

Binder Testing

Performance grading of the virgin and extracted and recovered binders was done in accordance with AASHTO M320. The recovered asphalt binder was treated as an RTFO-aged (rolling thin film oven) asphalt binder. Master stiffness curves for binders were generated using the dynamic shear rheometer (DSR) results at varying temperatures and loading frequencies. Analysis included evaluation of the high and low PG temperatures, the ΔT_{cr} parameter, and several rheological indices.

Anderson et al. (*11*) identified the difference between the bending beam rheometer (BBR) stiffness (*S*) and *m*-slope critical low temperature as a means of indexing the non-load associated cracking potential of asphalt binders. Asphalt binders that exhibit a greater difference between the *S* and *m*-slope low temperature have been recognized as being prone to non-load associated cracking. The parameter, defined as ΔT_{cr}, is shown in Equation 1.

$$\Delta T_{cr(\text{Stiffness})} - T_{cr\ (m-\text{slope})} \quad (1)$$

where

ΔT_{cr} = Difference in critical low-temperature PG grade;
$T_{cr(\text{Stiffness})}$ = Critical low-temperature grade predicted using the BBR stiffness (*S*); and
$T_{cr\ (m\text{-slope})}$ = Critical low-temperature grade predicted using the BBR *m*-slope.

In Equation 1, as the ΔT_{cr} decreases, the asphalt binder is considered to be more prone to non-load associated cracking. Initially, Anderson et al. (*11*) set a limit of $\Delta T_{cr} \leq -2.5$°C for when there is an identifiable risk of cracking and preventative action should be considered. Rowe recommended that at a $\Delta T_{cr} \leq -5$°C immediate remediation should be considered (*12*).

Glover et al. (*13*) proposed the rheological parameter, G'/(η'/G'), as an indicator of ductility based on a derivation of a mechanical analog to represent the ductility test consisting of springs and dashpots. Rowe re-defined the Glover parameter in terms of |G*| and δ based on

analysis of a Black Space diagram and suggested use of the parameter $|G^*|\cdot(\cos\delta)^2/\sin\delta$, termed the Glover-Rowe (G-R) parameter, in place of the original Glover parameter (*12*). Rowe proposed measuring the G-R parameter based on construction of a master curve from frequency sweep testing at 5°C, 15°C, and 25°C in the DSR and interpolating to find the value of G-R at 15°C and 0.005 rad/s to assess binder brittleness (*14*). A higher G-R value indicates increased brittleness. It has been proposed that a G-R parameter value of 180 kPa corresponds to damage onset whereas a G-R value exceeding 450 kPa corresponds to significant cracking based on a study relating binder ductility to field block cracking and surface raveling by Anderson et al. (*11*). The test results generated during the master stiffness curve analysis was utilized to determine the G-R parameter.

The Christensen-Anderson-Marasteanu Model (CAM) master curve parameters (ω_o, R, and T_d) have specific physical significance. As crossover frequency, ω_o, increases, the hardness of the binder decreases, which indicates lower degrees of aging. The rheological index, *R*-value, is defined as the difference between the log of the glassy modulus and the log of the dynamic modulus at the crossover frequency. As *R*-value increases, the master curve becomes flatter indicating a more gradual transition from elastic behavior to steady-state flow. Normally, *R*-value is higher for oxidized–aged asphalt (*15*). Mogawer et al. demonstrated that by plotting the crossover frequency versus *R*-value, the relative change in aging, or rejuvenating, can be tracked (*16*).

Mixture Testing

The Asphalt Mixture Performance Tester (AMPT) was used to perform dynamic modulus testing in unconfined uniaxial compression following AASHTO T342. The dimensions of the tested specimens were 100 mm in diameter by 150 mm tall. The average dynamic modulus isotherms were shifted to construct the master curve at a reference temperature of 21.1°C.

Fatigue testing was performed using the AMPT in uniaxial tension at various strain amplitudes. Analysis on the fatigue results was performed using the simplified viscoelastic continuum damage (SVECD) model developed by Underwood et al. (*17*). SVECD is a mode-of-loading independent, mechanistic model that allows the prediction of fatigue cracking performance under various stress–strain amplitudes at different temperatures from only a few tests. The SVECD model is composed of two material properties, the damage characteristic curve and the energy-based failure criterion. The damage characteristic curve defines how fatigue damage evolves in a mixture and is developed by plotting two calculated parameters at each loading cycle, the secant pseudo-stiffness (C) and the damage parameter (S). The exponential form shown in Equation 2 was used to fit the damage characteristic curves.

$$C = e^{aS^b} \tag{2}$$

Where a, b = damage model coefficients.

The SVECD fatigue failure criterion, called the G^R method, involves the released pseudo-strain energy. This concept focuses on the dissipated energy that is related to energy release from damage evolution only and is fully compatible and predictable using the SVECD model. The G^R characterizes the overall rate of damage accumulation during fatigue testing. A characteristic relationship, which is found to exist in both RAP and non-RAP mixtures, can be derived between the rate of change of the averaged released pseudo-strain energy during fatigue testing (G^R) and

the final fatigue life or number of cycles to failure (N_f). The equation to calculate G^R is as follows:

$$G^R = \frac{\frac{1}{2}\int_0^{N_f} \left(\varepsilon^R{}_{0,ta}\right)_i^2 (1-F_i)}{N_f{}^2} \quad (3)$$

where

$(\varepsilon^R{}_{0,t\alpha})_I$ = pseudo-strain amplitude at cycle i; and
F_i = pseudo-stiffness at cycle i.

In order to assess the low temperature cracking susceptibility, mixtures were tested in the Thermal Stress Restrained Specimen Test device in accordance with AASHTO TP10-93. Three replicate gyratory specimens 150 mm in diameter by 185 mm tall were fabricated and specimens were then cored and cut to 54 mm in diameter by 160 mm tall. The air voids of the final cut specimens were 6.5±1.0%.

Pavement Fatigue Life Evaluation

The layered viscoelastic critical distresses (LVECD) program was used to predict the long-term fatigue performance of pavements under traffic loading. Eslaminia et al. (*18*) developed the layered viscoelastic structural program with the material level continuum damage model to calculate the required stresses and strains for the fatigue behavior prediction using three-dimensional viscoelastic calculations under moving loads. The LVECD simulations were performed for both thin and thick pavement structures using the required parameters including design time, structural layout, traffic, and climate. The thin pavement structure had an asphalt layer of 100 mm and aggregate base of 200 mm; the thick pavement had an asphalt layer of 300 mm with the same base. The aggregate base and the subgrade were modeled using the linear elastic properties with the modulus values of 350 MPa and 100 MPa, respectively.

Two climates were evaluated: Boston, Massachusetts and Raleigh, North Carolina using pavement temperatures obtained from the Enhanced Integrated Climate Model. Also, a single tire with the standard loading of 80 kN at the center of pavement was utilized. The average annual daily truck traffic was assumed to be 2,000.

For fatigue cracking resistance evaluation, LVECD calculates the damage growth and the damage factor based on Miner's law (Equation 5). If the damage factor is equal to zero, the element does not experience any damage, while a damage factor of one indicates total failure of the element.

$$\sum_{i=1}^{T} D_i = \frac{N_i}{N_{fi}} \quad (4)$$

where

D = damage;

T = total number of periods;
N_i = traffic for period i; and
N_{fi} = allowable failure repetitions under the conditions that prevail in period i.

RESULTS AND DISCUSSION

The continuous high- and low-PG temperatures for the different virgin and extracted and recovered binders from one drum plant are shown in Figure 1 and Figure 2, respectively. The high PG temperatures from the lab produced mixtures were greater than those from the plant produced mixtures and there are slight differences with the different binder sources. The two PG 52-34 virgin binders did not quite meet the required performance grade on the low side. The difference between binders from the PMPC and LMLC mixtures was less pronounced on the low temperature side and all of the low grades were controlled by the m-value. In most cases for binders extracted from the 12.5 and 19 mm mixtures, PMPC mixtures showed colder temperatures.

The mixtures containing RAS had warmer temperatures than RAP only mixtures and the binders extracted from the 19-mm mixtures had warmer temperatures than those extracted from the 12.5-mm mixtures for the same recycled material content. The different binder sources for 12.5 mm and 19 mm may cause the difference in high- and low-temperature PG grade of extracted and recovered binders, so that the warmer high temperatures from the source 2 and source 3 virgin binders resulted in warmer high temperature of extracted and recovered binders from 19 mm mixtures than 12.5 mm mixtures. The slightly higher actual binder replacement for the 19 mm mixture (20.8% versus 18.9% for 12.5 mm) may contribute to the warmer temperatures, as well. The results of the PG grading analysis indicate that the LMLC materials were more highly aged than the PMPC materials and that the difference between the two depends on the mixture recycled content, effective binder content, virgin binder grade, and possibly binder source.

According to Figure 3, the ΔT_{cr} is negative for all binders, indicating they are m-controlled. The cracking warning (*11*) and cracking limit (*12*) lines are drawn in this figure as well. Most of the binders did not pass those criteria. For the 12.5-mm mixtures, the PMPC recovered binders showed larger ΔT_{cr} values than the LMLC recovered binders in most cases. This indicates that the aging which the asphalt is experiencing in the plant is changing the relaxation capacity (m-value) of the binder more than it is changing the stiffness (S-value) as compared to the aging the asphalt is experiencing in the lab. The recovered binders from 19-mm and PG 52-34 mixtures showed larger negative ΔT_{cr} values than the 12.5-mm and PG 58-28 mixtures, respectively.

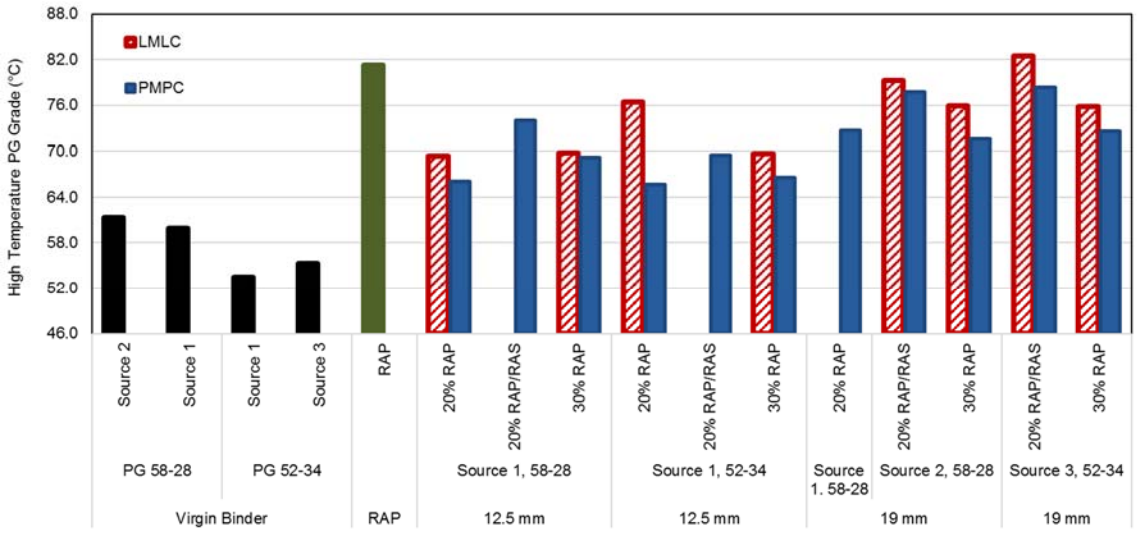

FIGURE 1 High PG temperatures for all binders.

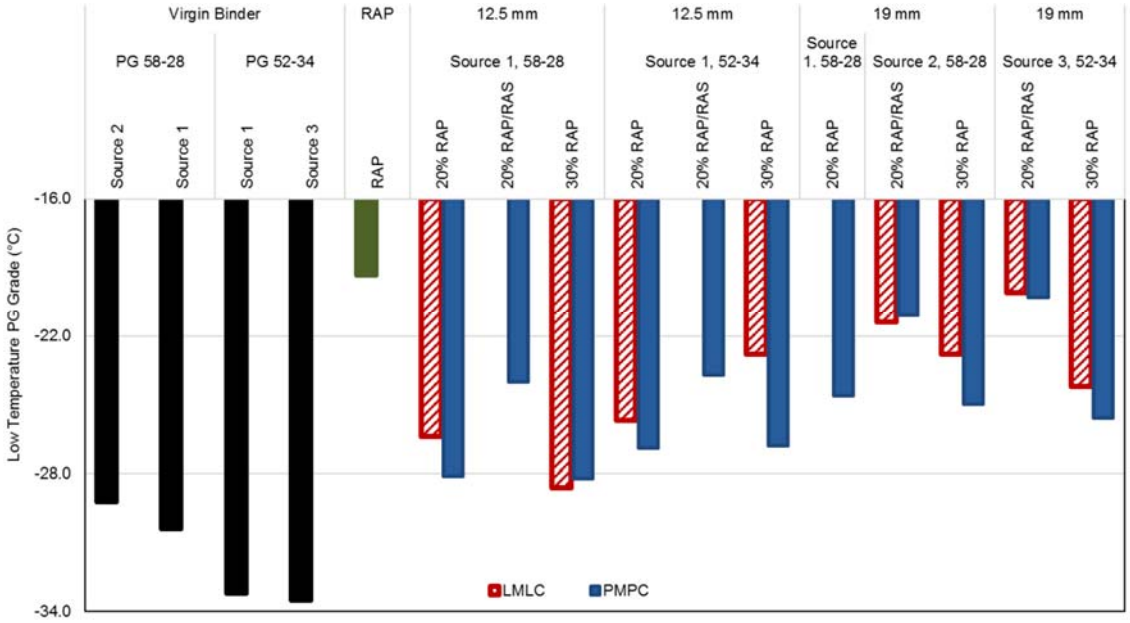

FIGURE 2 Low PG temperatures for all binders.

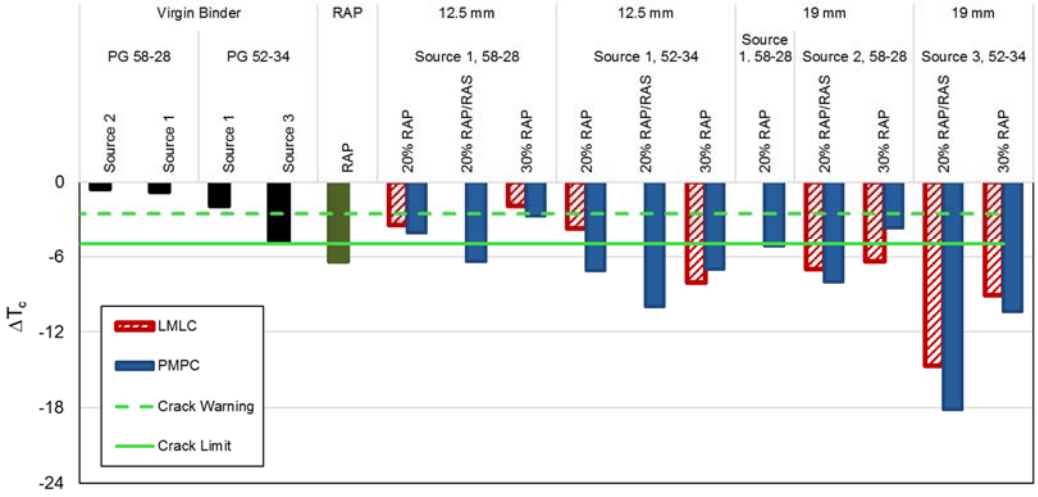

FIGURE 3 Delta T_{cr} values for all binders.

Direct comparisons of dynamic modulus mastercurves for plant and lab produced mixtures are shown in Figure 4. The results show that the lab produced mixtures generally had higher dynamic modulus curves than plant-produced mixtures. The difference between LMLC and PMPC dynamic modulus mastercurves was greater for 19-mm mixtures and the PG 58-28 base binder mixtures. Larger differences with a PG 58-28 base binder mixture have been observed with other groups of mixtures as well. The LMLC specimens generally had lower phase angles than the PMPC specimens, but there were no discernable trends in the differences with respect to NMAS or binder grade. However, the results of statistical analysis (T-test) for dynamic modulus and phase angle show that there was not a significant difference between dynamic modulus and phase angle of plant and lab produced mixtures, except for the PG 58-28, 12.5-mm, 20% RAP mixture.

Figure 5 compares the damage characteristic curves (*C* versus *S*) for the different plant- and lab-produced mixtures. Generally, these curves show how the material integrity decreases as damage is growing. The mixtures that have damage characteristic curves further up and to the right would be expected to perform better, since they are able to maintain their integrity better during fatigue loading (higher pseudo stiffness, *C*, with same amount of damage, *S*). However, the cracking performance of a mixture in the field depends on pavement structure as well and it is the combination of the rheological properties (modulus and phase angle) and damage characteristics that will determine how a mixture will perform in a particular pavement structure. The damage characteristic curves of lab-produced mixtures were very close to, or higher than the plant-produced mixtures for all 12.5-mm mixtures, while most of the 19-mm lab-produced mixtures showed slightly lower fatigue curves than plant produced mixtures. There is not much difference between the damage characteristic curves for the 19-mm mixtures, while 12.5-mm mixtures show a larger distinction between specimen types and mixture types.

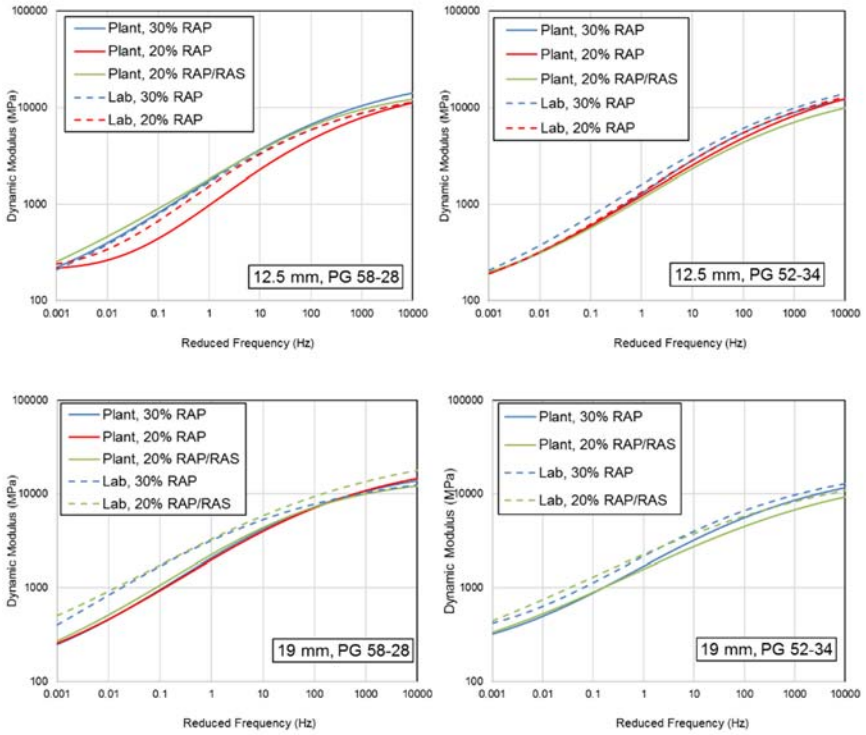

FIGURE 4 Comparison of plant-produced and laboratory-produced dynamic modulus master curves.

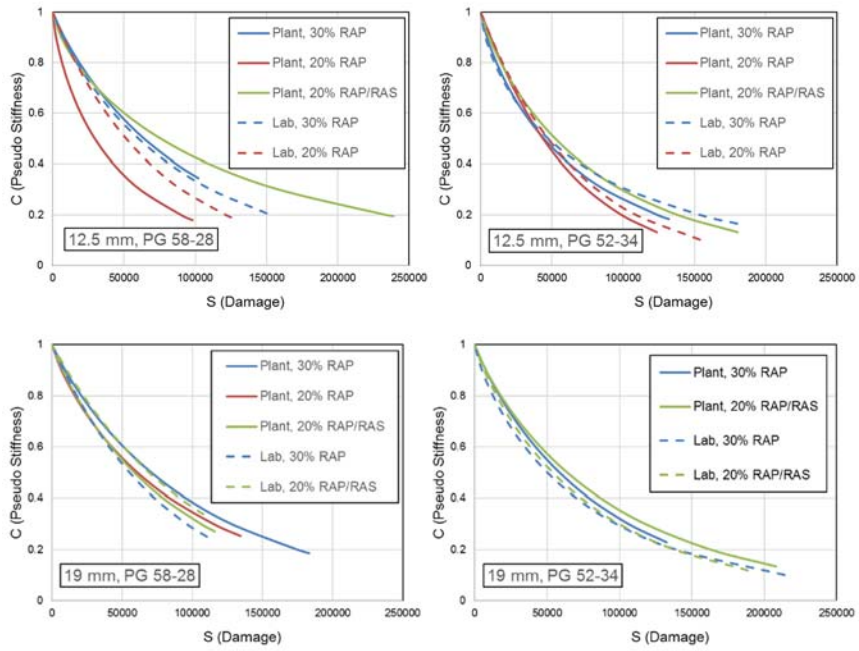

FIGURE 5 Comparison of plant-produced and laboratory-produced *C* versus *S* curves for SVECD fatigue.

Figure 6 compares the $G^R - N_f$ diagrams from plant- and lab-produced mixtures. Generally, lines that are further up and to the right would indicate better fatigue performance, but again, actual field performance will be determined by the combination of rheological and fatigue properties of the mixture and location of the material in the pavement structure in the field. The general trends indicate that the difference between plant- and lab-produced PG 52-34 mixtures was negligible, while a larger difference was observed for the PG 58-28 mixtures. Also, in most cases (except 19-mm RAP/RAS mixes), plant-produced mixtures showed slightly better fatigue behavior than lab-produced mixes, but it may not be a significant difference because of scatter in fatigue data.

The number of cycles to failure at a G^R value of 100 has been proposed as a fatigue index parameter. Figure 7 shows the ratio of number of cycles to failure for lab-produced mixtures to number of cycles for plant-produced mixtures at $G^R = 100$. The bars greater than 1.0 indicate higher number of cycles to failure for lab-produced mixtures. The results show that for both RAP/RAS mixtures, lab-produced mixtures had better fatigue performance than plant-produced mixtures, while for all high RAP mixtures (28.3% and 31.3% RAP), plant-produced mixtures had better behavior.

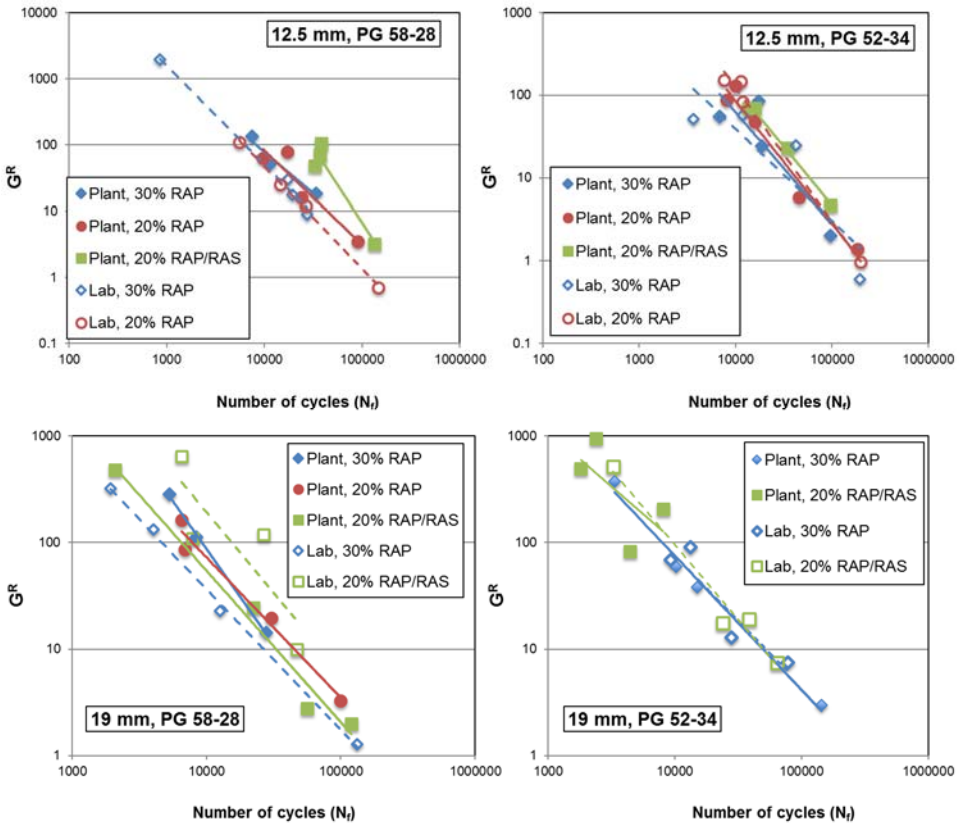

FIGURE 6 Comparison of plant-produced and laboratory-produced N_f versus G^R curves SVECD fatigue analysis.

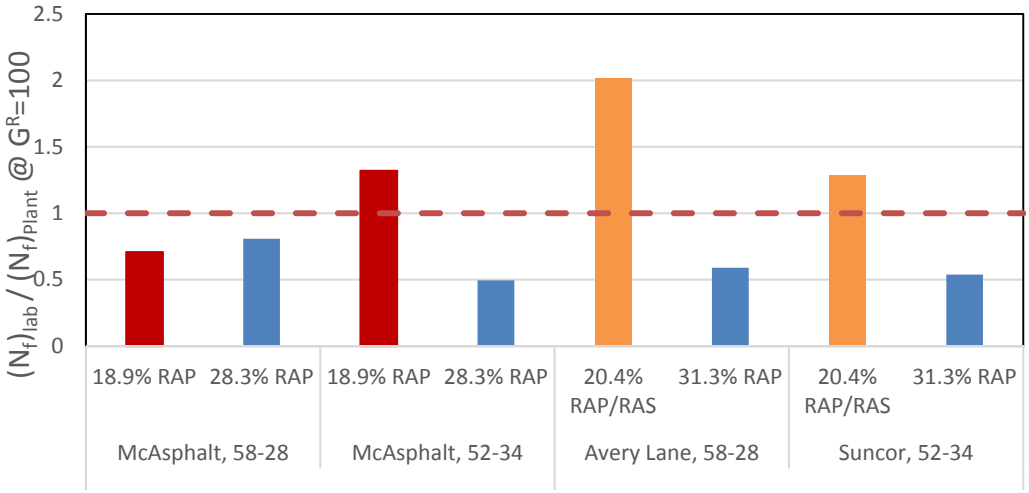

FIGURE 7 The ratio of (N_f) lab/(N_f) plant @ G^R = 100.

IMPACT OF REHEATING PLANT MIXTURE

The differences in properties measured on specimens that fabricated from reheated loose mixture (PMLC) and those fabricated without reheating (PMPC) are discussed in this section. Figure 8 shows the average dynamic modulus ratios for four sets of mixtures at four RAP contents. Each bar represents the average ratio for all measured values (tested over a range of frequencies) at each temperature. Generally, the ratios are observed to be larger at the higher temperatures and at the lower RAP contents. The binder in the RAP, having already been significantly aged from the field, will not undergo as much additional aging due to reheating as the virgin binder. Therefore, the ratios at the higher RAP contents are expected to be lower. The properties of the virgin binder, the RAP binder, plant operations, and temperatures will also influence the magnitude of this difference between specimens that are fabricated using reheated materials and those that are not.

Figure 9 shows average dynamic modulus master curves for a set of six mixtures; each plot shows the master curves constructed from measurements on LMLC, PMPC, PMLC, and field core specimens. The PMLC specimens are generally the stiffest, and the difference between the PMLC and PMPC specimens decreases with increasing RAP content for mixtures with both the PG 58-28 and PG 52-34 base binder. At the 25% RAP level (middle set of plots), the influence of the base binder on the differences can be observed; the softer binder is showing larger differences between the different specimen types.

Comparisons of the SVECD C versus S and N_f versus G^R curves for these same mixtures are shown in Figure 10 and Figure 11, respectively. These figures illustrate differences in the fatigue behavior of the various mixtures due to the impact of reheating the loose mixture. In some cases, the differences in behavior are negligible, while in others, there are large differences. However, there are not strong trends with respect to RAP content or virgin binder grade for these parameters.

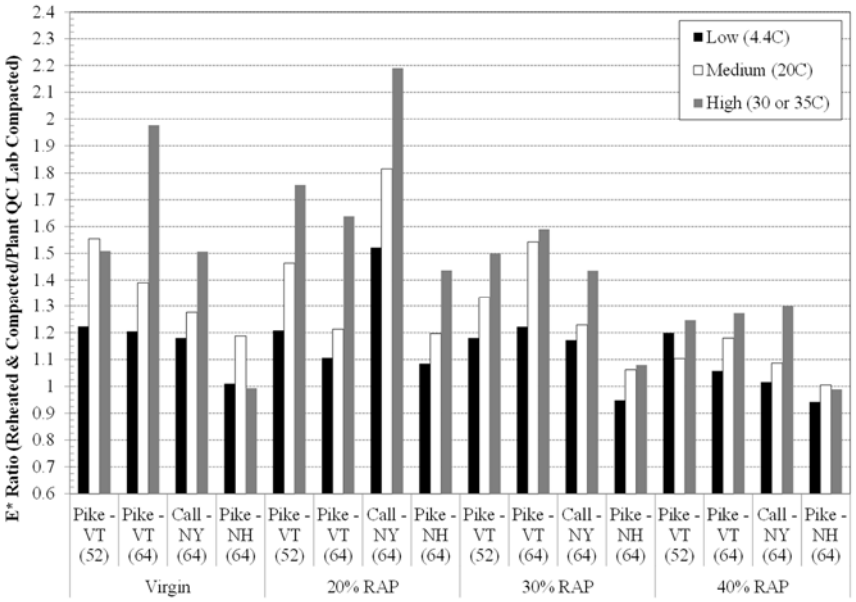

FIGURE 8 Average dynamic modulus ratios between specimens fabricated from loose mixture that was reheated and loose mixture that was not reheated.

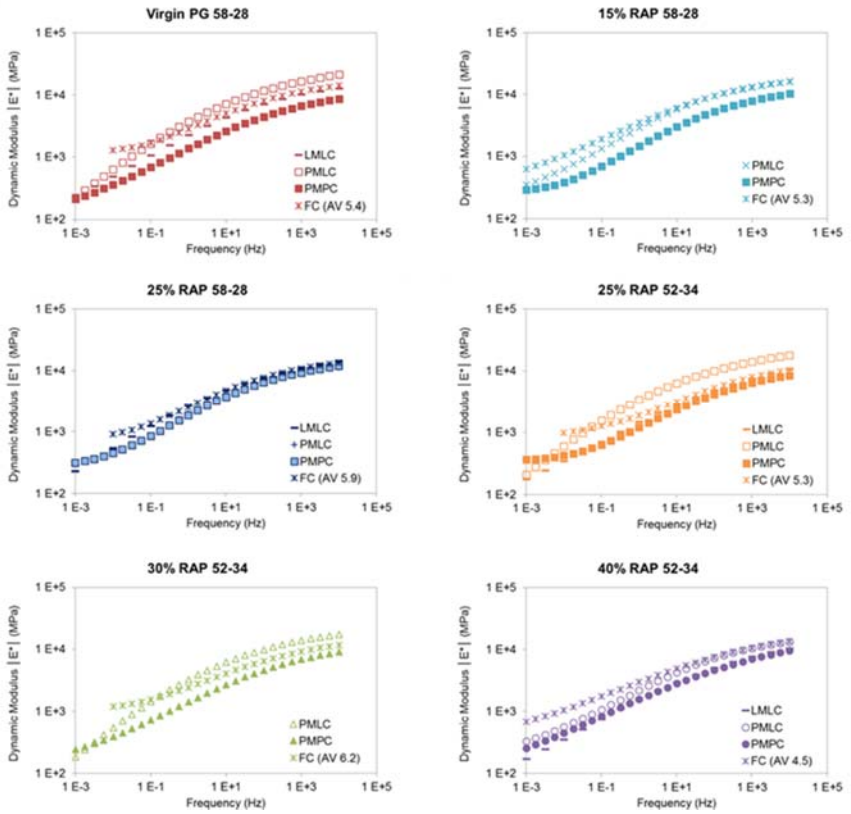

FIGURE 9 Average dynamic modulus master curves for various specimen fabrication methods.

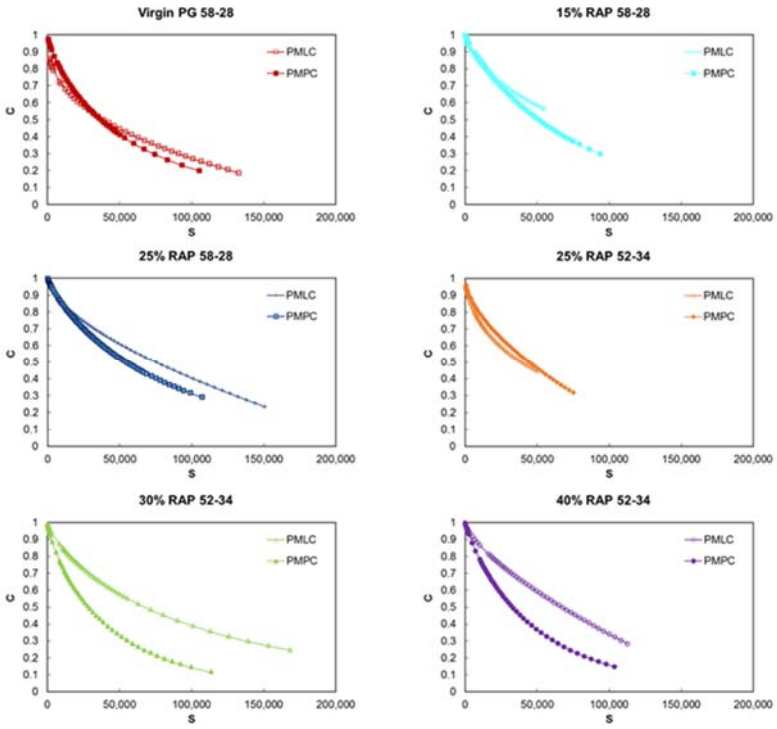

FIGURE 10 Average SVECD *C* versus *S* curves for various specimen fabrication methods.

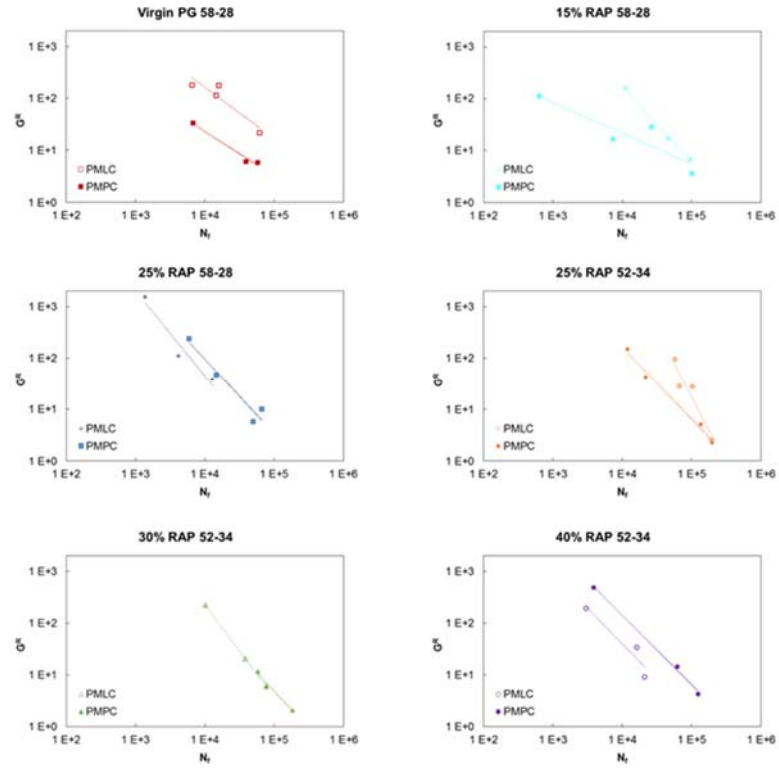

FIGURE 11 SVECD N_f versus G^R plots for various specimen fabrication methods.

A comparison of dynamic modulus master curves for another set of mixtures fabricated using both reheated and not reheated material is shown in Figure 12. The top figure, representing the specimens that were fabricated without reheating, shows differences in the material stiffnesses and expected trends with RAP content, excepting the 20% RAP mixture. The bottom figure shows the dynamic modulus curves from the reheated materials and all four mixtures have similar response; the effect of reheating has masked differences in the mixtures. The production temperatures and silo storage times for these mixtures are shown in the top figure; differences in the temperatures to which the materials were exposed and the time they were kept at elevated temperature could also cause differences in measured stiffnesses observed.

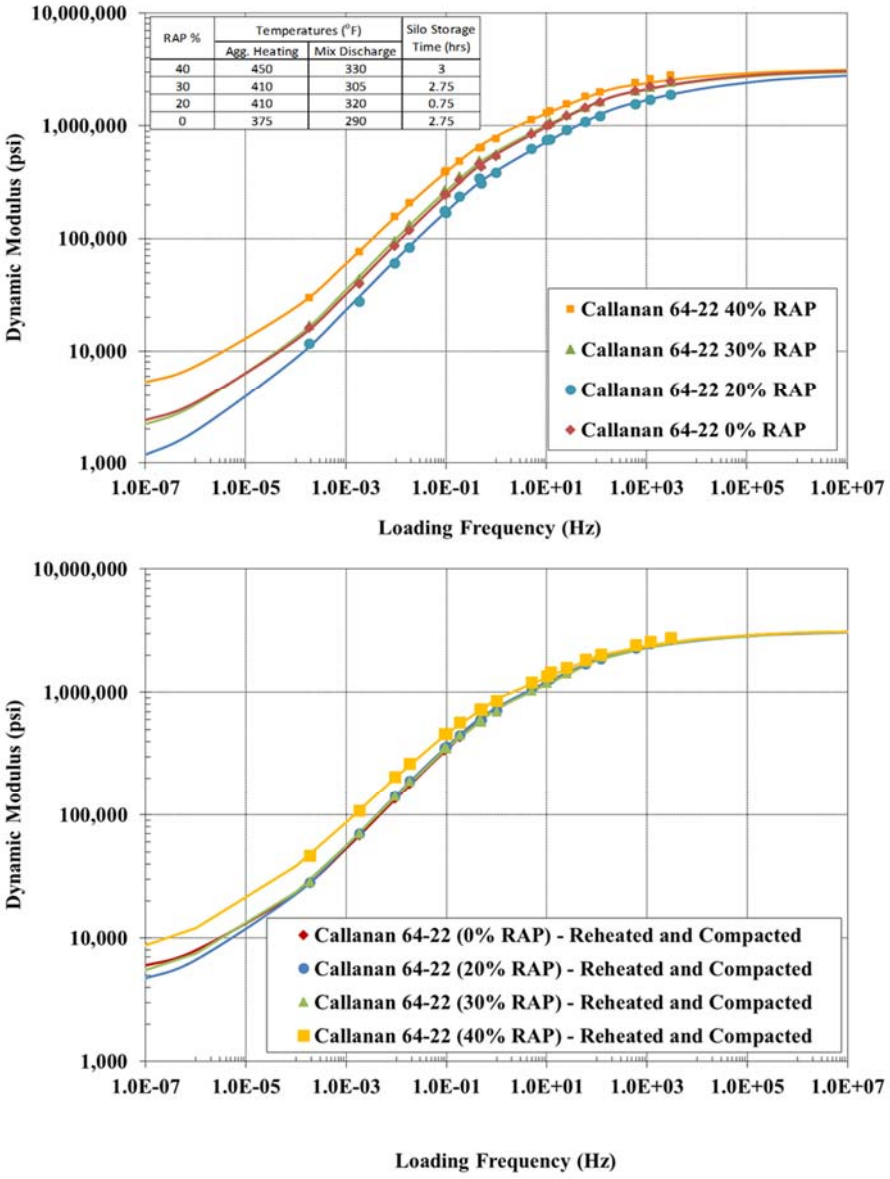

FIGURE 12 Dynamic modulus mastercurves for specimens fabricated without reheating and reheated and compacted.

IMPACT OF SILO STORAGE TIME

This section presents the results from two sets of mixtures: a virgin mixture and 25% RAP mixture were sampled from the plant at incremental silo storage times. Both mixtures had a 12.5 mm gradation, a target asphalt content of 5.4%, and a PG 64-22 virgin binder. The virgin mixture was sampled after silo storage times of 0, 2.5, 5, and 7.5 h after production began; the 25% RAP mixture was sampled at 0, 2.5, 5, 7.5, and 10 h. Specimens were produced by immediately compacting loose mix sampled from the plant without reheating the material. Mixture discharge temperatures were approximately 175°C, which is not unusual during shoulder seasons in the northeast. Virgin binder was also conditioned in the RTFO at five conditioning times (45, 85, 135, 170, and 300 min) to evaluate how well RTFO aging simulated the plant production and storage time associated with the virgin mixture in this study. More details can be found in Jacques et al. (*10*).

The G-R parameter analysis, shown in Figure 13, illustrates that as silo storage time increases, the extracted asphalt binder becomes more aged and migrates to areas where potential, non-load associated cracking is a concern. The results also show that the 25% RAP mixture initiates and moves closer to the threshold values than the asphalt binder from the virgin mixture. The measured crossover frequency and *R*-value shown in Figure 9 clearly indicates that a change in the CAM rheological indices occurs due to longer silo storage times, indicating that aging is occurring over time. The binder extracted from the RAP mixture shows larger changes than the extracted virgin binder.

The results of the RTFO aging for various times are also shown in Figure 13 and Figure 14. These results indicate that using the specified time of 85 min in the RTFO does not simulate the aging that occurred during plant production and silo storage for the virgin mixtures. In fact, it can be seen that RTFO conditioning does not show similar stiffness (G* and δ) and CAM rheological indices to 0 h of silo storage time until approximately 170 min, which is twice the amount specified in AASHTO T240. This clearly indicates that current laboratory conditioning methods do not necessarily simulate asphalt plant production. The large differences in this case are likely a result of the relatively high (175°C) production temperatures that would have aged the asphalt binder, especially under extended silo storage times.

Dynamic modulus master curves for the virgin and 25% RAP mixtures are shown in Figure 15. Both the virgin and RAP mixtures show an increase in dynamic modulus as the mixtures remain in the silo for longer periods. The RAP mixture shows greater increases with storage time than the virgin mixtures. Statistically, the 0, 2.5, and 5 h mixtures are all similar for the virgin material. The 7.5-h virgin mixture is statistically different from the 0- and 2.5-h storage times. The RAP mixture at 7.5 and 10 h shows significant differences from 0 h.

The average increases in stiffness, as compared to the 0-h mixtures are shown in Figure 16. On average, the 7.5-h virgin mixture is approximately 1.3 times stiffer than the 0-h mixture. Stiffening of the virgin mixtures implies that there is short-term aging or additional binder absorption occurring within the silo, particularly at longer storage times such as 7.5 h. The RAP mixtures show higher ratios than the virgin mixtures. The RAP mixture at 2.5 h has a similar ratio to the virgin mixture at 7.5 h. It is clear that the RAP mixture experiences greater stiffness changes than the virgin mixture as silo storage time increases. This could imply that there is blending or diffusion between RAP and virgin binders in the silo, in addition to short-term aging that is experienced with the virgin mixture.

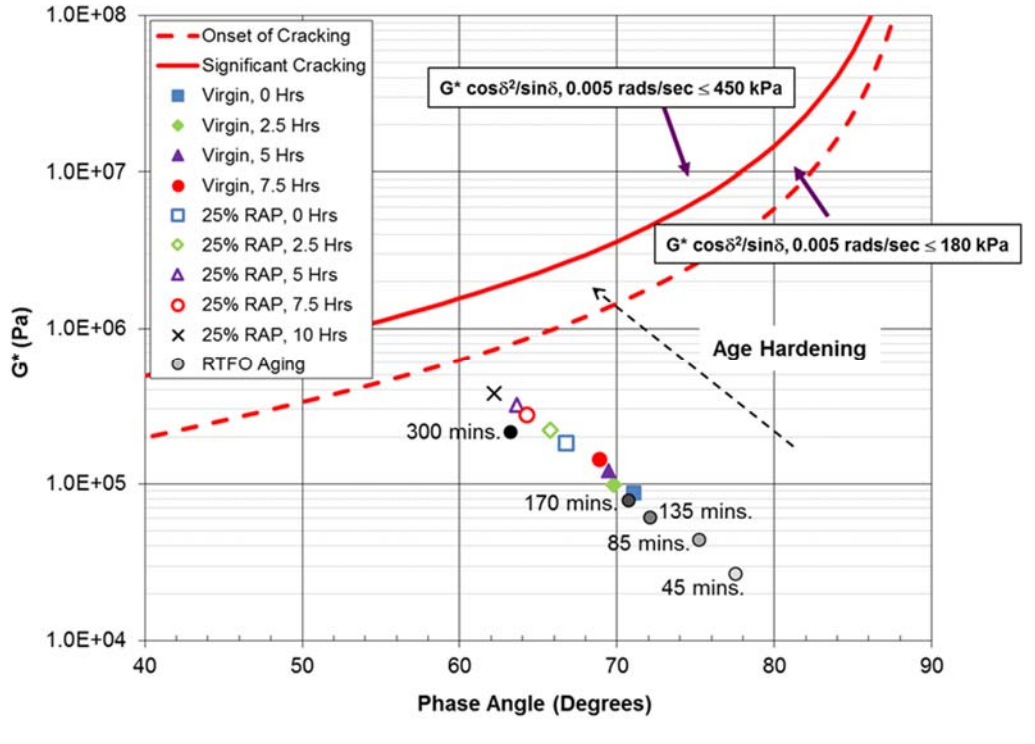

FIGURE 13 Effect of silo storage time and RTFO conditioning on retained asphalt binder: G-R parameter and Black Space plot.

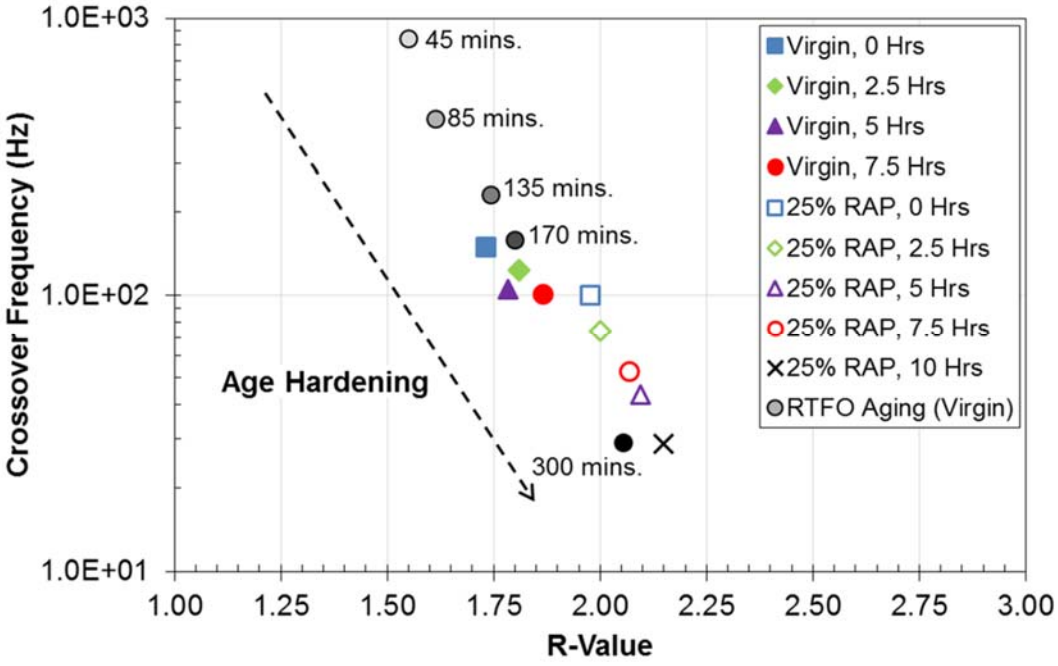

FIGURE 14 Effect of silo storage time and RTFO conditioning on retained asphalt binder: crossover frequency–*R*-value space.

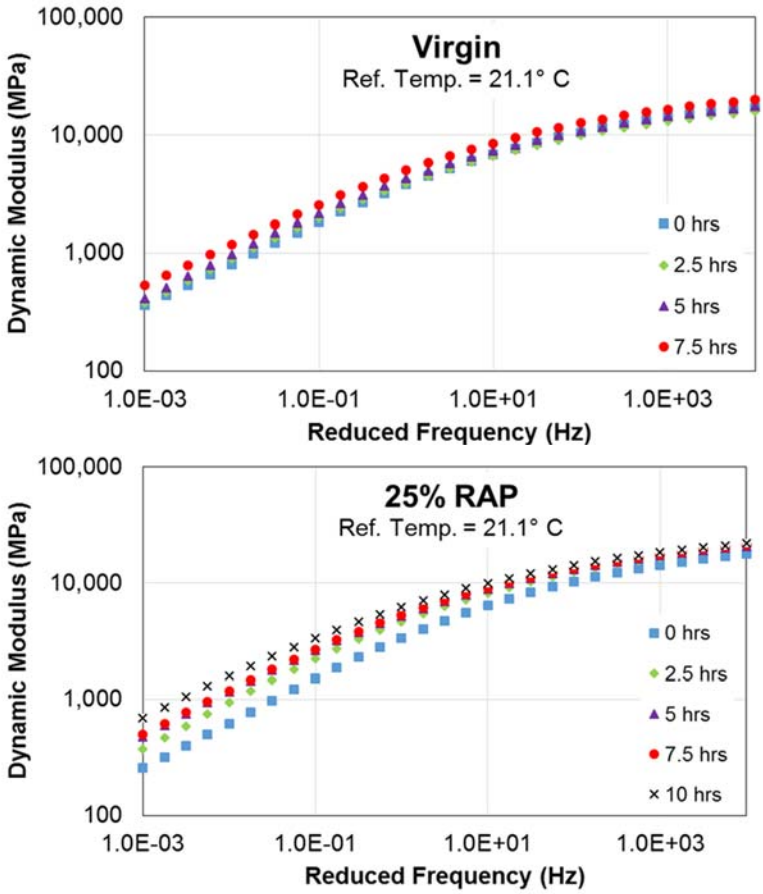

FIGURE 15 Dynamic modulus master curves for the virgin and 25% RAP mixtures.

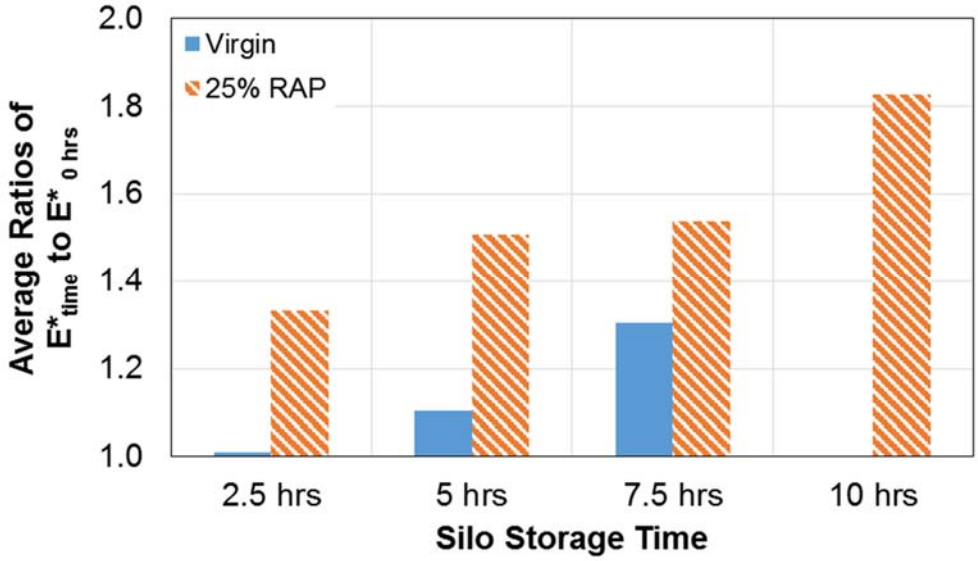

FIGURE 16 Dynamic modulus ratios.

The results from the SVECD testing and analysis on the virgin mixtures are shown in Figure 17. A clear increase in pseudo-stiffness is observed with an increase in silo storage time for the damage characteristic curves. There appears to be little distinction between the mixtures in the N_f versus G^R plots, but it is observed that the 7.5-h mixture has the largest slope (–1.528) which may indicate more susceptibility to fatigue cracking. It is important to keep in mind that the fatigue performance in the field also depends on the location within the pavement structure and loading conditions.

Figure 18 presents the results from LVECD analysis for virgin mixtures among two climate conditions for thin and thick pavements. Although LVECD was verified by several researchers (20, 21) for various conditions, this software has not been fully calibrated, and the transfer function to convert the predicted damage obtained from LVECD to cracking area in the field is still under development. Therefore, predictions presented in this paper are for relative comparisons; they use the number of elements that experienced more than 20% damage ($N/N_f > 0.20$) to evaluate the relative effects of silo storage time on the pavement performance. Figure 18 shows that an increase in silo storage time causes increases in fatigue damage for both types of pavements and climates, with increases of approximately 40% from 0- to 7.5-h storage times for the thin pavements and tripling of the damage for thick pavements (although magnitude of damage in thick pavements is much lower).

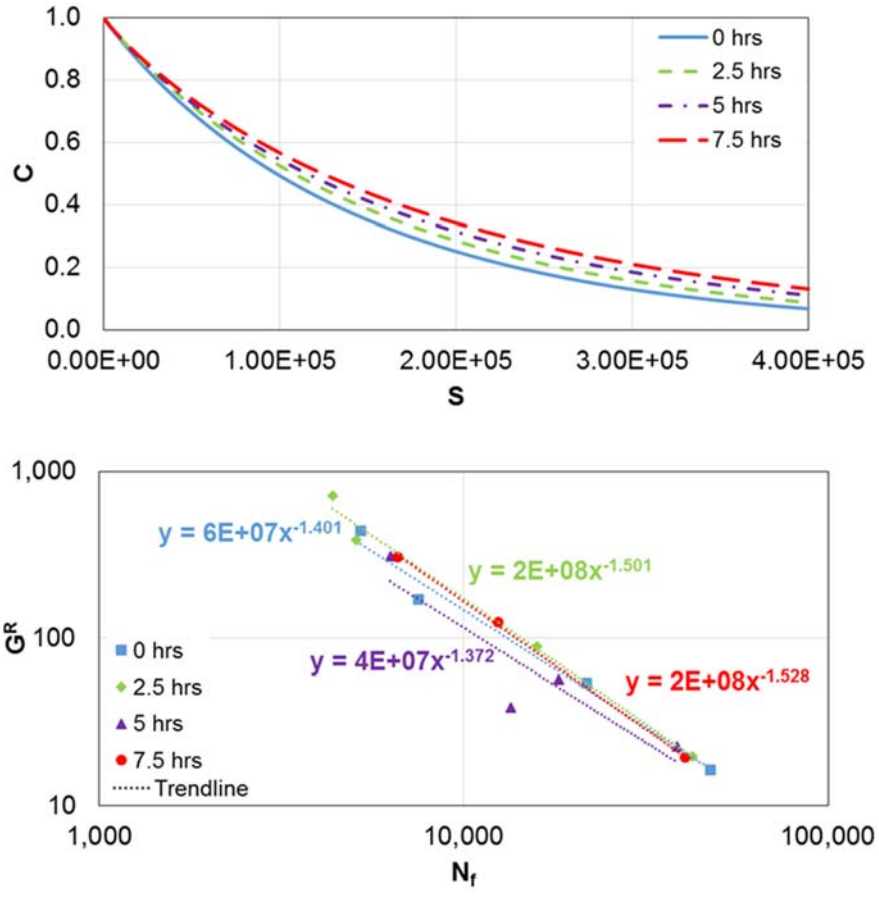

FIGURE 17 SVECD virgin mixture results: (*a*) damage characteristic curves and (*b*) fatigue failure criterion.

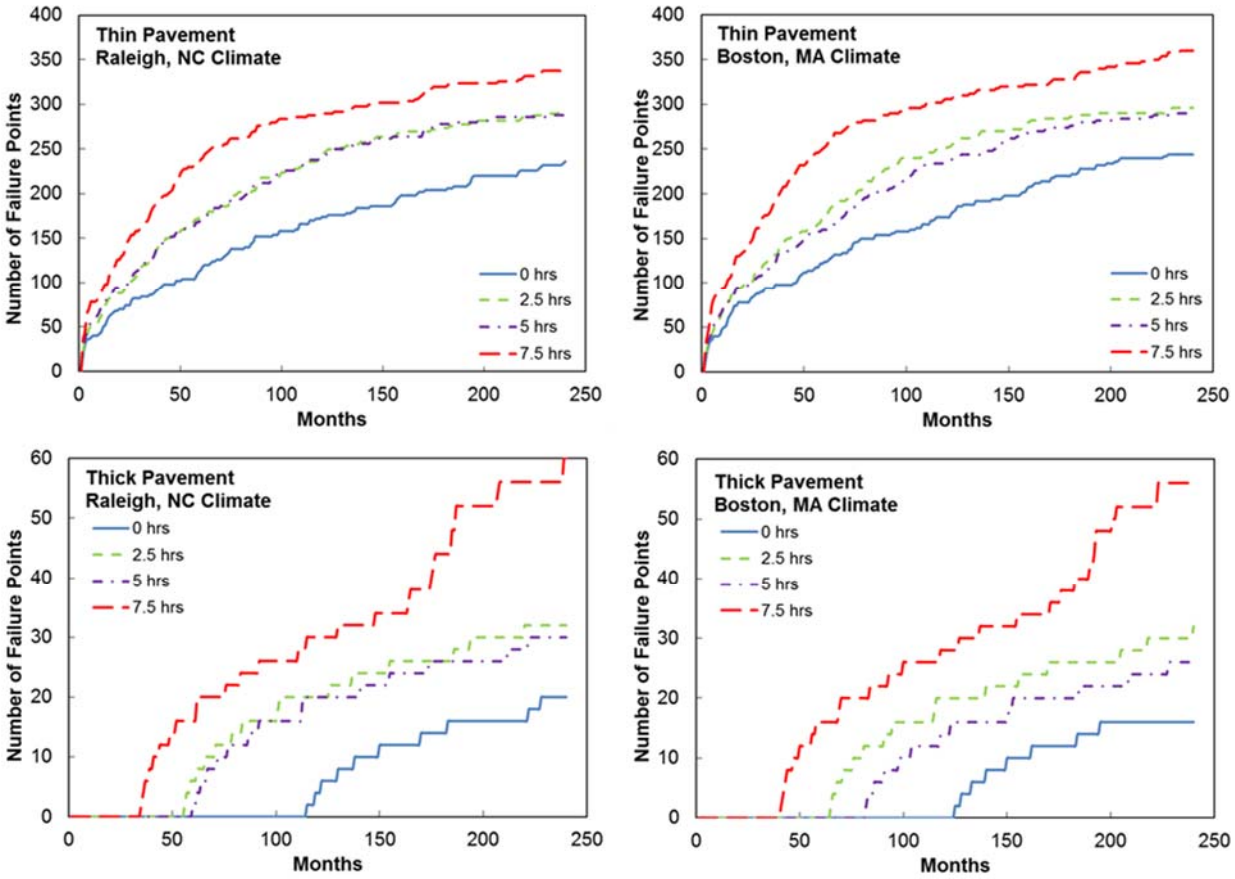

FIGURE 18 Comparison of fatigue resistance for virgin mixture using LVECD thick–thin pavements and two climate conditions.

SUMMARY AND CONCLUSIONS

This paper has presented summary results from three recently completed projects in the northeast United States to illustrate potential impacts from various mixture, fabrication, and plant-production parameters on measured asphalt mixture properties. Binders were evaluated using performance grading, rheological indices, and the G-R parameter. Mixtures were evaluated with complex modulus, SVECD fatigue, and pavement life evaluation with LVECD. The following observations were made based on the results and analysis.

- Lab-produced versus plant-produced materials. In general, laboratory produced materials were stiffer than plant produced materials and also had lower phase angles. The S-VECD fatigue curves change depending on the method as well. The PG of the binder and the amount of recycled material in the mixture impact the magnitude of the differences observed between the laboratory- and plant-produced materials.
- Impact of reheating mixtures for specimen fabrication: reheating material for specimen fabrication changes the measured properties as the materials undergo additional aging during the reheating. The magnitude of the differences depended on the aging susceptibility of

the materials. Generally, softer binder grades showed larger differences and the differences were smaller with higher recycle content.

- Effect of silo storage time. As mixtures are kept at elevated temperatures, additional aging may occur that results in stiffening and embrittlement of the materials. Both virgin and RAP mixtures experienced changes as a result of being stored in the silo, but the RAP mixture may have experienced larger changes. This indicates that there may be a combination of short-term aging within the silo and a blending or diffusion process occurring with the RAP mixture.

These studies have shown that current laboratory protocols don't always capture what happens in the plant and have highlighted the need to recognize potential impacts of fabrication methods and production parameters on measured properties. Additional work needs to be done to determine how the differences in measured properties translate to differences in actual field performance so that appropriate methodologies can be selected and adopted for use in performance-related specifications.

ACKNOWLEDGMENTS

The research team that completed these projects includes Richard Kim at North Carolina State University, Tom Bennert at Rutgers University, and Walaa Mogawer at Umass Dartmouth. The research team would like to acknowledge the New Hampshire DOT and participating agencies in TPF 5(230): Evaluation of Plant-Produced High-Percentage RAP Mixtures in the Northeast: FHWA, New Hampshire, Maryland, New Jersey, New York, Pennsylvania, Rhode Island, and Virginia for funding this work. Thanks also to Old Castle Materials for supplying the mixtures and production information from multiple plants.

REFERENCES

1. Daniel, J. S., C. Jacques, and S. Salehi. Performance of High RAP Pavement Sections in NH. *Final Report to New Hampshire Department of Transportation,* FHWA-NH-RD-15680B, 2015.
2. Daniel, J. S. and R. Rahbar-Rastegar. Correlation Between Laboratory and Plant Produced High RAP/RAS Mixtures. *Final Report to New Hampshire Department of Transportation,* 2016.
3. Daniel, J. S., T. Bennert, W. Mogawer, Y. R. Kim, A. Congalton, M. Elwardany, D. Mensching, and M. Sabouri. Evaluation of Plant-Produced High-Percentage RAP Mixtures in the Northeast. *TPF 5(230) Phase I Final Report,* 2014.
4. Daniel, J. S., T. Bennert, W. Mogawer, Y. R. Kim, A. Congalton, M. Elwardany, D. Mensching, and M. Sabouri. Evaluation of Plant-Produced High-Percentage RAP Mixtures in the Northeast. *TPF 5(230) Phase II Final Report,* 2015.
5. Daniel, J. S., T. Bennert, W. Mogawer, Y. R. Kim, D. Mensching, and M. Sabouri. Evaluation of Plant-Produced High-Percentage RAP Mixtures in the Northeast. *TPF 5(230) Phase III Final Report,* 2015.
6. Daniel, J. S., T. Bennert, W. Mogawer, Y. R. Kim, C. Jacques, and C. DeCarlo. Evaluation of Plant-Produced High-Percentage RAP Mixtures in the Northeast. *TPF 5(230) Silo Storage Study Additional Task Final Report,* 2016.
7. Sabouri, M., T. Bennert, J. S. Daniel, and Y. R. Kim. Evaluating Laboratory-Produced Asphalt Mixtures with RAP in Terms of Rutting, Fatigue, Predictive Capabilities, and High RAP Content

Potential. *Transportation Research Record: Journal of the Transportation Research Board, No. 2506*, 2015, pp. 32–44.
8. Mensching, D., J. S. Daniel, T. Bennert, M. Mederios, Jr., M. Elwardany, W. Mogawer, E. Hajj, and M. Alavi. Low Temperature Properties of Plant-Produced RAP Mixtures in the Northeast. *Electronic Journal of the Association of Asphalt Paving Technologists*, Vol. 83, 2014, pp. 37–79.
9. Mogawer, M., T. Bennert, J. S. Daniel, R. Bonaquist, A. Austerman, and A. Booshehrian. Performance Characteristics of Plant-Produced High RAP Mixtures. *Electronic Journal of the Association of Asphalt Paving Technologists*, Vol. 81, 2012, pp. 403–439.
10. Jacques, C., J. S. Daniel, T. Bennert, G. Reinke, A. Norouzi, C. Ericson, W. Mogawer, and Y. R. Kim. Effect of Silo Storage Time on the Characteristics of Virgin and Reclaimed Asphalt Pavement Mixtures. *Transportation Research Record: Journal of the Transportation Research Board*, 2016, 2016, pp. 76–85.
11. Anderson, M., G. King, D. Hanson, and P. Blankenship. Evaluation of the Relationship Between Asphalt Binder Properties and Non-Load Related Cracking. *Electronic Journal of the Association of Asphalt Paving Technologists*, Vol. 80, 2011, pp. 615–661.
12. Rowe, G. M. Prepared Discussion for the Association of Asphalt Paving Technologists Paper by Anderson et al.: Evaluation of the Relationship Between Asphalt Binder Properties and Non-Load Related Cracking. *Electronic Journal of the Association of Asphalt Paving Technologists*, Vol. 80, 2011, pp. 649–662.
13. Glover, C., R. Davison, C. Domke, Y. Ruan, P. Juristyarini, D. Knorr, and S. Jung. *Development of a New Method for Assessing Asphalt Binder Durability with Field Evaluation.* Publication FHWA-TX-05-1872-2, National Research Council, Washington, D.C, 2005.
14. Rowe, G. M., G. King, and M. Anderson. The Influence of Binder Rheology on the Cracking of Asphalt Mixes on Airport and Highway Projects. *ASTM Journal of Testing and Evaluation*, Vol. 42, No. 5, 2014.
15. Christensen, D. W., and D. A. Anderson. Interpretation of Dynamic Mechanical Test Data for Paving Grade Asphalt Cements. *Electronic Journal of the Association of Asphalt Paving Technologists*, Vol. 61, 1992, pp. 67–116.
16. Mogawer, W., T. Bennert, A. Austerman, and C. Ericson. Investigating the Aging Mitigation Capabilities of Rejuvenators in High RAP Mixtures Using Black Space Diagrams, Binder Rheology, and Mixture Tests. *Journal of the Association of Asphalt Paving Technologists,* Vol. 85, 2015.
17. Underwood, B. S., Y. R. Kim, and M. N. Guddati. Improved Calculation Method of Damage Parameter in Viscoelastic Continuum Damage Model. *International Journal of Pavement Engineering*, Vol. 11, No. 6, 2010, pp. 459–476. https://doi.org/10.1080/10298430903398088.
18. Eslaminia, M., S. Thirunavukkarasu, M. N. Guddati, and Y. R. Kim. Accelerated Pavement Performance Modeling Using Layered Viscoelastic Analysis. *Proceedings of the 7th International RILEM Conference on Cracking in Pavements*, Delft, Netherlands, 2012, pp. 20-22. https://doi.org/10.1007/978-94-007-4566-7_48.

Short-Term Laboratory Conditioning of Asphalt Mixtures

FAN YIN
National Center for Asphalt Technology

AMY EPPS MARTIN
EDITH ARÁMBULA-MERCADO
Texas A&M Transportation Institute

DAVID NEWCOMB
Texas A&M Transportation Institute

INTRODUCTION

Aging refers to the stiffening of asphalt binders and mixtures with time due to oxidation, molecular agglomeration, and other chemical processes. It occurs due to the heating of asphalt binder during production and construction in the short-term and due to oxidation over the long-term throughout the pavement's service life. The ability to simulate aging in asphalt mixtures produced in the laboratory has been studied extensively, and procedures have been adopted for use in mix design and performance evaluation. For example, AASHTO R 30 recommends a short-term oven aging (STOA) protocol of 2 h at compaction temperature for mix design, while 4 h at 275°F (135°C) is specified for mixtures subject to performance testing. In addition, a long-term oven aging (LTOA) protocol of 5 days at 185°F (85°C) on compacted specimens is recommended to simulate aging of asphalt mixtures during the first 7 to 10 years of pavement service life. While the comparison of stiffening in laboratory-produced and plant-produced mixtures was never exactly equivalent across all mixture types, there was an acceptance that the above-mentioned aging protocols were representative of plant and field aging. However, this occurred at a time when the amount of recycled materials used in asphalt mixtures was relatively low, polymer-modified asphalts were not common, and mixing temperatures remained relatively constant.

Over the past few decades, changes have occurred in asphalt mixture components, mixture processing, and plant design. These changes include an increased use of polymer modifiers and recycled materials, the advent of warm-mix asphalt (WMA) technologies, and drum-mix plants replacing batch-mix plants (BMPs). Although these changes are beneficial for economic, environmental, and engineering reasons, questions have been raised about the validity of the current mix design method in assessing the volumetric needs and physical characteristics of asphalt mixtures required to meet performance expectations. In addition, there is a need to further review the correlations of plant and field aging by laboratory aging protocols that considers the impacts of climate, aggregate type, recycled materials, WMA technologies, plant type, and production temperature.

The recently completed NCHRP Project 09-52: Short-Term Laboratory Conditioning of Asphalt Mixtures, focused on developing laboratory aging protocols to simulate asphalt aging and aggregate asphalt absorption of asphalt mixtures as produced in a plant and throughout the initial period of pavement performance (i.e., approximately 1 to 2 years after construction). In addition to developing these aging protocols, the research efforts were also devoted to identifying the effects of the following factors on the aging characteristics of asphalt mixtures:

WMA technology, aggregate asphalt absorption, plant temperature, plant type, presence of recycled materials, and asphalt source.

Materials used in this project were obtained from nine field sites located in eight states, as shown in Figure 1. Each field site was selected to include one or more of the factors listed above. Detailed descriptions of the asphalt mixtures included in each field site can be found in NCHRP Report 815 (Newcomb et al. 2015). Mineral aggregates and asphalt binders were sampled ahead of production and construction in order to fabricate LMLC specimens to replicate conditions during mix design. In addition, mixtures produced by the asphalt plant were sampled and compacted at or near the field site to prepare PMPC specimens. The PMPC specimens were regarded as the baseline of asphalt aging that occurred during plant production. Finally, field cores were sampled immediately after construction and at intervals of up to 2 years after construction to ascertain aging in the field.

In this project, the effects of both short-term and long-term aging on asphalt mixtures were primarily evaluated using the resilient modulus (M_R) test per ASTM D7369 at 77°F (25°C) and the Hamburg Wheel-Tracking Test (HWTT) per AASHTO T 324 at 122°F (50°C). In addition, a limited amount of dynamic modulus (E*) testing was conducted in accordance with AASHTO TP 79-13. The M_R test is effective for evaluating the aging of asphalt mixtures for two reasons: (1) M_R stiffness is governed by asphalt binder properties; and (2) the test is applicable to characterizing field cores, which can have limited thickness.

SIMULATION OF PLANT AGING

The first part of the project focused on validating a laboratory STOA protocol for asphalt loose mix prior to compaction to simulate asphalt aging and aggregate asphalt absorption during plant production. Guidance on laboratory STOA protocols for preparing LMLC specimens was obtained from results in NCHRP Project 09-49: Moisture Susceptibility of Warm-Mix Asphalt

FIGURE 1 Locations of field sites used in NCHRP Project 9-52.

(Epps Martin et al. 2014). Among the various STOA protocols investigated, the best correlation in mixture stiffness between LMLC specimens and PMPC specimens or cores at construction was obtained by conditioning the loose mix for 2 hours at 240°F (116°C) and 275°F (135°C) for WMA and hot-mix asphalt (HMA), respectively. These short-term aging protocols were adopted for this research effort and were further evaluated with more than 40 additional asphalt mixtures with various components and production parameters. For data analysis, the volumetric parameters and laboratory test results of LMLC specimens fabricated using the selected STOA protocols were compared against those of corresponding PMPC specimens and cores at construction. The results were plotted against the line of equality to determine whether an equivalent level of asphalt aging was achieved between laboratory and plant production.

Figure 2 presents the volumetric correlations for LMLC specimens (x-axis) versus PMPC specimens (*y*-axis) in terms of theoretical maximum specific gravity (G_{mm}) and percent binder absorbed (P_{ba}). As illustrated in Figure 2*a*, most of the data points fell on the line of equality indicating equivalent G_{mm} values were achieved by LMLC and PMPC specimens. The exceptions were mixtures from the Iowa field site that were produced with highly absorptive aggregates. A reasonable correlation in term of P_{ba} values was also observed in Figure 2*b* when comparing the two specimen types, with the exception of the same subset of Iowa mixtures. For these mixtures, the aggregate asphalt absorption that occurred during plant production was greater than that produced by the selected laboratory STOA protocols, which was possibly due to a higher-than-planned temperature during plant production. Based on the results shown in Figure 2, practically equivalent mixture volumetrics were observed for PMPC specimens and LMLC specimens for a wide range of asphalt mixtures. Therefore, the selected laboratory STOA protocols of 2 h at 275°F (135°C) for HMA and 2 h at 240°F (116°C) for WMA were considered suitable to simulate the aggregate asphalt absorption during plant production.

Figure 3 presents the M_R stiffness correlation of LMLC specimens (*x*-axis) versus PMPC specimens and cores at construction (*y*-axis). As shown in Figure 3*a*, most of the data points fell on the line of equality, which indicated that M_R stiffness for LMLC specimens with the selected laboratory STOA protocols of 2 h at 275°F (135°C) for HMA and 2 h at 240°F (116°C) for WMA closely mimicked that for PMPC specimens. The biggest explainable exceptions

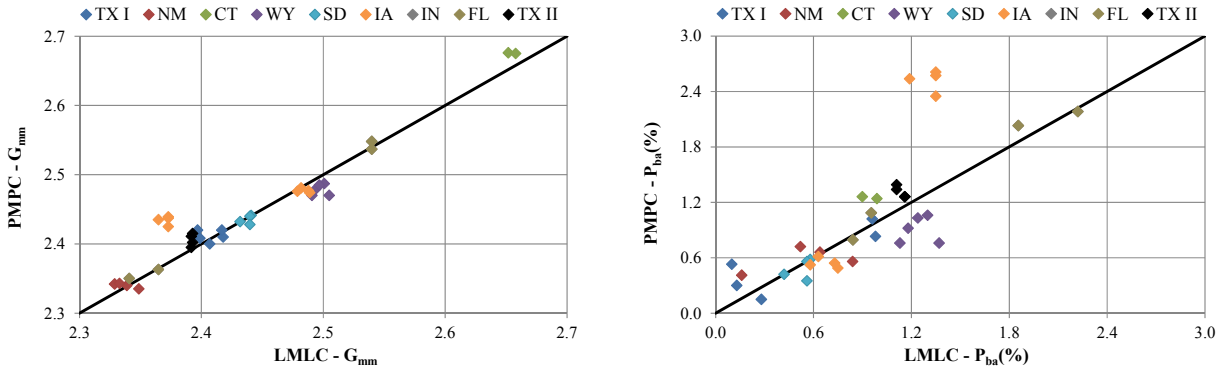

(a) (b)

FIGURE 2 Mixture volumetrics correlations for LMLC versus PMPC specimens: (*a*) G_{mm} values and (*b*) P_{ba} values.

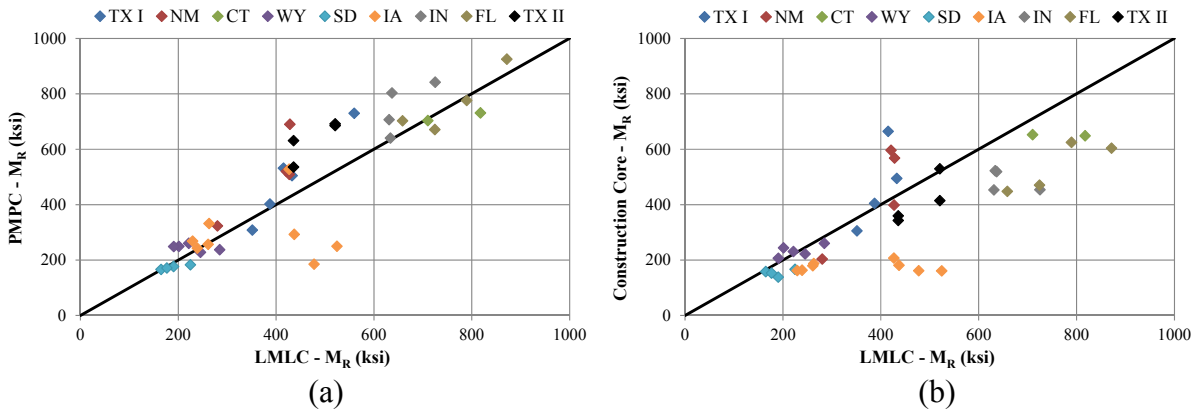

FIGURE 3 M_R stiffness correlation: (*a*) LMLC versus PMPC specimens and (*b*) LMLC specimens versus cores at construction.

were for the high-absorptive mixtures from Iowa which were affected by the laboratory conditioning, the high RAP mixture from New Mexico, and the rapidly aging asphalt mixture from Texas II. Although a reasonable correlation was observed in Figure 3*b* between the cores at construction and the LMLC specimens, the cores exhibited lower M_R stiffness, possibly due to the higher air voids (AV) and different aggregate orientation in the construction cores. Previous studies have shown that more horizontal aggregate orientation in field cores, as compared to laboratory specimens, can lead to anisotropic behavior resulting in lower mixture stiffness values measured in the M_R test (Yin et al. 2013; Zhang et al. 2011).

Figure 4 presents the correlation of E* stiffness results at 68°F (20°C) and 10 Hz for LMLC specimens (*x*-axis) versus PMPC specimens (*y*-axis) from the Connecticut, Indiana, and Texas II field sites. Consistent with the results shown in Figure 3, a good correlation in E* stiffness was observed for LMLC specimens versus PMPC specimens. The only outlier shown in Figure 4 corresponded to BMP PMPC specimens of HMA from the Indiana field site, which showed a significantly lower E* stiffness as compared to corresponding LMLC specimens. Besides this outlier, the rest of the E* results indicated the laboratory samples achieved a degree of aging similar to that caused by heating and mixing during plant production.

The comparison of the HWTT rut depth at 5,000 load cycles for LMLC specimens (*x*-axis) versus PMPC specimens and cores at construction (*y*-axis) is illustrated in Figure 5. Although a substantial variability in the rut depth measurements was shown in Figure 5*a*, there was a reasonable correlation between LMLC and PMPC specimens for mixtures with fairly low rut depth values (i.e., less than 5 mm at 5,000 load cycles). The reduced correlation for mixtures with high rut depth values was likely due to the occurrence of stripping during the test. The comparison between LMLC specimens and cores at construction showed a different trend in Figure 5*b*, where the majority of the data points were located above the line of equality. Thus, cores at construction showed a greater susceptibility to rutting in the HWTT as compared to corresponding LMLC specimens. The degradation and debonding of the plaster needed to fit the cores into the testing mold was likely a significant contributing factor to higher rut depth measurements for cores at construction, and a consequent poor correlation with the LMLC specimens.

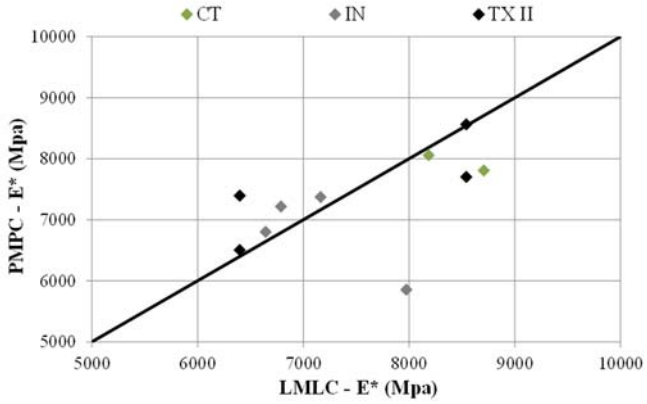

FIGURE 4 E* Stiffness at 20°C/10-Hz correlation for LMLC versus PMPC specimens.

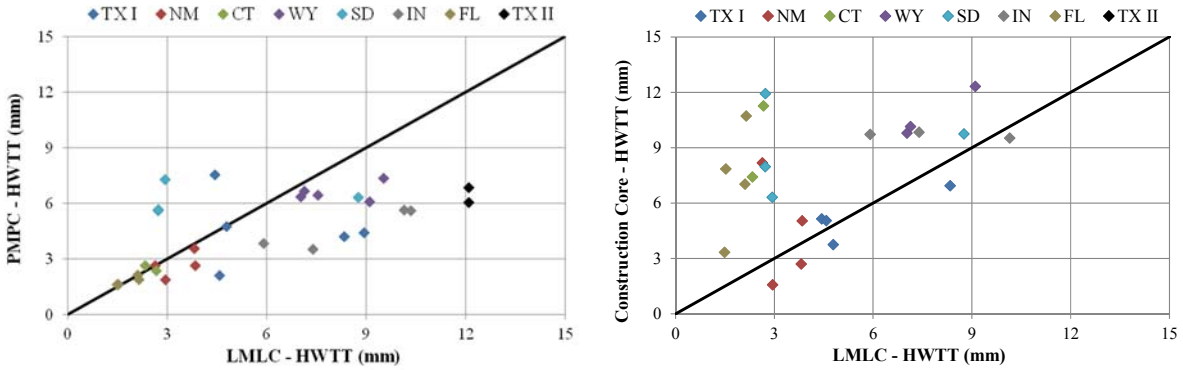

(a) (b)

FIGURE 5 HWTT rut depth correlation: (*a*) LMLC versus PMPC specimens and (*b*) LMLC versus cores at construction.

In summary, based on to the M_R and E* test results, good correlations in mixture stiffness between LMLC specimens with the selected laboratory STOA protocols and PMPC specimens and cores at construction were obtained for a wide range of asphalt mixtures from nine field sites. In addition, an approximately equivalent rutting resistance was observed for LMLC specimens and PMPC specimens in terms of HWTT rut depths at 5,000 load cycles. A higher rutting susceptibility in the HWTT was shown for cores at construction when compared to corresponding LMLC specimens, which was possibly caused by the need to plaster the cores to fit the height of the HWTT molds. Thus, the simulation of asphalt aging during plant production and construction by the laboratory STOA protocols of 2 h at 135°C for HMA and 116°C for WMA was verified in this project and considered appropriate for a wide range of asphalt mixtures.

CORRELATION TO FIELD AGING

The objective of the second part of the project was to develop a correlation between field aging (i.e., 1 to 2 years after construction) and laboratory LTOA protocols that could accommodate various mixture components and production parameters. The two LTOA protocols evaluated were 5 days at 185°F (85°C) per AASHTO R 30 and 2 weeks at 140°F (60°C), both applied to compacted specimens. The modeling of LTOA of asphalt mixtures is more challenging as the number of variables affecting the degree of aging increases. For instance, mixture parameters such as total AV, the interconnectivity of AV, asphalt binder film thickness (FT), and asphalt source interact in complex ways with the field in-service temperature and time (Kemp and Predoehl 1981; Kari 1982; Rolt 2000; Farrar et al 2013).

Previous literature indicated that pavement in-service time at the time of coring was commonly used to quantify field aging of asphalt mixtures. However, this approach failed to differentiate field sites with different construction dates and climates. To address this shortcoming, the cumulative degree days (CDD) was used as a field aging metric in this project. As expressed in Equation 1, the CDD is calculated as the sum of the daily high temperature above freezing for all the days being considered from the time of construction to the time of core sampling. As compared to the parameter of pavement in-service time, the CDD allowed the analysis to account for both pavement temperature (i.e., climate) and time.

$$CDD = \begin{Bmatrix} \sum (T_{d\max} - 32), & \text{if } T_{dmax} \geq 32 \\ 0, & \text{if } T_{dmax} < 32 \end{Bmatrix} \quad (1)$$

where:

$T_{d\max}$ = daily max. temperature, °F.

Figure 6 presents the CDD values for seven out of nine field sites shown in Figure 1, obtained from weather stations near the construction sites, with data points highlighted in black representing the time when field cores were sampled. The Connecticut and Texas II field sites were not included in this part of the project because no post-construction cores were obtained due to the traffic concerns of the agency or time constraints of the project. As illustrated in Figure 6, the CDD values were noticeably different for various field sites and therefore, were able to provide a distinct indication of the individual climatic characteristics. Specially, the average secant slopes of the curves for Texas, New Mexico, and Florida field sites were significantly steeper than those located in colder climate zones, like Wyoming, South Dakota, Iowa, and Indiana, due to differences in ambient temperatures. Thus, based on the CDD concept, mixtures placed in two different climates could be expected to age differently over the same period.

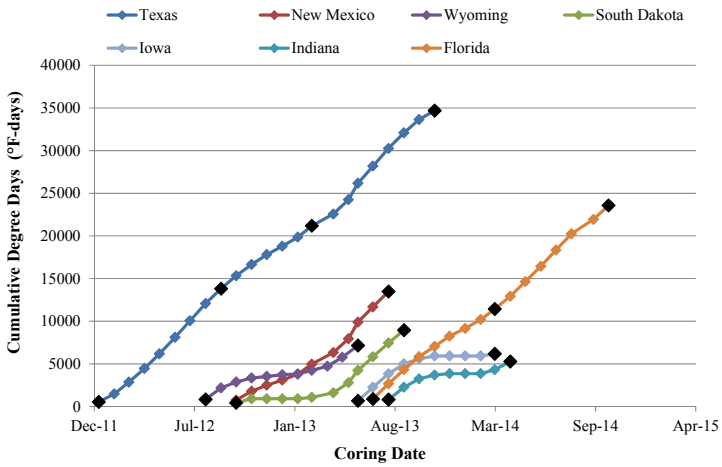

FIGURE 6 CDD curves for various field sites.

To illustrate the effect of field aging on mixture stiffness, a parameter termed M_R ratio was proposed, which is defined as the fraction of M_R stiffness of either field or laboratory aged specimens over that of unaged specimens. The aged specimens referred to LMLC specimens with STOA plus LTOA protocols and field cores obtained 1 to 2 years after construction, and the unaged specimens corresponded to LMLC specimens with STOA protocol only and field cores obtained immediately after construction. Considering that M_R stiffness proved to be effective in quantifying asphalt aging, mixtures with a higher M_R ratio were considered more sensitive to aging and more likely to exhibit an increase in mixture stiffness with time.

Figure 7 presents the plot of the CDD values for post-construction cores obtained from seven field sites versus their associated M_R ratio values. The data points represent the average M_R ratio values for each field site, and the curve represents an exponential function expressed in Equation 2. As illustrated, aging was more severe early in the pavement life, as indicated by the initial increase in M_R ratio values, but the rate of aging decreased with time.

$$M_R\,Ratio = 1 + \alpha * e^{\left[-\left(\frac{\beta}{CDD}\right)^{\gamma}\right]} \tag{2}$$

where

CDD = cumulative degree days for cores after specific in-service times; and
α, β, and γ = fitting coefficients.

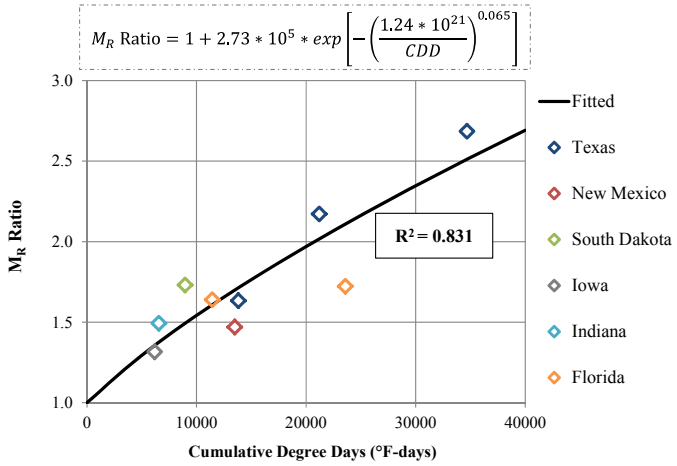

FIGURE 7 M_R ratio versus CDD values for post-construction cores.

According to the results previously described, the selected laboratory STOA protocols of 2 h at 275°F (135°C) for HMA and 240°F (116°C) for WMA were representative of PMPC specimens and cores at construction in terms of mixture volumetrics, stiffness, and rutting resistance. Therefore, the correlation between field aging and laboratory LTOA protocols could be identified based on the M_R ratio results of laboratory and field aged specimens. Figure 8 presents the M_R ratio results for the two laboratory LTOA protocols evaluated in this project. The average M_R ratio values for the LTOA protocols on compacted specimens of 2 weeks at 140°F (60°C) and 5 days at 185°F (85°C) were approximately 1.48 and 1.78, respectively. The higher M_R ratio value observed for the 5-day protocol indicated the aging of asphalt mixtures was more sensitive to temperature than time.

In order to identify the correlation of field aging with laboratory LTOA protocols, the average M_R ratio values for long-term aged LMLC specimens were plotted as markers by crossing the exponential curve determined by Equation 2, as shown in Figure 9. The vertical and horizontal error bars represent one standard deviation from the average M_R ratio values and their corresponding CDD values for the post-construction cores. As illustrated, the laboratory LTOA protocol of 2 weeks at 140°F (60°C) was able to produce mixture aging equivalent to an average of 9,100 CDD values, and the other protocol of 5 days at 185°F (85°C) per AASHTO R 30 produced mixture aging similar to approximately 16,000 CDD values. A similar analysis was also performed using the HWTT results, and correlations of approximately 10,000 and 19,000 CDD values were obtained for the 2-week and 5-day protocols, respectively.

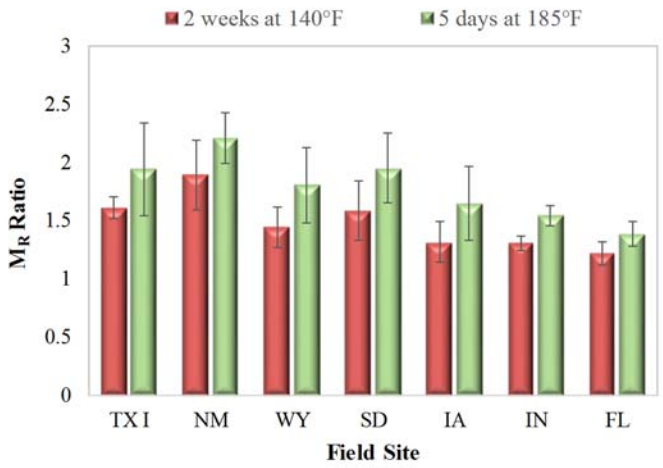

FIGURE 8 M_R ratio results for long-term aged LMLC specimens.

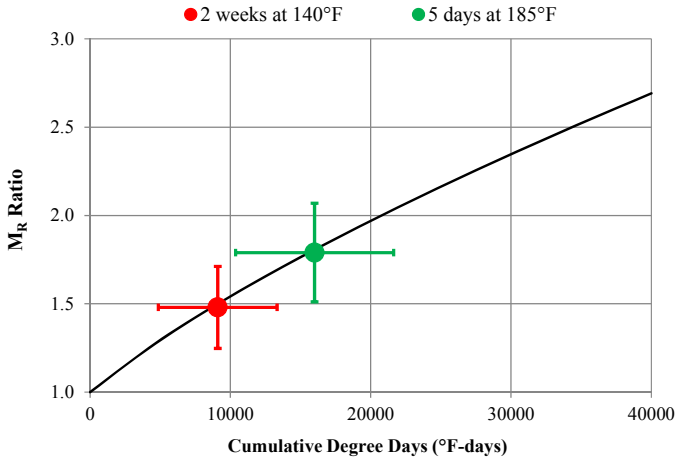

FIGURE 9 M_R ratio correlation between field aging and laboratory LTOA protocols.

Based on the M_R and HWTT results obtained in this project, the two LTOA protocols of 2 weeks at 140°F (60°C) and 5 days at 185°F (85°C) were representative of field aging of approximately 9,600 and 17,500 CDD values, respectively. These two critical CDD values were the average of those determined based on M_R stiffness and HWTT rutting resistance results. Using the information shown in Figure 6, the pavement in-service time for each field site corresponding to the critical CDD values was determined, as summarized in Table 1. The protocol of 2 weeks at 140°F (60°C) was equivalent to approximately 7 months in-service in warmer climates and 12 months in-service in colder climates. As for the 5-day protocol at 185°F (85°C), it was representative of field aging of approximately 12 months and 23 months in-service for warmer climates and colder climates, respectively. Therefore, the LTOA protocol specified in AASHTO R 30 was not sufficient to simulate field aging of 7 to 10 years after production and construction as originally suggested in the Strategic Highway Research Program (SHRP) (Bell et al. 1994).

TABLE 1 Correlation of Pavement In-Service Time with Laboratory LTOA Protocols

Field Project	Climate	2 weeks at 140°F (60°C)	5 days at 185°F (85°C)
Texas	Warmer climate	6 months	11 months
New Mexico		8 months	14 months
Florida		7 months	12 months
Average		**7 months**	**12 months**
Wyoming	Colder climate	12 months	23 months
South Dakota		12 months	23 months
Iowa		12 months	23 months
Indiana		11 months	22 months*
Average		**12 months**	**23 months**

FACTORS AFFECTING MIXTURE AGING

The last part of the project focused on identifying mixture components and production parameters with significant effects on the performance of short-term and long-term aged asphalt mixtures. M_R stiffness and M_R ratio results were the parameters used to discriminate mixtures with different short-term and long-term aging characteristics, respectively. For example, those with higher initial M_R stiffness values after STOA and higher M_R ratio values after LTOA were expected to be more sensitive to aging than those with lower values. Mixture stiffness results for the variable mixture were plotted against those for the control mixture for each of the following factors: WMA technology, production temperature, plant type, inclusion of recycled materials, aggregate asphalt absorption, and binder source. Based on the distribution of the data points relative to the line of equality, the effect of those factors on the aging characteristics of asphalt mixtures was identified, as illustrated in Figure 10. Table 2 provides a summary of the factor analysis results obtained; more detailed information can be found in NCHRP Report 815 (Newcomb et al. 2015).

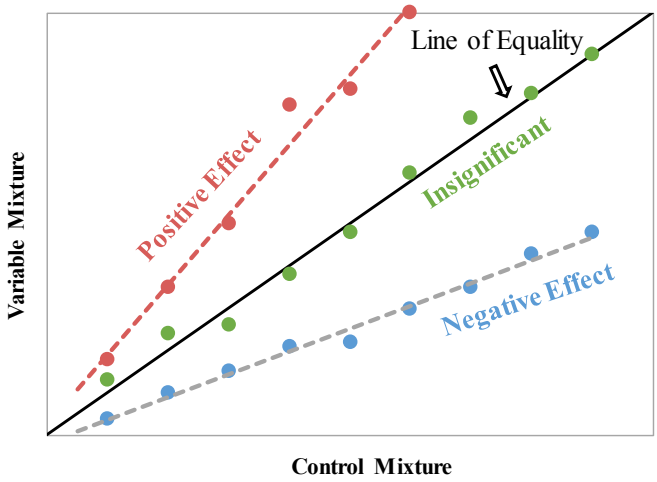

FIGURE 10 Identification of factors with significant effects on aging characteristics.

TABLE 2 Aging Factor Analysis Summary

Factors	Significant Effect on Aging?	
	Short-Term	Long-Term
WMA technology (WMA versus HMA)	Yes (lower stiffness)	Yes (faster aging)
Recycled materials (RAP/RAS versus control)	Yes (higher stiffness)	Yes (slower aging)
Aggregate asphalt absorption (High versus low abs.)	Yes (lower stiffness)	Yes (faster aging)
Binder source	Yes (same PG ≠ same properties)	N/A
Production temperature	No	No
Plant type	No	No

As illustrated in Table 2, among the factors evaluated in this project, WMA technology, recycled materials, aggregate asphalt absorption, and binder source showed a significant effect on the aging characteristics of asphalt mixtures, while the effect from production temperature (i.e., 30°F difference) and plant type was insignificant. A brief discussion of the significant factors follows.

- WMA technology showed a significant effect on both short-term and long-term aging characteristics of asphalt mixtures. Lower mixture stiffness was observed for the short-term aged WMA mixtures as compared to their control HMA counterparts, possibly due to the reduced production temperature. However, the majority of the WMA mixtures evaluated in this project showed a faster aging rate, and their stiffness eventually was expected to equal that of HMA after approximately 17 months in warmer climates and 29 months in colder climates.
- The inclusion of recycled materials also had a significant effect on the aging characteristics of asphalt mixtures. Those with recycled materials, often using softer virgin binders, had higher initial stiffness but showed a slower rate of stiffness increase with aging than the control mixtures without recycled materials. The greater sensitivity to aging by the control mixtures was attributed to the larger amount of virgin binders in the mixtures, which had higher oxygen diffusivity and were more susceptible to aging than the recycled binders.
- Aggregate asphalt absorption, specifically the effective binder content in the mixture, showed a significant effect on the aging characteristics. The short-term aged mixtures using high absorptive aggregates exhibited lower stiffness and decreased rutting resistance than their counterpart mixtures using low absorptive aggregates, which was attributed to the thicker effective FT from volumetric compensation during the mix design process. However, the difference in mixture properties between the two mixtures reduced with field aging, due to the higher volume of effective binders in the high aggregate asphalt absorption mixtures that was available for aging.
- Binder source had a significant effect on the short-term aging characteristics of asphalt mixtures, while its effect on the long-term aging characteristics was not studied. Different mixture performance in terms of stiffness and rutting resistance should be expected from asphalt mixtures using the same PG-graded binders from different sources.

SUMMARY

In summary, this project was successful in validating the proposed STOA protocols of 2 h at 275°F (135°C) and 240°F (116°C) for preparing HMA and WMA mixtures, respectively, in the laboratory that were comparable to those produced at the asphalt plant. Desirable correlations between LMLC specimens versus PMPC specimens and field cores at construction in terms of mixture volumetric, stiffness, and rutting resistance were achieved by asphalt mixtures with a wide range of mixture components and production parameters. In addition, the CDD concept was proposed as a novel metric to quantify field aging of asphalt mixtures, which was able to account for the differences in construction dates and climates for various field sites. Research efforts were also devoted to identify the correlation of field aging with laboratory LTOA protocols based on mixture property ratio results. The two protocols of 2 weeks at 140°F (60°C) and 5 days at 185°F (85°C) were representative of field aging at approximately 9,600 and 17,500 CDD values, respectively. Field aging at 9,600 CDD values was equivalent to approximately 7 months in-service in warmer climates and 12 months in-service in colder climates. As for the field aging at 17,500 CDD values, approximately 12 and 23 months in-service were required for warmer climates and colder climates, respectively. Finally, the effects of various factors in terms of mixture components and production parameters on the aging characteristics of asphalt mixtures were identified. WMA technology, recycled materials, aggregate asphalt absorption, and binder source showed a significant effect; while the effect from production temperature and plant type was insignificant. For future research, a follow-up study has been proposed to monitor the longer-term performance of the asphalt mixtures included in NCHRP Project 09-52 and to validate or refine the long-term aging model based on CDD and mixture property ratios.

REFERENCES

Bell, C. A., A. J. Wieder, and M. J. Fellin. Laboratory Aging of Asphalt-Aggregate Mixtures: Field Validation. SHRP-A-390, 1994.

Epps Martin, A., E. Arambula, F. Yin, L. Garcia Cucalon, A. Chowdhury, R. Lytton, J. Epps, C. Estakhri, and E. S. Park. *NCHRP Report 763: Evaluation of the Moisture Susceptibility of WMA Technologies*, 2014.

Farrar, M. J., T. F. Turner, J. Planche, J. F. Schabron, and P. M. Harnsberger. Evolution of the Crossover Modulus with Oxidative Aging. *Transportation Research Record: Journal of the Transportation Research Board*, *No. 2370*, 2013, pp. 76–83. https://doi.org/10.3141/2370-10.

Kari, W. J. Effect of Construction Practices on the Asphalt Properties in the Mix. *Proceedings of the Annual Conference of Canadian Technical Asphalt Association*, Vol. 27, 1982, pp. 310–334.

Kemp, G. R., and P. H. Predoehl. A Comparison of Field and Laboratory Environments on Asphalt Durability. *Association of Asphalt Paving Technologists*, Vol. 50, 1981, pp. 492–537.

Newcomb, D., A. Epps Martin, F. Yin, E. Arambula, E. Sug Park, A. Chowdhury, R. Brown, C. Rodezno, N. Tran, E. Coleri, D. Jones, J. T. Harvey, and J. M. Signore. *NCHRP Report 815*: *Short-Term Laboratory Conditioning of Asphalt Mixtures*, 2015. https://doi.org/10.17226/22077.

Rolt, J. (2000) "Top-Down Cracking: Myth or Reality?" *The World Bank Regional Seminar on Innovative Road Rehabilitation and Recycling Technologies*, Amman, Jordan.

Yin, F., L. Garcia Cucalon, A. Epps Martin, E. Arambula, A. Chowdhury, and E. S. Park. Laboratory Conditioning Protocols for Warm-Mix Asphalt. *Electronic Journal of the Association of Asphalt Paving Technologists*, Vol. 82, 2013, pp. 177–212.

Zhang, Y., R. Luo, and R. Lytton. Microstructure-Based Inherent Anisotropy of Asphalt Mixtures. *Journal of Materials in Civil Engineering*, Vol. 23, No. 10, 2011, pp. 1473–1482. https://doi.org/10.1061/(ASCE)MT.1943-5533.0000325.

Characterization of Pavement Performance Based on Field Validation Test Site Data Interpreted by an Asphalt Composition Model of Binder Oxidation

ADAM T. PAULI
MIKE FARRAR
SHIN-CHI HUANG
Western Research Institute

INTRODUCTION

It is now well documented that a major contributing factor to pavement distress cracking in asphalt pavements is asphalt binder deterioration by oxidation (Kandhal and Chakaraborty 1996; Kandhal et al. 1998). Petersen et al. (1994) promoted the concept that asphalt microstructure, which is assumed to be a three-dimensional association of polar constituents variously distributed in a less polar liquid phase, is directly influenced by oxidation of the asphalt binder. Microstructuring in asphalt, which leads to pavement embrittlement, occurs at various length scales ranging from nano- to microscale. Oxidation of asphalt binder therefore leads to age hardening of the binder via microstructuring, and thus directly contributes to the embrittlement and eventual failure of pavements (Petersen and Harnsberger 1998, 1996; Petersen 1984, 1975).

Over the past 20 years several studies have been reported which relate laboratory aging of asphalt binder with field aged asphalt pavements with respect to material property testing of the binder, mix, and pavement cores to access pavement performance (Button et al. 1996; Soleimani et al. 2009; Hesp et al. 2009; Wright et al. 2011; Jin et al. 2013; Gu et al. 2015; McGovern et al. 2016; Menapace et al. 2016; Rose et al. 2016; Li et al. 2016).

One of the earliest of these reports by Button et al. (1996) discusses a set of test pavements constructed throughout the state of Texas (e.g., Texarkana, Sherman, San Benito, and Ft. Worth) to evaluate a variety of asphalt binders modified with different additives in both a laboratory and field setting to access the influence of the additives on pavement cracking and rutting. Additive types included in this study ranged from a selection polymers (e.g., latex–EVA, latex–styrene-butadiene-styrene (SBS), finely dispersed polyethylene, and vulcanized SBS) to either a manganese or carbon black complex prepared in base oil derived from one of five asphalt sources where the base asphalts were either AC-10 or AC-20 penetration grade. Laboratory testing reported in the Button et al. (1996) study included viscosity and penetration, DSR, BBR, DTT, indirect tension and resilient modulus testing, GPC, FTIR, and asphaltene precipitation by heptane analyses of unaged and artificially accelerated aged materials and binder material extracted from test pavement field cores. One finding in particular stands out in this report where it was observed that the loss tangent correlated quite well with longitudinal cracking.

Several years later Soleimani et al. (2009) reported on the utilization of the loss tangent as a "surrogate performance indicator for the control of thermal cracking." In this study the authors report on the testing and performance evaluation of some 20 different contract pavement sites constructed in Ontario, Canada, where BBR and DSR analyses were performed on recovered binder materials. It was specifically noted in these studies that longer isothermal conditioning times were needed, and subsequently performed on binder materials, than that

normally recommended for by current specifications for DSR and BBR analyses. Thus, cracking distress was found to correlate well, among the test protocols, including DSR-derived loss tangent for this large set of materials.

OXIDATION KINETICS OF ASPHALT BINDER COLLOIDAL SUSPENSIONS

A phenomenological approach recently proposed by Pauli and Huang (2013), forgoes the investigation of carbonyl production to study asphalt binder microstructure composition, brought about by oxidation, to investigate changes in rheological behavior. The rate of change in the flow property of age hardened binders, commonly quantified by the change in dynamic viscosity as a function of aging time, $d\eta(t,T)/dt_{age}$, is shown to directly relate to the production of new polar species, predominately carbonyls. These "new" polar species, which fractionate by chromatographic methods with unoxidized asphaltenes, may be thought to constitute "new" asphaltene material with the corresponding consumption of free solvent

$$\phi_{fs} \equiv \left(1 - K\chi_A\right) \tag{1}$$

given the asphaltene mass fraction χ_A, and solvation factor K. Here the free solvent is directly associated with maltenes, which themselves are composed of saturates, naphthenic aromatic and polar aromatic (resin) "SARA" fractions.

A phenomenological rate law has been proposed by Pauli and Huang (2013) which constitutes the general microstructural component reaction,

$$\chi_m^0 + \chi_a^0 + O_2 \xrightarrow{k} \chi_m^- + \chi_a^0 + \chi_a^+ \tag{2}$$

The kinetics rate of change is then defined in terms of the dynamic viscosity, derived from the Pal-Rhodes equation (Pauli 2014), raised to the exponent $-1/[\eta]$ where $[\eta] = 2/5$,

$$\eta^{-1/[\eta]} = \eta_0^{-1/[\eta]}\phi_{fs} = \eta_0^{-1/[\eta]}\left(1 - K\chi_A\right) \tag{3}$$

given $\chi_m^0 + \chi_a^0 = \chi_m^- + \chi_a^0 + \chi_a^+ = 1$, and assuming $d(\chi_a^0)/dt_{age} = d(\eta_0^{-0.4})/dt_{age} = 0$, thus,

$$\begin{aligned}
&\frac{d}{dt_{age}}\left(\eta^{-1/[\eta]}\right) \\
&= \frac{d}{dt_{age}}\left(\eta_0^{-1/[\eta]}\phi_{fs}\right) \\
&= \frac{d}{dt_{age}}\left\{\left(\eta_0^{-1/[\eta]}\right)(1 - K\chi_a^0)\right\} \\
&= \eta_0^{-1/[\eta]}\left[K[t_{age}]\frac{d(\chi_a^+[t_{age}])}{dt_{age}} + \chi_a^+\frac{d(K[t_{age}])}{dt_{age}} + \chi_a^0\frac{d(K[t_{age}])}{dt_{age}}\right] \\
&= \eta_0^{-1/[\eta]}\left[K[t_{age}]\frac{d(\chi_a^+[t_{age}])}{dt_{age}} + \left(\chi_a^+ + \chi_a^0\right)\frac{d(K[t_{age}])}{dt_{age}}\right]
\end{aligned} \tag{4}$$

Here χ_m^0 and χ_a^0 represent initial compositional classes of maltene and asphaltene mass fractions, respectively, and χ_m^- and χ_a^+ represent mass fractions of remaining maltene and "new" asphaltene material, respectively, after reaction with oxygen for a given amount of aging time t_{age} at temperature *T*.

Assuming first-order kinetics as proposed by Petersen and Harnsberger (1998, 1996), the concentration in newly formed asphaltenes, as defined by the mass fraction χ_a^+, can be expressed by

$$\chi_a^+[t_{age},T] = \chi_m^0(1-e^{-kt}) = (1-\chi_a^0)(1-e^{-kt}) \tag{5}$$

Drawing on expressions 3 to 5, the phenomenological rate expression for the change in asphalt viscosity with aging time is thus expressed by

$$\begin{aligned} r &= \frac{d}{dt_{age}}\left(\eta^{-1/[\eta]}\right) = \chi_m^0\eta_0^{-1/[\eta]}\left[\left((1-e^{-k(T)t})+\chi_a^0\right)\frac{d(K[t_{age}])}{dt_{age}} - K[t_{age}]ke^{-k(T)t}\right] \\ &= \chi_a^0\chi_m^0\eta_0^{-1/[\eta]}\frac{d(K[t_{age}])}{dt_{age}} - \chi_m^0\eta_0^{-1/[\eta]}K[t_{age}]ke^{-k(T)t} + \chi_m^0\eta_0^{-1/[\eta]}\frac{d(K[t_{age}])}{dt_{age}}(1-e^{-k(T)t}) \end{aligned} \tag{6}$$

A solvation factor is thus defined as a function of aging time $K[t_{age}]$, while the rate constant $k(T)$, is defined as a function of temperature.

THERMO-RHEOLOGICAL BEHAVIOR OF ASPHALT BINDER MODELED AS A COLLOIDAL SUSPENSION

Studies reported in Pauli (2014) consider dynamic shear rheology measurements of "low" shear rate (0.1 rad/s) viscosities of asphalts and n-heptane soluble maltenes as inputs to the Pal-Rhodes model to develop correlations relating flow properties of asphalts to compositional properties. Rheological and compositional properties determined for 20 SHRP asphalts, including dynamic viscosity of neat asphalt η (Pa*s, @ T = 25°C, ω = 0.1 rad/s), dynamic viscosity of n-heptane soluble maltenes η_{nC_7} (Pa*s, @ 25°C, ω = 0.1 rad/s), mass fractions of isooctane insoluble asphaltenes χ_{isoC_8}, the mass fractions of SEC-I (size-exclusion chromatography) material χ_{SECI}, and rheological phase angles **d** (@ 25°C, 0.1 rad/s). Plots of $\left(\eta/\eta_{nC_7}\right)^{-1/[\eta]}$ as a function of $\phi_{fs} \equiv (1 - K\chi_{isoC_8})$,

$$\left(\eta/\eta_{nC_7}\right)^{-1/2.5} = 1 - K\chi_{isoC_8} \tag{7}$$

determined for these 20 SHRP asphalts, given the mass fractions of isooctane insoluble asphaltenes χ_{isoC_8} and [η] = 2.5 resulted in linear functions where the slope of the line

corresponded to a solvation constant, *K*, determined to be 3.3 for $\eta_r \to 1$ as $\chi_{isoC_8} \to 0$, given the following conditions for *K*,

$$K = \begin{cases} 3.3, & \chi \approx < 0.25 \\ < 3.3, & \chi \approx > 0.25 \end{cases} \tag{8}$$

This correlation was found to be self-consistent suggesting that at $\chi_{isoC_8} = 0$, $\eta = \eta_0$. Here $K = 3.3$ represents a limit of maximum asphaltene mass fraction as $\chi_{isoC_8} \le 0.303$. This model requires that *K* be an adjustable parameter at higher concentrations as well as being a function of temperature and strain rate.

Similar correlations exist for viscoelastic variables when compared among asphalts derived from different crude sources, where $\left(\eta/\eta_{nC_7}\right)^{-1/[\eta]}$ is a measure of the elastic-to-viscous character. The phase angle, for example, derived from the complex modulus $\mathbf{G}^*(\omega)$

$$\omega\eta^*(\omega) = \mathbf{G}^*(\omega) \tag{9}$$

is a function of the loss (viscous) modulus **G"**, and storage (elastic) modulus **G'**, where, based on oscillatory measurements of viscoelasticity,

$$\mathbf{G}^*(\omega) = \mathbf{G}'(\omega) + i\mathbf{G}''(\omega) \tag{10}$$

The rheological phase angle is then defined as the inverse tangent of the ratio of the loss (viscous) modulus **G"**, to the storage (elastic) modulus **G'**,

$$\boldsymbol{\delta} = \tan^{-1}\left(\mathbf{G}''/\mathbf{G}'\right) \tag{11}$$

Given that asphalt fractions, e.g., solubility defined asphaltenes and maltenes, represent phases of a colloidal suspension, alternative material phases generated by other material property specific separation schemes could also represent continuous and associated phases in asphalt. Thus, asphalt has been separated based on molecular mass or size employing SEC (Branthaver et al. 1993). Here, the pore size distribution of a SEC stationary phase column packing determines retention times of retained materials as a function of molecular weight. With this technique, an asphalt solution introduced onto a column packed with the stationary phase material "retains" molecular species based on molecular size, thus constituting an alternative method of defining of suspended colloidal phase materials. Plots of the phase angle $\boldsymbol{\delta}$ (@ 25°C, 0.1 rad/s), are thus found to correlate with both iso-octane insoluble asphaltene mass fractions χ_{isoC_8}, and SEC-I mass fractions χ_{SEC-I} determined for the 20 SHRP asphalts [Robertson *et al*. 2001]. These correlations are expressed by

$$\boldsymbol{\delta}/\left(\boldsymbol{\delta}_0 = 90°\right) \approx 1 - \chi_{SEC-I} \approx 1 - \chi_{isoC_8} \tag{12}$$

where $\boldsymbol{\delta} \to (\boldsymbol{\delta}_0 = 90°)$ and where $\chi_{SEC-1} \to 1$ as $\boldsymbol{\delta} \to 0$.

By showing the relationship between phase angle and colloidal dispersed phases, e.g., asphaltenes or SEC fractions, it has been hypothesized that the concentration of newly formed asphaltenes can be related to a phase angle function $\boldsymbol{\delta}(T, t_{age})$ that is dependent on temperature and aging time. A dynamic suspended phase mass fraction $\left[\chi^*(T, t_{age})\right]_{T_{age},\omega}$ can thus be defined by

$$\left[\chi^*(T, t_{age})\right]_{T_{age},\omega} \equiv \left[1 - \left(\boldsymbol{\delta}(T, t_{age})/\boldsymbol{\delta}_0\right)\right] \tag{13}$$

which in turn may be related to the rheological phase angle by

$$\boldsymbol{\delta}\left(T, t_{age}\right) = \boldsymbol{\delta}_0\left(1 - \chi_a^+\left(T, t_{age}\right)\right) = \boldsymbol{\delta}_0\left[1 - \chi_m^0(1 - e^{-kt})\right] \tag{14}$$

with all variables being defined above.

EXPERIMENTAL

Data Mining of Field Validation Test Site Field Performance Date

Western Research Institute (WRI) with the support and assistance of the FHWA Turner-Fairbank Highway Research Center, beginning in 1999, constructed and monitored nine field test sites in the United States and Canada. In 2012 the National Center for Asphalt Technology (NCAT) joined the Asphalt Research Consortium (ARC) team and took the lead in constructing six field

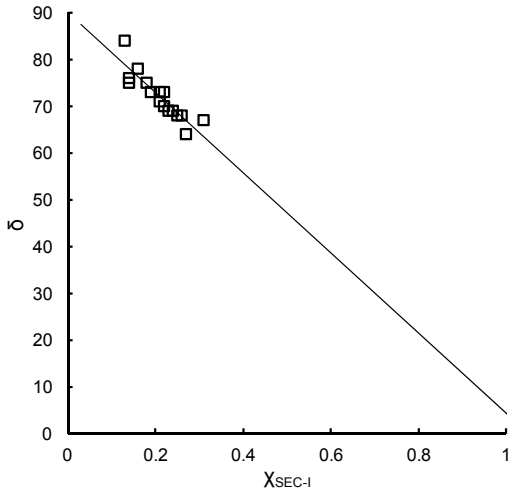

FIGURE 1 DSR determined phase angle δ (25°C, 0.1 rad/s) plotted as a function of SEC-I mass fraction χ_{SEC-I} determined for 20 SHRP asphalts by preparative size exclusion liquid chromatography.

validation test sites: five in 2012 and one in 2013. The first four field test sites, constructed between 1999 and 2002, were initially designed to support and evaluate the SHRP PG asphalt binder system. These sites were referred to as "comparative" test sites since on a particular project all the test sections were constructed with the same PG asphalt and the only variable between test sections was the source of the asphalt.

In 2007 these four sites, along with two other sites constructed by WRI in 2006 and 2007 were absorbed into the ARC. The sites constructed in 2006 and 2007 were designed to not only support the PG asphalt binder system, but also to validate existing and new technologies such as WMA, RAP mix design innovation, the *Mechanistic Empirical Pavement Design Guide* (MEPDG), and FP III and ARC products. Since 2007 the sites have been more commonly referred to as "validation" sites rather than "comparative" test sites. In 2009 and 2010, two additional sites were constructed in Manitoba and a final site near Phoenix, Arizona, in 2013.

In studies that followed, field performance data and corresponding rheology and compositional (physico-chemical) data derived for binder and core samples taken from the Arizona US-93 validation site were data mined to develop correlations for the purpose of understanding the nature of binder oxidation and its impact on pavement cracking performance. One of the prime objectives of the validations sites, was just as the name implies, to validate predictive theories, models and test methodology developed throughout the course of ARC. Thus, a description and purpose of this validation site is presented in the next section.

Description and Purpose of the Validation Site

With regard to the investigation of oxidation propensities in asphalt pavements, the Arizona US 93 validation site continues to provide invaluable data, and thus provides great insights into this mode of pavement distress. The Arizona US-93 validation site is roughly 50 mi north of Wickenburg and begins at about milepost 153. During construction of the test sites in 2001, two 2½-in. lifts of dense-graded asphalt pavement (19-mm NMAS, PG 76 – 16) were placed over a granular base, followed by a ¾-in. lift of a rubber-modified asphalt friction course. The friction course was only placed in the driving and passing lanes, not the shoulders (Figure 2).

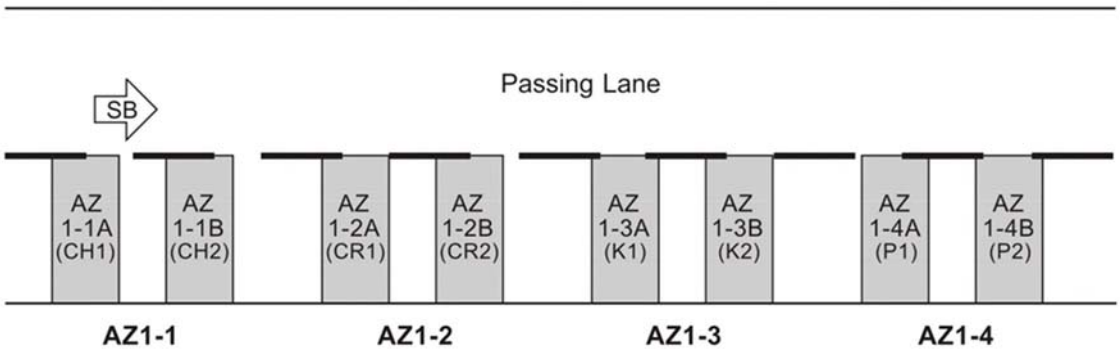

FIGURE 2 FHWA–ARC–WRI US-93 Arizona validation site layout [WRI-3] (constructed 2001). The Arizona US-93 validation site is roughly 50 mi north of Wickenburg and begins at about milepost 153. Constructed as two 2½-in. lifts of dense-graded asphalt pavement (19-mm NMAS, PG 76–16) placed over a granular base, followed by a ¾-in. lift of a rubber-modified asphalt friction course. The friction course was only placed in the driving and passing lanes, but not the shoulders.

As one of the first four field test sites constructed by WRI, this site was designed specifically to support and evaluate the SHRP PG asphalt binder system. At this site all test sections were constructed with the same PG asphalt with the only variable between test sections being the source of the asphalt. During the years following construction, the dominate distress has been transverse and longitudinal cracking.

Mechanical Testing

The following sets of bullets characterize the types of testing protocols conducted over the past 20 years with respect specifically to the Arizona US-93 validation site:

- Unaged, RTFO, RTFO/pressure aging vessel (PAV) (SHRP: $G^*/\sin\delta$; $G^* \sin\delta$; *m*-value; creep stiffness; DSR frequency sweeps –30°C to 70°C); strain sweeps to 20% at intermediate temperature).
- Recovered binder from loose mix (SHRP: $G^*/\sin\delta$; $G^* \sin\delta$; *m*-value; creep stiffness; DSR frequency sweeps –30°C to 70°C; strain sweeps to 20% at intermediate temperature).
- Recovered binder from cores (SHRP: $G^*/\sin\delta$; $G^* \sin\delta$; *m*-value; creep stiffness; DSR frequency sweeps –30°C to 70°C; strain sweeps to 20% at intermediate temperature).
- Mix testing and compositional analysis [E*, indirect tensile test (IDT) creep and strength, fatigue and rut testing; aggregate gradation, AC content].

Chemical Testing (Binder)

- Mid-infrared spectroscopy (carbonyl and sulfoxide quantification with oxidation);
- Asphaltene/compatibility measurements;
- Differential scanning calorimetry; and
- Elemental analyses.

Pavement Distress Surveys

In strict accordance with the *Long-Term Pavement Performance* (LTPP) *Distress Identification Manual* (DIM), pavement distress surveys have been conducted every year 2002 through 2013.

Climatic Data

The closest weather station to the project is the Bagdad, Arizona, station about 10 mi from the project. In LTPPBind the station ID is AZ0586. The station elevation is 1,049 m. From the LTPPBind program the mean high air temperature is 38.4°C and the mean low temperature is –7.1°C (Table 1).

Pavement Distress Surveys

Formal distress surveys have been performed on all WRI test sites beginning the year after construction and continued on an annual basis. All pavement distress surveys were performed in strict accordance with the *Distress Identification Manual for the Long Term Pavement*

TABLE 1 GPS Coordinates Climatic Data (Note: the closest weather station to the project is the Bagdad, Arizona, station about 10 mi from the project. In LTPPBind the Station ID is AZ0586. The station elevation is 1,049 m. From the LTPPBind program the mean high air temperature is 38.4°C and the mean low temperature is –7.1°C.)

Site	Latitude, N (°)	Longitude, W (°)	Elevation (m)
AZ1-1A	34.4883	113.37866	875
AZ1-1B	34.48712	113.37569	896
AZ1-2A	34.4843	113.36678	929
AZ1-2B	34.48425	113.36303	926
AZ1-3A	34.48346	113.35761	935
AZ2-3B	34.48277	113.35303	-0-
AZ1-4A	34.48151	113.34593	972
AZ1-4B	34.48151	113.34593	972

Performance Program (2003) by Nichols Consulting Engineers (NCE) personnel with the assistance of WRI personnel. NCE is part of the LTPP program team, and the NCE pavement distress rater who performed the surveys was a certified DIM rater. Transverse profiling was performed with a Dipstick profiler at 15.25-m intervals.

Truck Loading

Traditional 18-kip equivalent single-axle loading (ESAL), or the new MEPDG truck axle load spectra, which are expressed by the number of load applications of various axle configurations (single, dual, tridem, and quad) within a given weight classification range, have not been compiled for any of the WRI test sites. However, the truck loading information is available from traffic studies performed by the respective DOTs.

Sample Collection

Samples of all construction materials were collected during the actual time of construction. Loose mix samples were collected either from the windrow in front of the paver or from the paver hopper. Asphalt samples were collected from the sample collection port of the hot-mix plant, generally when the state DOT was also collecting asphalt samples. Asphalt samples were collected when it was certain that a specific asphalt source was being used and not during any transition periods between sources.

On November 17, 2005, three cores from the south bound lane shoulder were collected from each of the sections. The cores were shipped to WRI in Laramie, Wyoming, and selected cores were sectioned as shown in Figure 3.

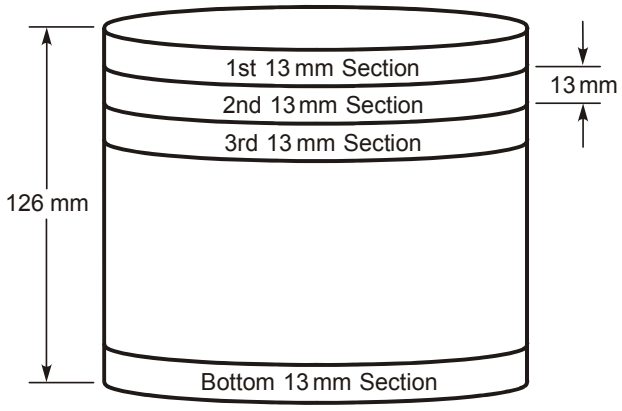

FIGURE 3 Sketch of sectioned field core.

RESULTS AND DISCUSSION

FHWA–ARC–WRI US-93 Arizona Validation Site Field Survey Results

Pavement distress survey data compiled from the US-93 Arizona validation site included transverse cracking of low and moderate severity, fatigue cracking of low severity, and longitudinal cracking/non-wheelpath of low, moderate, and high severity. Tables 2 through 7 report these pavement distress survey data over an 11-year life span. Figures 4, 7, and 10 correspondingly depict these data in line-marker plots. It can be noted immediately that cracking performance data varied, dramatically in some instances, specifically between sections constructed from the same binder. For example, comparisons made between AZ1-1A(CH1) and AZ1-1B(CH2) with respect to longitudinal and fatigue cracking differed substantially, as depicted in Figures 8 and 11. Longitudinal cracking/non-wheelpath, by comparison, was much more similar for the "duplicated" sections, as depicted in Figure 4. Figures 5, 8, and 11 help show these trends, or lack of trend. Figure 5, for example, depicts good correlation between transverse cracking: sum of low severity and moderate severity (total length, m), from two different sections, labeled A and B, constructed from the same binder source. Comparatively Figure 8 depicts an inversion correlation between fatigue cracking: low severity, (area, m^2) from two different sections, labeled A and B, constructed from the same binder source, whereas Figure 11 effectively shows` no correlation for longitudinal cracking/non-wheelpath: low, moderate and high severity, (total length, m), surveyed over an 11-year span, for two sections, labeled A and B, constructed from the same binder source.

Based on these observations it was thus decided that a statistical approach would be taken to report field survey data to evaluate performance by combining data for each of the two sections constructed from the same binder source. Figures 6, 9, and 12 therefore depict cumulative transverse, fatigue, and longitudinal cracking, respectively, surveyed over an 11-year span, summed for the two sections, labeled A and B, constructed from the same binder source. The final data used to compare to material test properties was represented as cumulative summed cracking (i.e., the sum of transverse, fatigue and longitudinal cracking), as depicted in Figure 13.

TABLE 2 Transverse Cracking: Sum of Low Severity and Moderate Severity (Total Length, m), Section A, Reported for an 11-Year Life Span

Year	AZ1-1	AZ1-2	AZ1-3	AZ1-4
2001	0	0	0	0
2002	0	0	0	0
2003	0	0	0	0
2004	0	0	0.3	0
2005	0	0	0	0
2006	1	0	0	0
2007	8	0.3	0	7.4
2008	17.1	3.5	0	54
2009	70.7	12.4	4.4	85.5
2010	87.4	31.8	11	108.4
2011	112.1	66.9	36.9	122.1
2012	135.4	114.1	75.4	147

TABLE 3 Transverse Cracking: Sum of Low Severity and Moderate Severity (Total Length, m), Section B, Reported for an 11-Year Life Span

Year	AZ1-1	AZ1-2	AZ1-3	AZ1-4
2001	0	0	0	0
2002	0	0	0	0
2003	0	0	0	0
2004	0	0	0	0
2005	0.7	0	0	0
2006	4.8	0	0	23.4
2007	10.3	0	0.9	60.6
2008	62.2	3.2	6.7	70.3
2009	86.4	7.5	17.4	99.9
2010	97.5	24.8	34.5	123.6
2011	118.2	47.3	39.3	126.6
2012	128.7	60.8	56.2	119.9

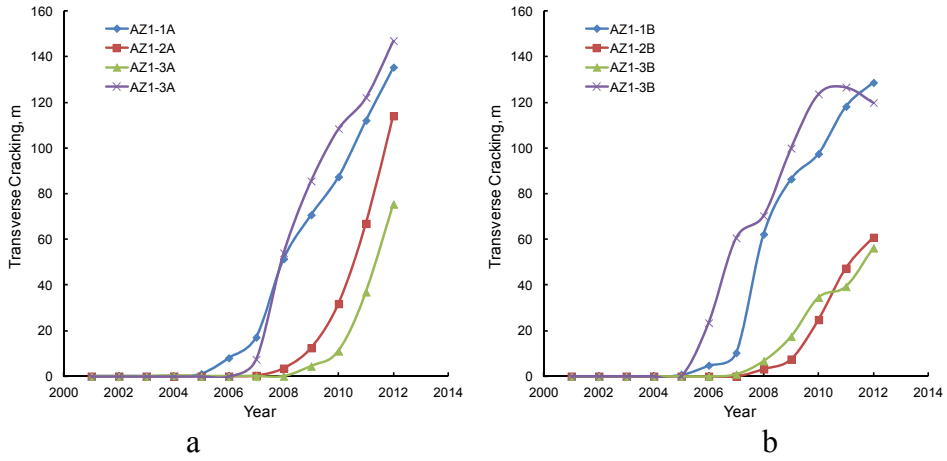

FIGURE 4 Transverse cracking: sum of low severity and moderate severity (total length, m) surveyed over an 11-year span, for two sections labeled A and B, each constructed from the same binder source.

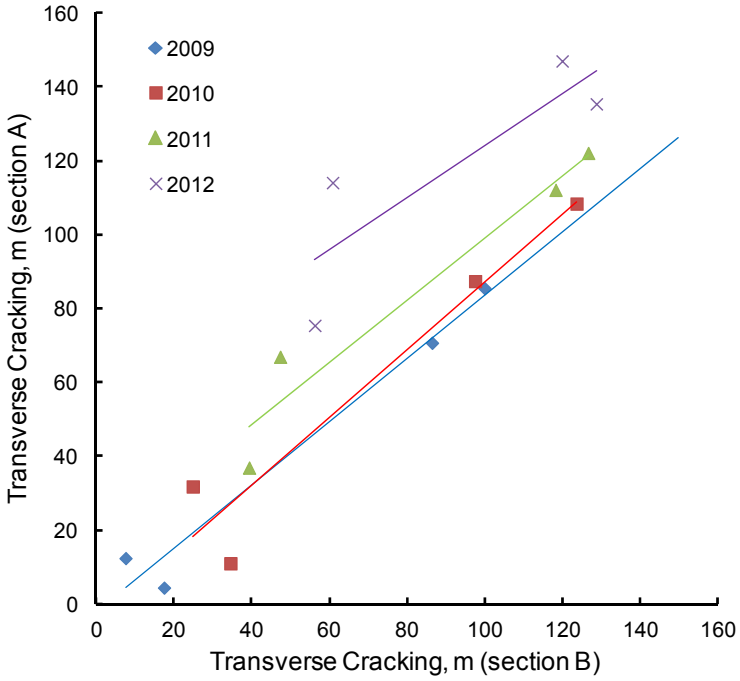

FIGURE 5 Correlation between transverse cracking: sum of low severity and moderate severity (total length, m), from two different sections, labeled A and B, constructed from the same binder source.

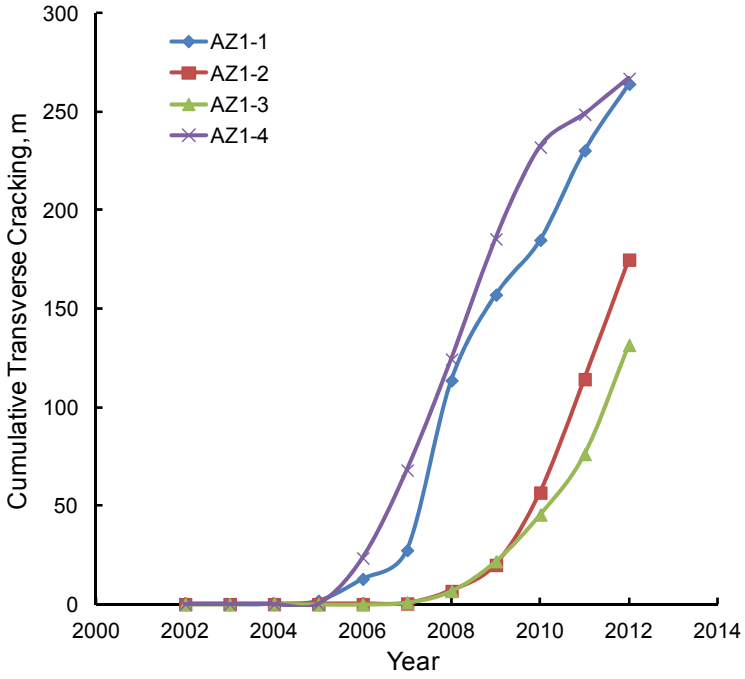

FIGURE 6 Cumulative transverse cracking: sum of low severity and moderate severity (total length, m), surveyed over an 11-year span, summed for two sections, labeled A and B, constructed from the same binder source.

TABLE 4 Fatigue Cracking: Low Severity, (Area, m^2), Section A, Reported for an 11-Year Life Span

Year	AZ1-1	AZ1-2	AZ1-3	AZ1-4
2001 (Y0)	0	0	0	0
2002	0	0	0	0
2003	0	0	0	0
2004	0	0	0	0
2005	0.4	0	0	0
2006	3.9	0	0	0.4
2007	3.7	0	0	0.8
2008	18.1	8.1	0.6	2.1
2009	11.5	8.9	3.1	2.7
2010	12.4	9	3.1	5.1
2011	13	10.2	3.2	5.5
2012 (Y11)	13.1	14.7	4.5	8.5

TABLE 5 Fatigue Cracking: Low Severity, (Area, m^2), Section B, Reported for an 11-Year Life Span

Year	AZ1-1	AZ1-2	AZ1-3	AZ1-4
2001	0	0	0	0
2002	0	0	0	0
2003	0	0	0	0
2004	0	0	0	0
2005	0	0.7	1.8	1
2006	0	3.3	14.5	28.1
2007	0	3.3	24.4	30.8
2008	1	7.5	31.6	33.6
2009	0.9	10.4	41.6	43.2
2010	0.9	10.8	64.1	52.3
2011	2.3	18.5	86.6	73.7
2012	2.6	20.9	124.8	123.7

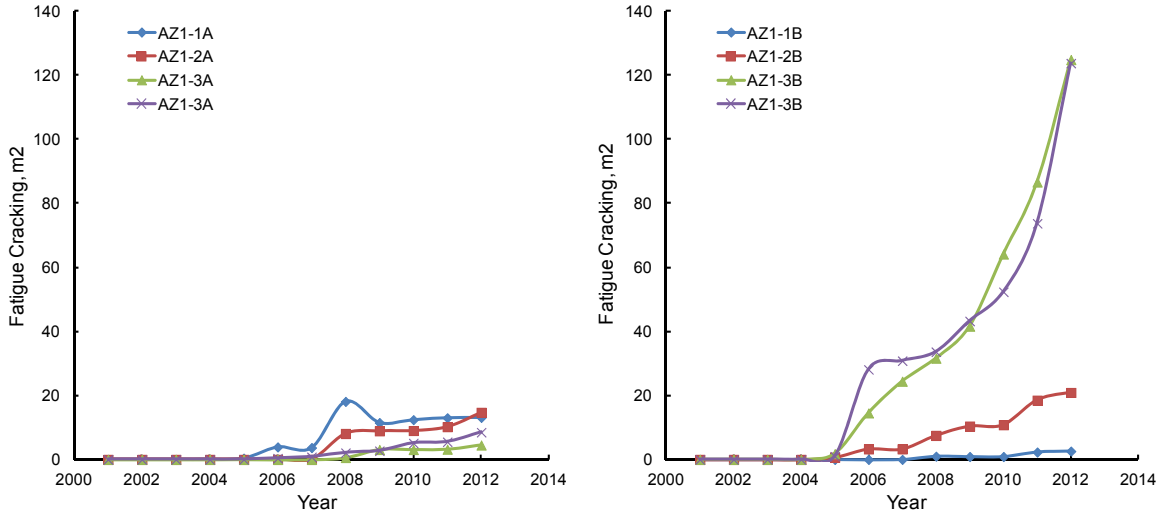

FIGURE 7 Fatigue cracking: low severity, (area, m^2), surveyed over an 11-year span, for two sections labeled A and B, each constructed from the same binder source.

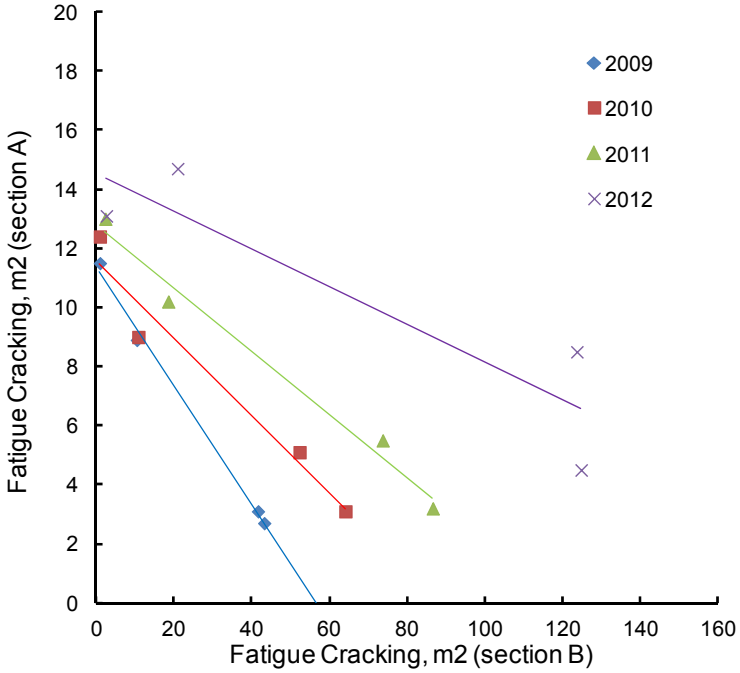

FIGURE 8 Correlation between fatigue cracking: low severity, (area, m^2) from two different sections, labeled A and B, constructed from the same binder source.

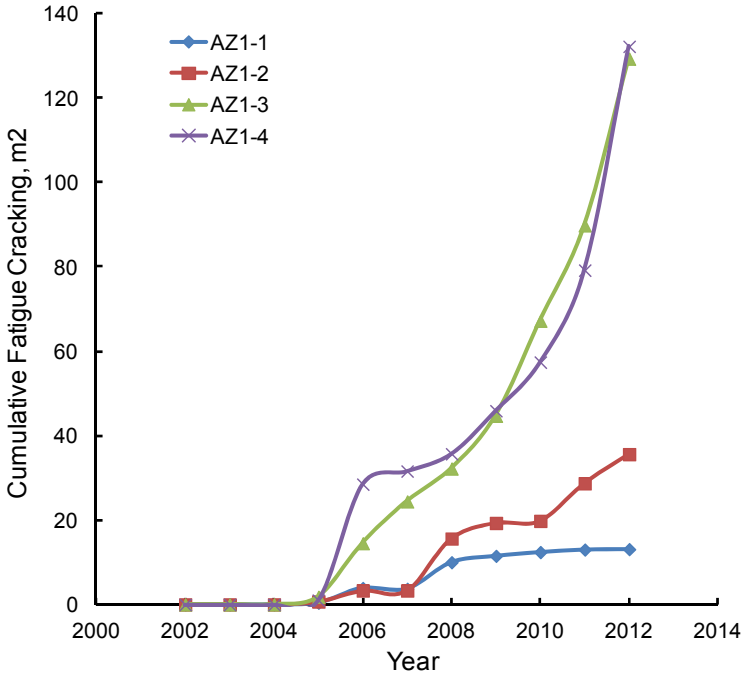

FIGURE 9 Cumulative fatigue cracking: low severity, (area, m^2), surveyed over an 11-year span, summed for two sections, labeled A and B, constructed from the same binder source.

TABLE 6 Longitudinal Cracking/Non-Wheelpath: Sum of Low, Moderate, and High Severity, (Total Length, m), Section A, Reported for an 11-Year Life Span

Year	AZ1-1	AZ1-2	AZ1-3	AZ1-4
2001	0	0	0	0
2002	0	0	0	0
2003	0	0	0	0
2004	45	0	0	68.3
2005	77.9	0	0	86.9
2006	130.6	60.4	6.3	116.2
2007	137.4	120.1	19.6	119.6
2008	142.6	145	45.5	162.2
2009	157	184.5	55.7	201.5
2010	170.4	193	55.8	211.4
2011	191.1	215.9	205.3	227.8
2012	196.1	217.7	209.2	230.8

TABLE 7 Longitudinal Cracking/Non-Wheelpath: Sum of Low, Moderate, and High Severity, (Total Length, m), Section B, Reported for an 11-Year Life Span

Year	AZ1-1	AZ1-2	AZ1-3	AZ1-4
2001	0	0	0	0
2002	0	0	0	0
2003	0	0	0	0
2004	168.2	0	0	29
2005	200	0	0	48.4
2006	279	32.8	4.5	28.5
2007	291.4	70.9	17.5	39.6
2008	291.6	65.9	19.7	38.8
2009	296	97.8	14.5	45.4
2010	303.2	96.9	23.3	58.4
2011	303.1	161.5	91.5	98.6
2012	308.9	164.7	57.6	96

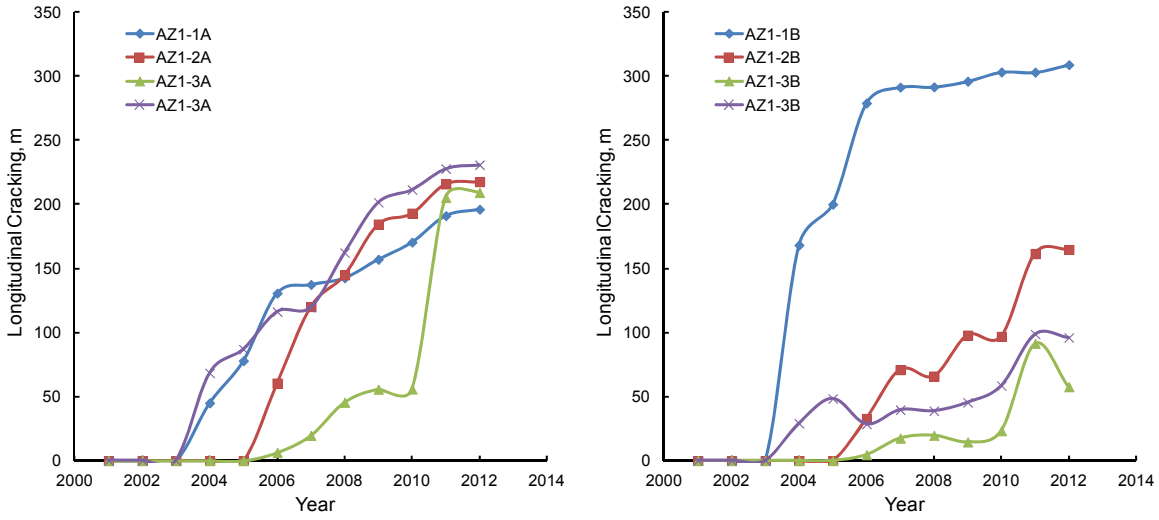

FIGURE 10 Longitudinal cracking/non-wheelpath: sum of low, moderate, and high severity, (total length, m), surveyed over an 11-year span, for two sections labeled A and B, each constructed from the same binder source.

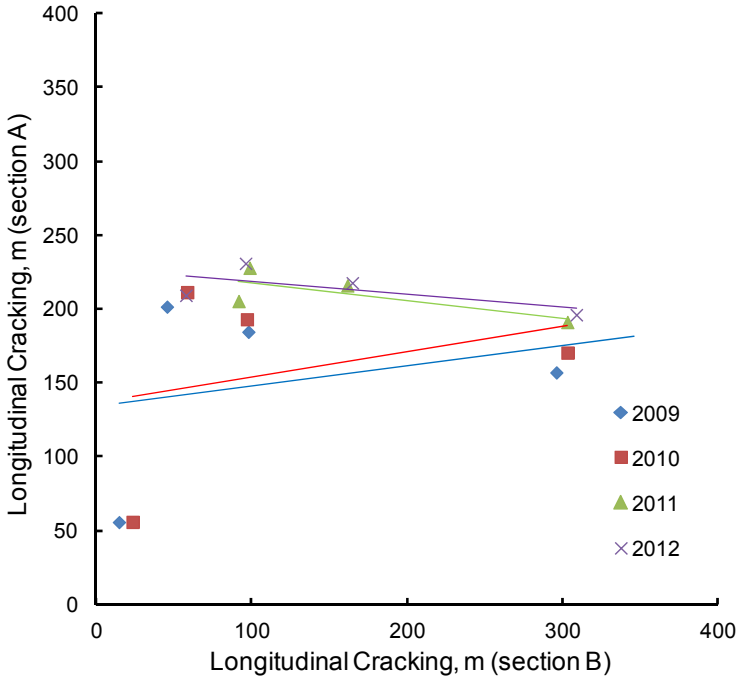

FIGURE 11 Correlation between longitudinal cracking/non-wheel path: sum of low, moderate, and high severity, (total length, m), surveyed over an 11-year span, for two sections, labeled A and B, constructed from the same binder source.

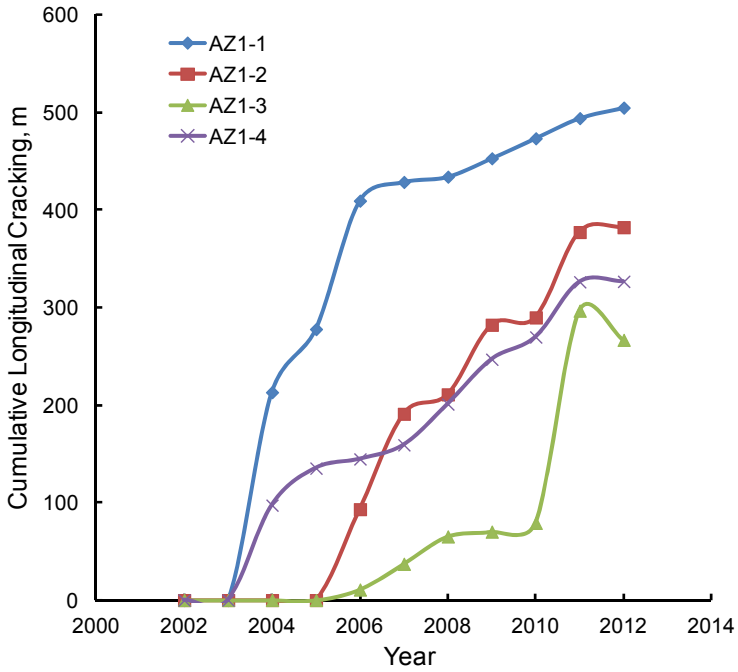

FIGURE 12 Cumulative longitudinal cracking/non-wheelpath: sum of low, moderate, and high severity, (total length, m), surveyed over an 11-year span, summed for two sections, labeled A and B, constructed from the same binder source.

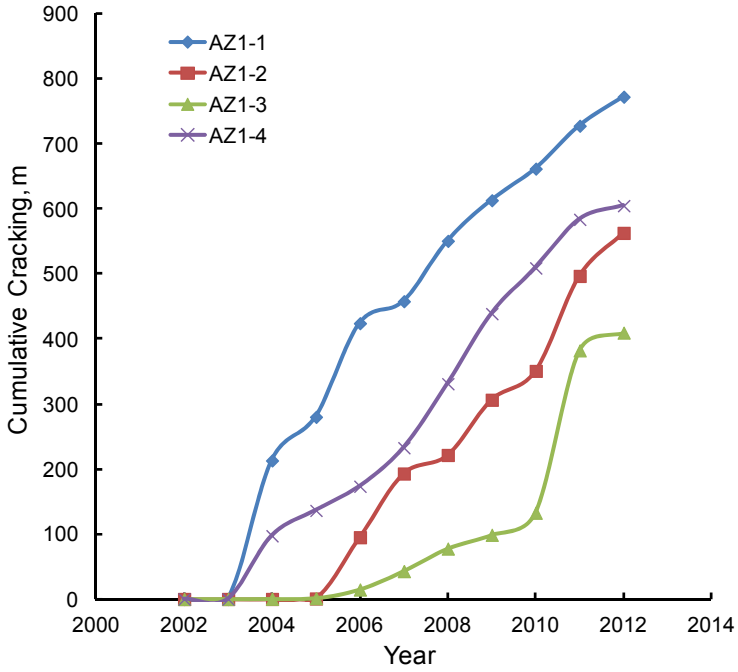

FIGURE 13 Cumulative summed longitudinal cracking/non-wheelpath, fatigue cracking: low severity, $(m^2)^{1/2}$, and transverse cracking: sum of low severity and moderate severity (total length, m), surveyed over an 11-year span, summed for two sections, labeled A and B, constructed from the same binder source.

Temperature Dependent Phase Angle Analysis of Neat, Aged, and Core Sample Binder

Establishing that cumulative summed cracking data be used as the basis for quantifying field performance, laboratory test data comparisons were thus made using rheological data derived from the same neat and aged binders retained from the field validation site, as well as from binder materials derived from field cores taken periodically during performance surveys. Binder materials from these field cores were subsequently sliced in accord with studies conducted by Qin et al. (2014) and extracted by the same methodologies.

Tables 8 through 11 report DSR phase angle δ for extracted binder from the first 13-mm core slice, cored November 17, 2005, and for RTFO/PAV aged binder aged at 95°C, 100°C, and 110°C, all measured at 10 rad/s, determined over the temperature range of 0°C to 80°C (10°C intervals). Figures 14 through 17 correspondingly depicts line-marker plots of phase angle as a function of temperature for each of the four material binder types reported in Tables 8 through 11. In each of these figures are notable temperature regions of trend-line crossover, indicated by the enclosing oval, that extend between 40°C to 60°C.

Figures 18 through 21 then depict correlation plots of phase angle (δ at 10 rad/s) for extracted core binders and RTFO/PAV aged binders, respectively, correlated to cumulative cracking. Plots specifically depicted in Figures 18 and 19 show strong linear functions of the phase angle at constant frequency as a function of cumulative cracking δ_ω at a temperature of 50°C, which subsequently corresponds to the central value of δ_ω within the temperature region of trend-line crossover indicated by the enclosing oval in Figures 14 through 17. Whereas, at temperatures above and below the temperature of 50°C, the correlation is better approximated as second order.

Figures 22 and 23 finally depict more appropriate correlation plots where cumulative cracking (2012 survey) is plotted as a function of phase angle (DSR 10 rad/s, 50°C), for top slice extracted core binders obtained in 2005 (Figure 22) and for binder materials RTFO/PAV aged at three different temperatures.

TABLE 8 DSR Phase Angle δ, 10 rad/s; Extracted Binder from First 13-mm Core Slice, Cored November 17, 2005

Temperature, °C	δ, AZ1-1	δ, AZ1-2	δ, AZ1-3	δ, AZ1-4
0	17	20	14	14
10	22	28	22	21
20	27	37	30	28
30	31	45	41	38
40	33	48	51	38
50	43	55	62	52
60	50	61	70	61
70	59	67	77	72
80	68	74	82	78

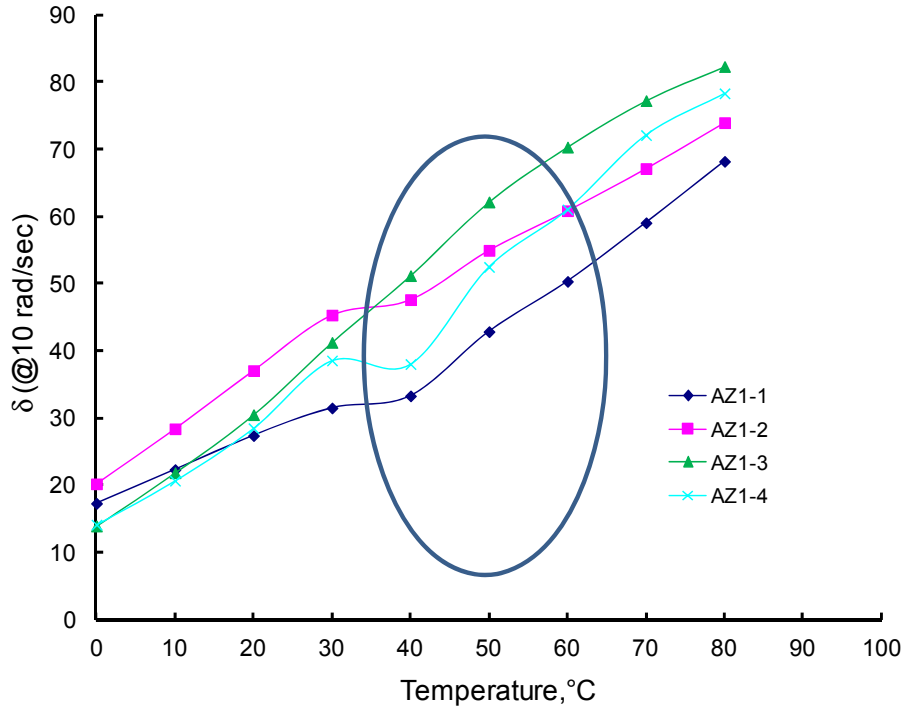

FIGURE 14 Phase angle (DSR 10 rad/s) versus temperature plots of extracted binder from top slice of sectioned field cores (obtained in 2005).

TABLE 9 DSR–RTFO/PAV 95°C Aged Binder Phase Angle Data, δ, 10 rad/s Determined Over the Temperature Range of 0°C to 80°C (10°C Intervals)

Temperature, °C	δ, AZ1-1	δ, AZ1-2	δ, AZ1-3	δ, AZ1-4
0	19	19	-0-	14
10	25	28	24	22
20	32	37	35	32
30	39	46	45	43
40	42	49	50	43
50	51	55	61	57
60	59	60	67	65
70	68	66	74	73
80	76	72	79	79

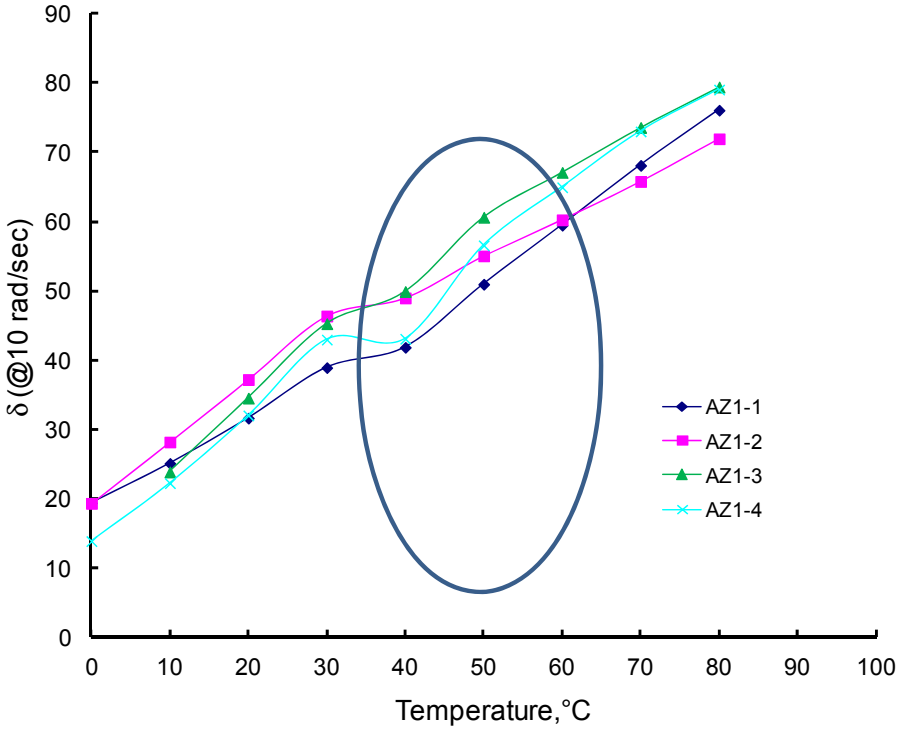

FIGURE 15 Phase angle (DSR 10 rad/s) versus temperature plots of RTFO/PAV 95°C aged binders.

TABLE 10 DSR–RTFO/PAV 100°C Aged Binder Phase Angle Data, δ, 10 rad/sec Determined Over the Temperature Range of 0°C to 80°C (10°C Intervals)

Temperature, °C	δ, AZ1-1	δ, AZ1-2	δ, AZ1-3	δ, AZ1-4
0	20	21	17	14
10	26	30	26	22
20	32	39	36	31
30	36	41	36	43
40	45	51	-0-	43
50	54	56	62	56
60	64	62	69	64
70	71	68	76	73
80	78	75	82	79

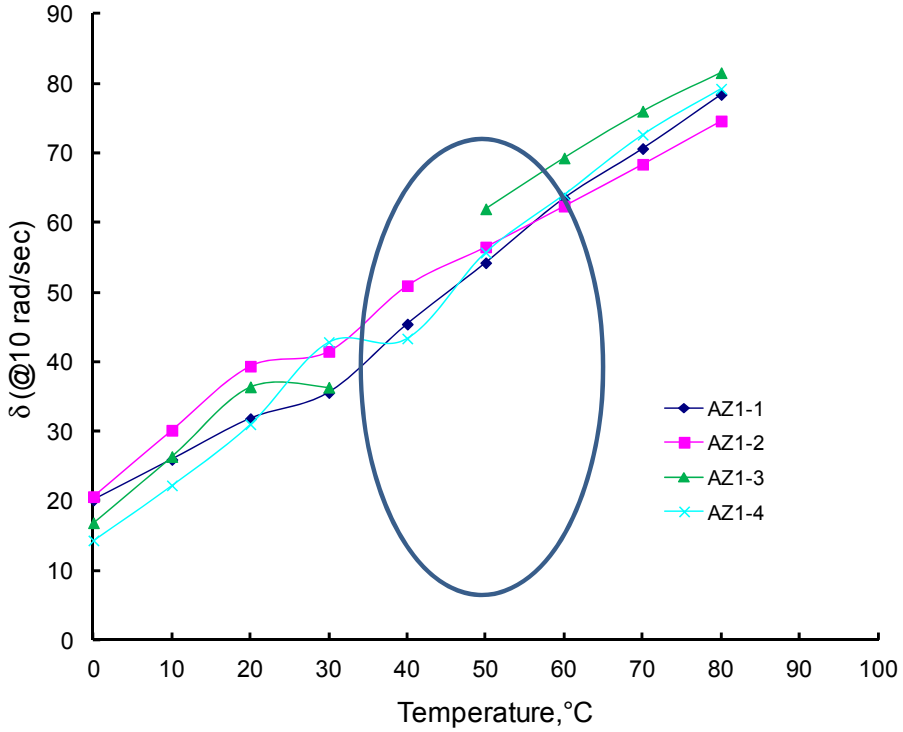

FIGURE 16 Phase angle (DSR 10 rad/s) versus temperature plots of RTFO/PAV 100°C aged binders.

TABLE 11 DSR–RTFO/PAV 110°C, Aged Binder Phase Angle Data, δ, 10 rad/sec Determined Over the Temperature Range of 0°C to 80°C (10°C Intervals)

Temperature, °C	δ, AZ1-1	δ, AZ1-2	δ, AZ1-3	δ, AZ1-4
0	19	20	15	14
10	24	29	24	22
20	29	37	33	31
30	35	44	36	41
40	37	47	45	43
50	47	53	56	56
60	54	58	63	62
70	63	63	70	71
80	71	70	76	79

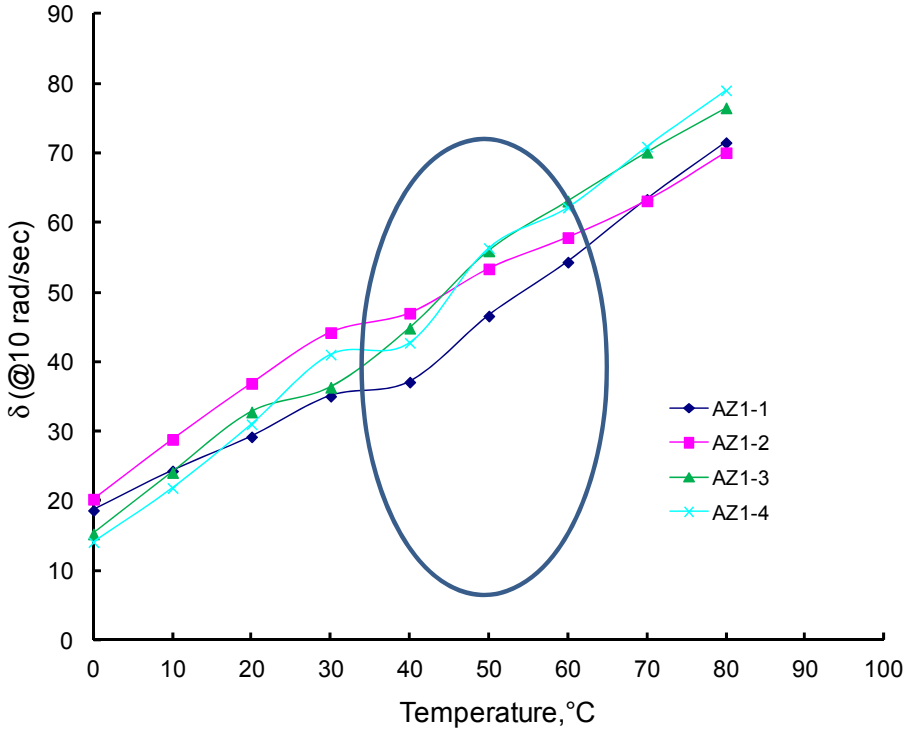

FIGURE 17 Phase angle (DSR 10 rad/s) versus temperature plots of RTFO/PAV 110°C aged binders.

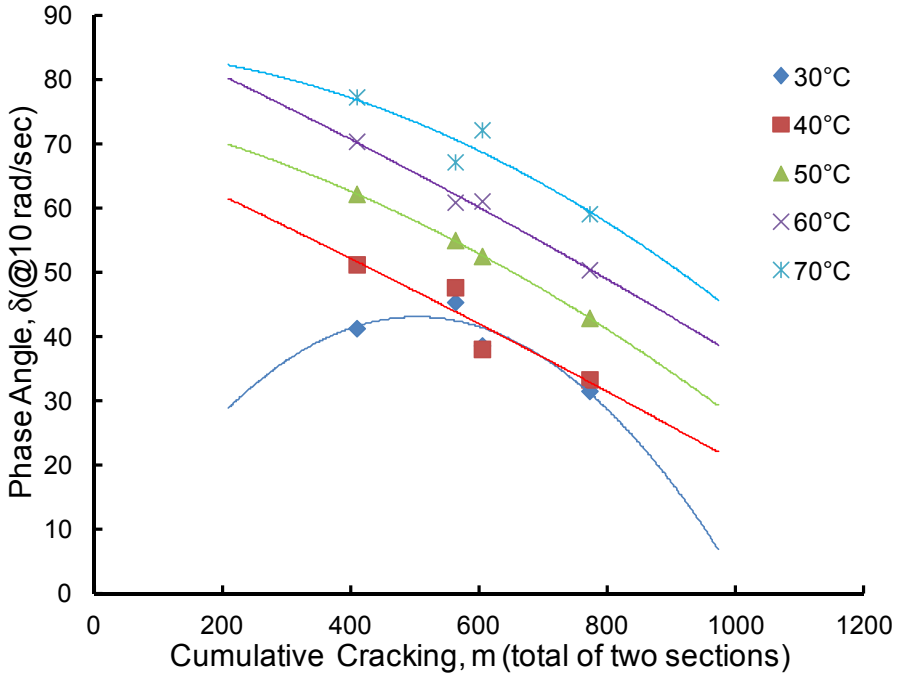

FIGURE 18 Correlation plot of phase angle (DSR 10 rad/s) of extracted core binders (obtained in 2005), correlated to cumulative cracking.

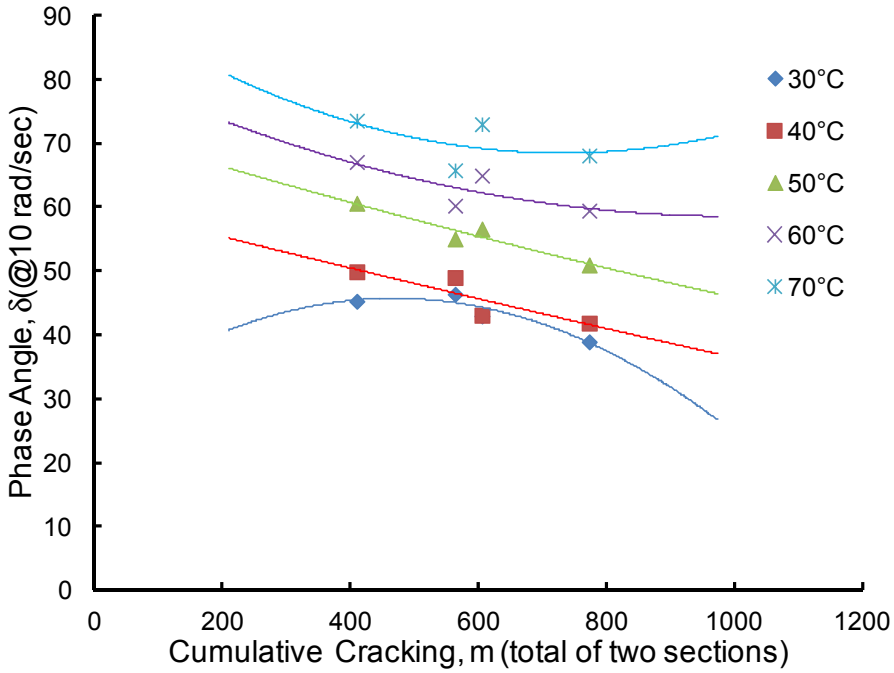

FIGURE 19 Correlation plot of phase angle (DSR 10 rad/s) of RTFO/PAV 95°C binders, correlated to cumulative cracking.

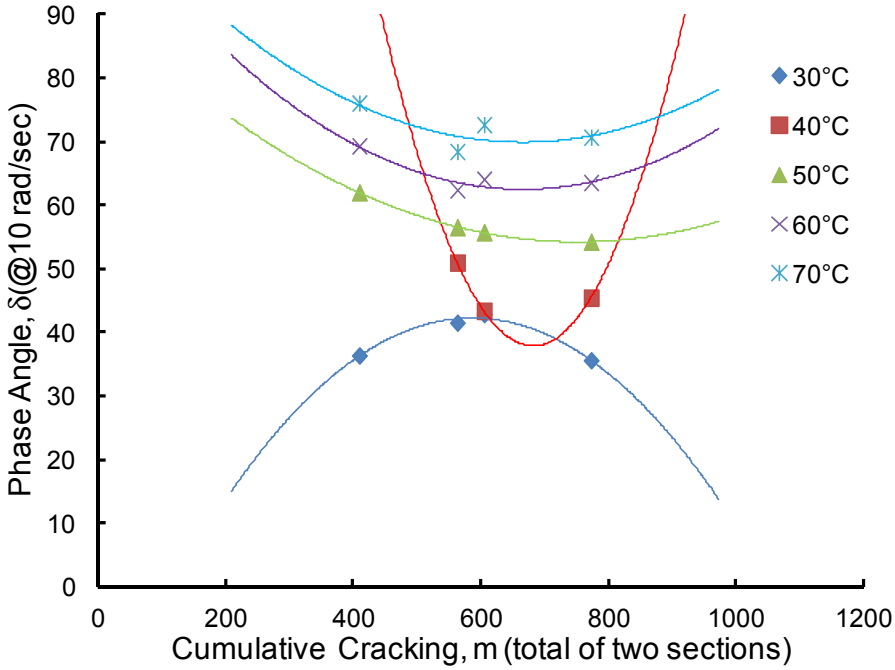

FIGURE 20 Correlation plot of phase angle (DSR 10 rad/s) of RTFO/PAV 100°C binders, correlated to cumulative cracking (2012 survey).

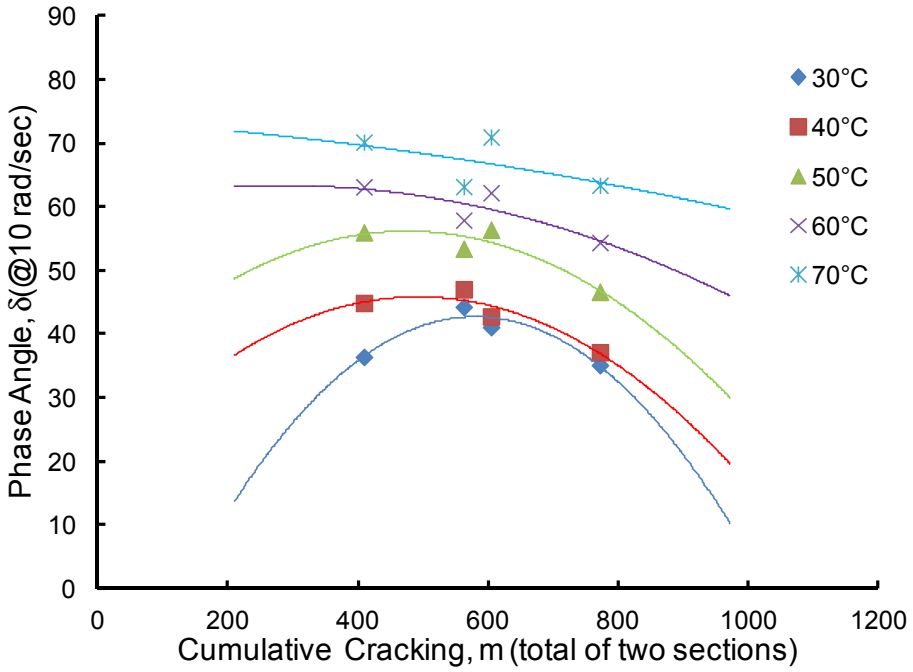

FIGURE 21 Correlation plot of phase angle (DSR 10 rad/s) of RTFO/PAV 110°C binders, correlated to cumulative cracking (2012 survey).

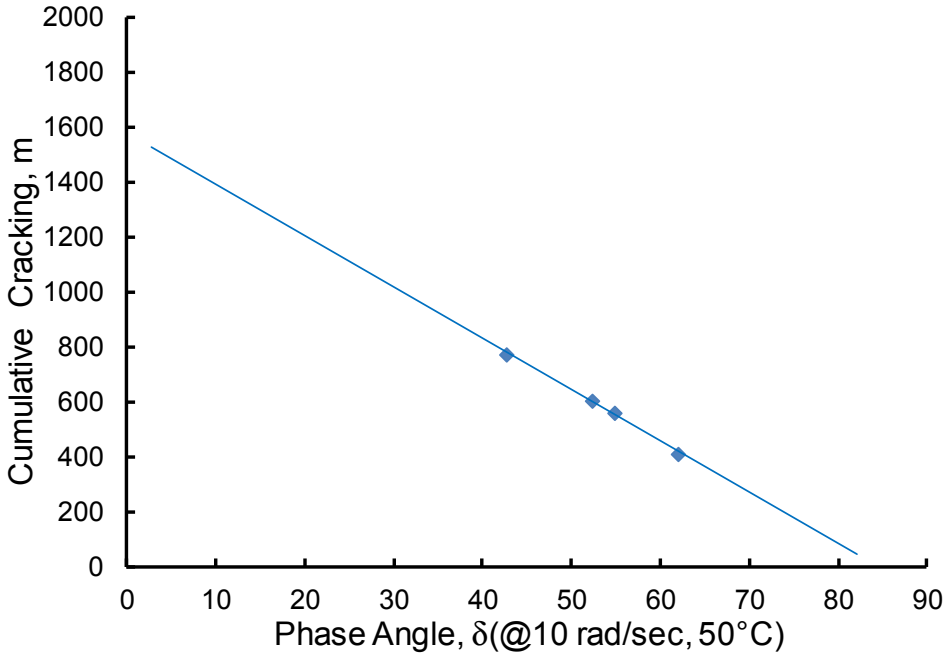

FIGURE 22 Cumulative cracking (2012 survey) plotted as a function of phase angle (DSR 10 rad/s, 50°C) of top slice extracted core binders (obtained in 2005).

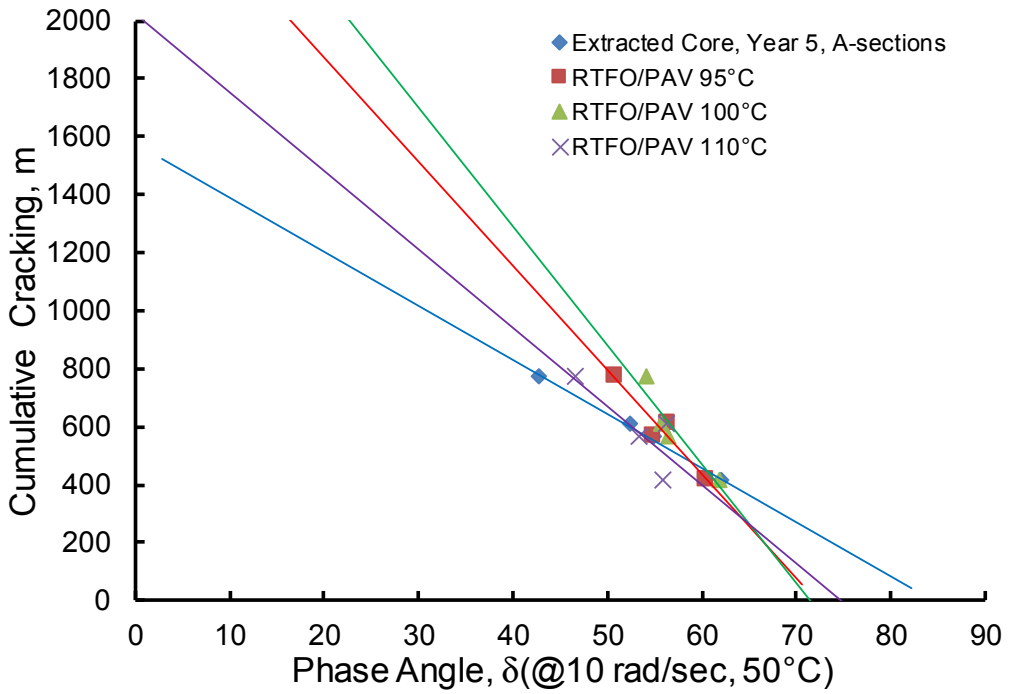

FIGURE 23 Cumulative cracking (2012 survey) plotted as a function of phase angle (DSR 10 rad/s, 50°C) of top slice extracted core binders (2005), and binders RTFO/PAV aged at three different temperatures.

Comparisons of Complex Modulus of Core Sample Binders to RTFO/PAV-Aged Binders

In an attempt to compare the extent of aging of the laboratory aged binders to binder materials extracted from top slice cores, complex modulus data (at 10 rad/s) are reported in Table 12 at 20°C increments between 10°C and 80°C. Figures 24 through 27 further depict bar graphs of complex modulus (at 10°C, 30°C, 50°C, and 80°C, and each at 10 rad/s) for the four AZ-binders top slice extracted (2005) core binders and RTFO/PAV aged binders aged at different temperatures.

In the bar graphs depicted, complex modulus is most consistent among the four material types at 10°C, but then tend to deviate at higher temperatures. In all cases binder materials extracted from top slice cores have higher complex modulus compared to lab aged materials. For 50°C data in particular (Figure 26) 95°C aged and 110°C aged RTFO/PAV materials tend to be closer in value to extracted core materials, supporting the correlations depicted in Figures 19 and 20.

TABLE 12 Complex Modulus (at 10 rad/s) Data Reported at Different Temperatures for Four AZ-Binders Representing Top Slice Extracted (2005) Core Binders and RTFO/PAV-Aged Binders Aged at Three Different Temperatures

Material (conditioning)	AZ1-1	AZ1-2	AZ1-3	AZ1-4
10°C				
Extracted Core	42975000	41023000	81650000	84435000
RTFO/PAV 95°C	39678000	51205000	84731000	92282000
RTFO/PAV 100°C	36661000	44526000	65775000	88622000
RTFO/PAV 110°C	38433000	41994000	77019000	91226000
30°C				
Extracted Core	8875000	3876800	9655000	11426000
RTFO/PAV 95°C	4239800	4084000	7188100	9709700
RTFO/PAV 100°C	2055200	2349700	3911800	6673600
RTFO/PAV 110°C	5429000	3702300	6757400	9108700
50°C				
Extracted Core	714960	302880	288070	934510
RTFO/PAV 95°C	333460	296590	359520	714780
RTFO/PAV 100°C	177910	203070	267930	590200
RTFO/PAV 110°C	472360	267550	481680	609280
80°C				
Extracted Core	20215	7996	5752	16873
RTFO/PAV 95°C	6475	7706	5938	10699
RTFO/PAV 100°C	2415	5370	4189	9257
RTFO/PAV 110°C	11084	8528	8448	8695

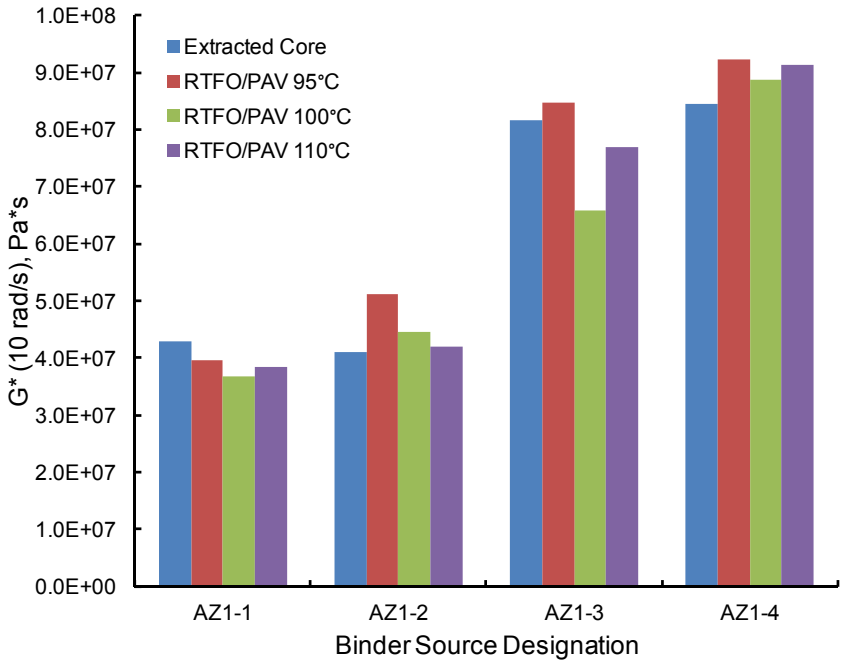

FIGURE 24 Bar graph of complex modulus (at 10°C, 10 rad/s) for four AZ-binders representing top slice extracted (2005) core binders and RTFO/PAV-aged binders aged at different temperatures.

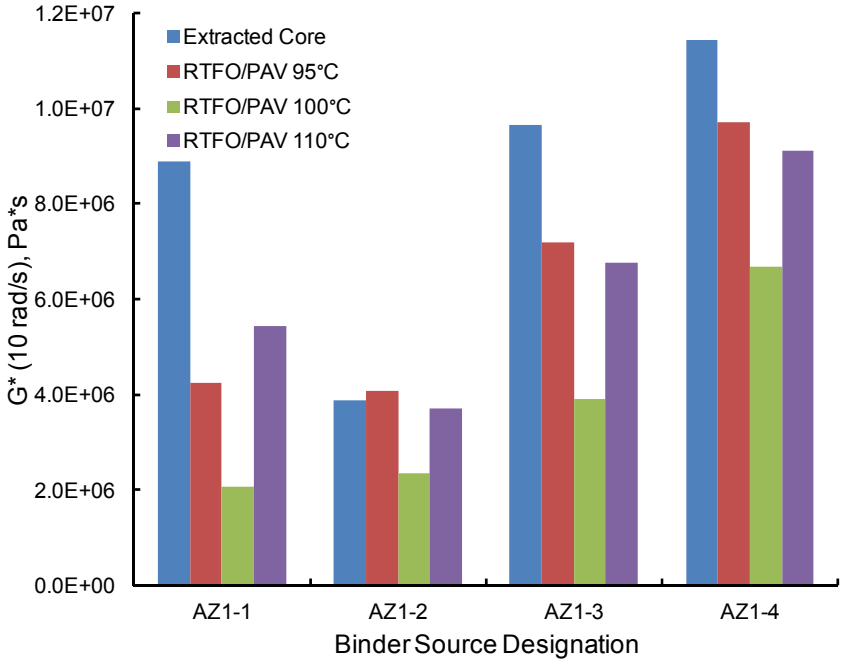

FIGURE 25 Bar graph of complex modulus (at 30°C, 10 rad/s) for four AZ-binders representing top slice extracted (2005) core binders and RTFO/PAV-aged binders aged at different temperatures.

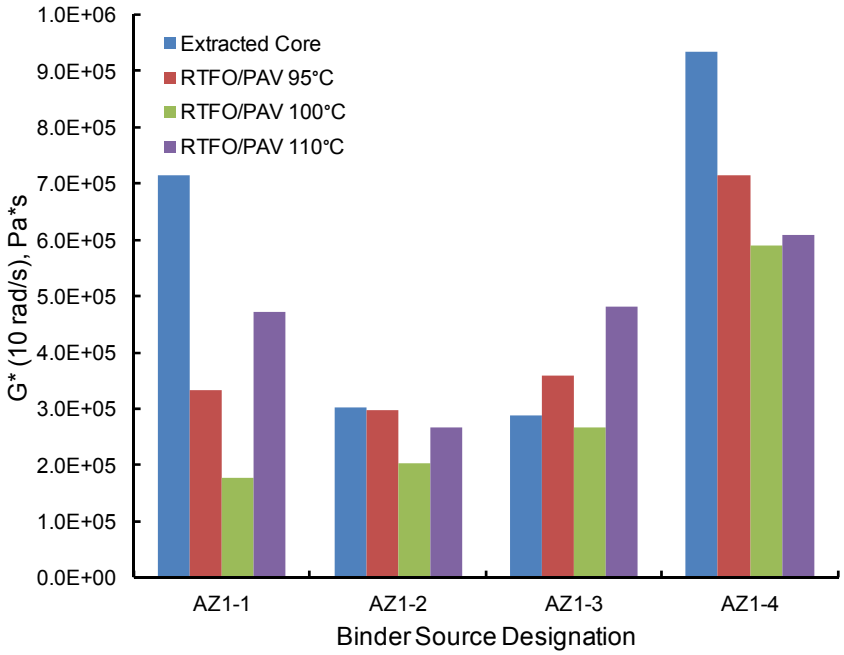

FIGURE 26 Bar graph of complex modulus (at 50°C, 10 rad/s) for four AZ-binders representing top slice extracted (2005) core binders and RTFO/PAV-aged binders aged at different temperatures.

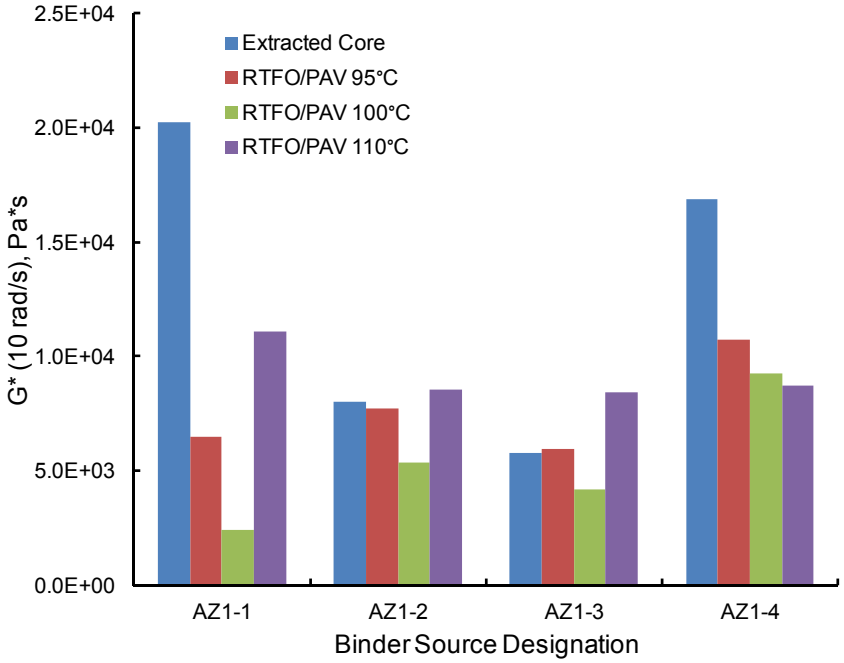

FIGURE 27 Bar graph of complex modulus (at 80°C, 10 rad/s) for four AZ-binders representing top slice extracted (2005) core binders and RTFO/PAV-aged binders aged at different temperatures.

CONCLUSION

Results presented in the present study demonstrate rather straightforward and elegantly simple correlations between the measured phase angle of binder materials extracted from the top slice portion of recovered pavement cores derived from test pavement sites at the time in the life cycle of the pavement when cracking is just beginning to occur and cumulative cracking that is noted several years after this time. The interpretation of these correlations lies in the observation that the phase angle may be a compositional measurement of the brittle elastic material which builds up in asphalts during oxidations, formally referred to here as oxidation product asphaltenes. Therefore, a dynamic suspended phase mass fraction $\left[\chi^*(T,t_{age})\right]_{T_{age},\omega}$ is defined in terms of the phase angle as $\left[\chi^*(T,t_{age})\right]_{T_{age},\omega} \equiv \left[1-\left(\boldsymbol{\delta}(T,t_{age})/\boldsymbol{\delta}_0\right)\right]$. Although not reported in the present paper, a second ARC field site constructed in August 2006 in Rochester, Minnesota, in Olmsted County on County Road 113 is showing identical correlations lending confidence to the approach reported here.

The one aspect of the present study which should warrant some concern for current performance specifications is the observation that aging in asphalt derived field core samples, specifically for the top layer materials appears to be much more age hardened that would be predicted by current protocols. It is specifically noted that stiffness modulus produced at laboratory aging temperatures in excess of 100°C still do not approach the age hardened state of field-aged materials for most of the samples considered in this study.

REFERENCES

Branthaver, J. F., J. C. Petersen, R. E. Robertson, J. J. Duvall, S. S. Kim, P. M. Harnsberger, T. Mill, E. K. Ensley, F. A. Barbour, and J. F. Schabron. SHRP-A-368; Binder Characterization and Evaluation, Volume 2: Chemistry. Strategic Highway Research Program, 1993.

Button, J. W., C. P. Hastings, and D. N. Little. Effects of Asphalt Additives on Pavement Performance. Report No. FHWA/TX-97/187-26. Texas Department of Transportation Research and Technology Transfer Office, 1996

Gu, F., X. Luo, Y. Zhang, and R. L. Lytton. Using Overlay Test to Evaluate Fracture Properties of Field-Aged Asphalt Concrete. *Construction & Building Materials*, Vol. 101, 2015, pp. 1059–1068. https://doi.org/10.1016/j.conbuildmat.2015.10.159.

Hesp, S. A. M., A. Soleimani, S. Subramani, T. Phillips, D. Smith, P. Marks, and K. K. Tam. Asphalt Pavement Cracking: Analysis of Extraordinary Life Cycle Variability in Eastern and Northeastern Ontario. *International Journal of Pavement Engineering*, Vol. 10, No. 3, 2009, pp. 209–227. https://doi.org/10.1080/10298430802343169.

Jin, X., Y. Cui, and C. J. Glover. Modeling Asphalt Oxidation in Pavement With Field Validation. *Petroleum Science and Technology*, Vol. 31, No. 13, 2013, pp. 1398–1405. https://doi.org/10.1080/10916466.2012.665115.

Kandhal, P. S., and S. Chakaraborty. Effect of Asphalt Film Thickness on Short and Long Term Aging of Asphalt Paving Mixtures. NCAT Report No. 96-01, 1996.

Kandhal, P. S., K. Y. Foo, and R. B. Mallick. A Critical Review of VMA Requirements in Superpave. NCAT Report No. 98-1, 1998.

Li, P., Z. Ding, Z. Zhang, and D. Zhang. Comparative Evaluation of Laboratory and Field Ageing of Asphalt Binder Using a Nonlinear Differential Model. *Road Materials and Pavement Design*, Vol. 17, No. 2, 2016, pp. 434–445. https://doi.org/10.1080/14680629.2015.1071717.

McGovern, M. E., W. G. Buttlar, and H. Reis. Field Assessment of Oxidative Aging in Asphalt Concrete Pavements With Unknown Acoustic Properties. *Construction & Building Materials*, Vol. 116, 2016, pp. 159–168. https://doi.org/10.1016/j.conbuildmat.2016.04.117.

Menapace, I., E. Masad, G. Papavassiliou, and E. Kassem. Evaluation of Ageing in Asphalt Cores Using Low-Field Nuclear Magnetic Resonance. *International Journal of Pavement Engineering*, Vol. 17, No. 10, 2016, pp. 847–860. https://doi.org/10.1080/10298436.2015.1019503.

Pauli, A. T. Chemomechanics of Damage Accumulation and Damage Recovery Self-Healing in Bituminous Asphalt Binders. Dissertation, 2014.

Pauli, A. T., and S.-C. Huang. Relationship between Asphalt Compatibility, Flow Properties, and Oxidative Aging. *International Journal of Pavement Research and Technology*, Vol. 6, No. 10, p. 20131-7.

Petersen, J. C. Chemical Composition of Asphalts Related to Asphalt Durability: State of the Art. *Transportation Research Record: Journal of the Transportation Research Board*, *No. 999*, 1984, pp. 13–30.

Petersen, J. C. Quantitative Method Using Differential Infrared Spectrometry for the Determination of Compound Types Absorbing in the Carbonyl Region in Asphalts. *Analytical Chemistry*, Vol. 47, No. 1, 1975, pp. 112–117. https://doi.org/10.1021/ac60351a037.

Petersen, J. C., and P. M. Harnsberger. Asphalt Aging: Dual Oxidation Mechanism and Its Interrelationships with Asphalt Composition and Oxidative Age Hardening. *Transportation Research Record: Journal of the Transportation Research Board*, *No. 1638*, 1998, pp. 47–55. https://doi.org/10.3141/1638-06.

Petersen, J. C., and P. M. Harnsberger. Factors Affecting the Kinetics and Mechanisms of Asphalt Oxidation and the Relative Effects of Oxidation Products on Age Hardening, 1996. http://www.anl.gov/PCS/acsfuel/preprint%20archive/41_4_ORLANDO_08-96.htm.

Petersen, J. C., R. E. Robertson, J. F. Branthaver, P. M. Harnsberger, J. J. Duvall, S. S. Kim, D. A. Anderson, D. W. Christensen, and H. U. Bahia. SHRP-A-367: Binder Characterization and Evaluation, Volume 1. Strategic Highway Research Program, 1994.

Robertson, R. E., J. F. Branthaver, P. M. Harnsberger, J. C. Petersen, S. M. Dorrence, J. F. McKay, T. F. Turner, A. T. Pauli, S.-C. Huang, J.-D. Huh, J. E. Tauer, K. P. Thomas, D. A. Netzel, F. P. Miknis, T. Williams, J. J. Duvall, F. A. Barbour, and C. Wright. Fundamental Properties of Asphalts and Modified Asphalts, Volume I: Interpretive Report, FHWA-RD-99-212. Federal Highway Administration, U. S. Department of Transportation, 2001.

Rose, A. A., Y. Cui, and C. J. Glover. A Comparison of Two Approaches for Incorporating Air Voids in Asphalt Pavement Oxidation Modeling With a Multiyear, Multisite Set of Field Core Data. *Petroleum Science and Technology*, Vol. 34, No. 3, 2016, pp. 223–231. https://doi.org/10.1080/10916466.2015.1122626.

Soleimani, A., S. Walsh, and S. A. M. Hesp. Asphalt Cement Loss Tangent as Surrogate Performance Indicator for Control of Thermal Cracking. *Transportation Research Record: Journal of the Transportation Research Board, No. 2126*, 2009, pp. 39–46. https://doi.org/10.3141/2126-05.

Wright, L., A. Kanabar, E. Moult, S. Rubab, and S. Hesp. Oxidative Aging of Asphalt Cements from an Ontario Pavement Trial. *International Journal of Pavement Research and Technology*, Vol. 4, No. 5, pp. 259–267.

Evaluation of Two Comparative Test Projects in Minnesota and the Relationship Between Binder Composition, Binder Aging, and In-Service Mixture Performance

GERALD REINKE
ANDREW HANZ
Mahy Construction

When the presentation was made at Session 462 the subtitle was shown as "Everything Old Is New Again." This was not so much intended as a hook for the presentation as an acknowledgement that in our efforts to produce something new we often lose sight of the meaningful and informative research that has gone before. In some measure this document is intended to create a bridge between work that goes back more than 50 years and still informs us today in our efforts to understand the impact of bituminous mixture aging on performance.

BACKGROUND INFORMATION

In 1977 Kandhal (1977) reported on research conducted in Pennsylvania covering pavements constructed in 1961 to 1962 and another study of pavements constructed in 1964. These pavements were monitored for approximately 10 years. Cores were taken periodically and recovered binder properties determined including penetration at 25°C, absolute viscosity at 60° C and ductility at 15.5°C at 5 cm/min. For the 1961–1962 pavements, Table 1 summarizes the results after approximately 11 years in service.

Figure 1 is a reproduction of Figure 7 from Kandhal's 1977 report to which has been added markups to emphasize specific points made by Kandhal regarding recovered binder ductility and pavement distress.

TABLE 1 Ductility and Pavement Condition of 1961 and 1962 Pennsylvania Pavements as Reported by Khandal (1977)

Ductility Value at 60°F (15.5°C), 5 cm/min, cm	Pavement Condition Observed
More than 10	Satisfactory
8 to 10	Loss of fines (matrix)
5 to 8	Raveling
3 to 5	Cracking, needs resurfacing
Less than 3	Very poor, extensive cracking

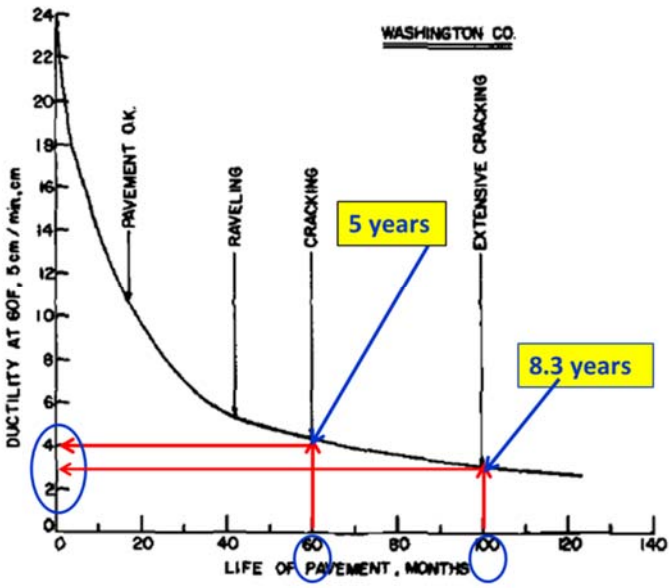

FIGURE 1 Reproduction of Kandhal's Figure 7 (1977).

Figure 1 emphasizes that at 5 years of service cracking had occurred at a ductility of 4 cm and at 8.3 years extensive cracking had occurred at approximately 3 cm of ductility. We will show in the course of this report that there are ultimately relationships between ductility at 15°C and rheological parameters more directly related to pavement performance. While Kandhal's work is, by his own admission, empirical it is an important stepping stone on the path towards understanding the drivers of pavement performance. In the conclusion to his 1977 paper Kandhal made the point that "After the penetration of asphalt drops below 30 due to hardening, the pavements containing asphalt with low ductilities are likely to show poorer service than pavements containing asphalts of the same penetration but with high ductilities." Simply stated, not all asphalts are created equally and as we shall see there are more fundamental binder properties available to us today to better articulate that fact than was available to Kandhal in the 1970s.

Charles Glover and co-workers at Texas A&M have published extensively in the area asphalt oxidation kinetics and aging and the impact of binder aging on mixture performance. For purposes of this discussion his work as reported in Glover (2005) will be covered. In the 2005 report Glover referred to the work already cited by Kandhal as well as other researchers who highlighted the importance of loss of ductility of binders with aging in the deterioration of asphalt pavements (R. G. Clark, 1958; R. Clark, 1956; Halstead, 1963). Out of his research on the ductility properties of aged binders and determination of rheological properties of those same binders Glover arrived at the relationship showing that for binders having ductilities measured at 15°C and 1 cm/min of less than 10 cm there was a good correlation with the rheological parameter G'/(η'/G')measured at 44.7°C and 10 rad/s. As the work by Kandhal and Clark had shown it was when ductility dropped below 10 cm that pavement distress began to develop. Glover's work has been merely summarized here and a reading of Chapter 4 in the 2005 report will provide extensive background to the development of Glover's rheological parameter.

As part of the 2005 report Glover proposed a binder aging procedure that approximated binder properties obtained from extended mixture aging studies. That procedure consists of

1. Using pans 4 cm x 7 cm in size;
2. Adding 2.4 g of RTFO binder residue to each pan (FT is ≈0.857 mm);
3. Age the binder in the pans at 90°C for 32 h at 20 ATM air pressure;
4. After aging use the DSR to determine G' and η' @ 44.7°C and 10 rad/s;
5. Convert the result to G'/(η'/G') @ 15°C and 0.005 rad/s by dividing by 2000;
6. If the result is >0.003 MPa/s the binder fails, this corresponds to a ductility of 3 cm; and
7. A crack warning limit of <0.0009 MPa/s was established which corresponds to a ductility value of 5 cm.

Based on the pan dimensions in point 1 it would be possible to arrange 4 of the 4- x-7-cm pans on a standard 150-mm diameter PAV pan which would provide 9.6 g of aged residue per pan. In addition to arriving at a parameter based on rheological measurements that correlated to historical pavement performance studies based on low-temperature ductility, Glover also emphasized through his aging procedure the need to age binders more severely than the standard PAV procedure used for binder specification determination.

Simon Hesp of Queens University in Kingston, Ontario has written numerous papers showing that the results of tests that he has developed are correlated to onset of pavement cracking (Hesp et al., 2009). The most important of these tests are the Double Edge Notched Tension Test (DENT) and the Extended Bending Beam Rheometer test. Using the DENT test, a Crack Tip Opening Displacement (CTOD) result is obtained that Hesp has correlated to pavement cracking. The Extended BBR test determines the low-temperature grade loss of a binder PAV residue after 72 h of isothermal conditioning at the low PG grade temperature. The DENT test is basically a force ductility test performed at 15°C but at three different notch widths at a standard 5 cm/min pull rate. In essence Hesp has gone back in some respects to Kandhal's roots in looking at a ductility test but one that produces an analytical result. Hesp showed that after 5 years in service that binders recovered from field mix on Ontario Highway 655 with the least pavement distress tended to have the best CTOD results. The binders with the lowest low temperature limiting grades after 3 days of Extended BBR conditioning at –12°C and –24°C also exhibited the best field performance. It is not clear from the reports the thickness of mix that was extracted and therefore some of the variability CTOD results compared to pavement distress could be due to not testing binder from the top 12 mm of pavement. See Section 5 of S. G. Hesp (2009) for more details

The last background paper to be discussed is also the most recent and was published by Anderson et al. (2011). In their work Anderson et al. determined the rheological properties and ductility of binders recovered from airfield pavements of different ages as well as PAV binders aged up to 80 h in the PAV. In this paper the authors introduced the parameter ΔT_c and related it to the Glover parameter of G'/(η'/G') @ 15°C and 0.005 rad/s. Figure 2 shows the manner in which the Glover suggested value of 0.003 MPa/sec as a criterion suggestive of when a binder would be prone to cracking relates to ΔT_c values beyond which distress could also be expected. The data represented by colored symbols show the values for the indicated binders at unaged, 20, 40, and 80 h of PAV aging. The open circles are binders that were recovered from different airfield pavements at different aging times in service.

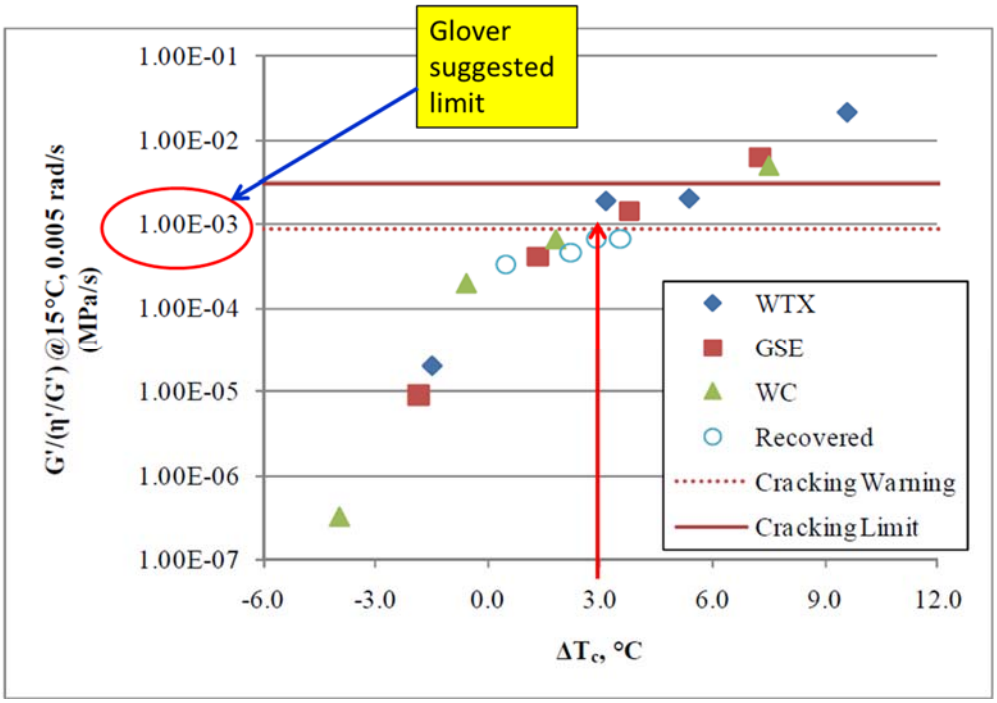

FIGURE 2 Relationship between G'/(η'/G') and ΔT_c taken from Anderson et al. (2011).

PRELIMINARY INFORMATION

When Anderson et al. (2011) introduced the ΔT_c parameter he used bending beam data and subtracted the BBR stiffness critical temperature (temperature where stiffness = 300 MPa) from the creep or *m*-value critical temperature (where the slope of the log stiffness plot at 60 s of BBR creep = |0.300|). For aged binders this value calculated in this fashion will generally be a positive number because most aged binders are *m*-value controlled and therefore the value of *m*–*S* will generally be positive. In the years since the Anderson paper was published several researchers picked up on the ΔT_c concept but began calculating it as *S*-critical temperature–*m*-value critical temperature (*S*-*m*) which will generally result in negative values for ΔT_c for aged binders. The more negative the number the more substantially *m*-controlled the binder and since that is generally not considered a beneficial binder property the ΔT_c being more negative seemed appropriate.

For the ΔT_c information discussed in this paper the 4-mm DSR test procedure was used to determine the rheological equivalents of BBR stiffness and *m*-value critical values. The 4-mm DSR test and method of calculating BBR equivalent values were developed by WRI and reported at several meetings (Sui C. Farrar, 2010; Sui C., 2011; Michael Farrar, 2012; Farrar, 2012).

In a discussion prepared for and published with the Anderson et al. 2011 paper, Geoff Rowe showed how the Glover parameter of G'/(η'/G') can be converted to a stiffness value determined by the relationship G*(cosδ)2/sinδ. Based on Rowe's analysis the crack warning limit of 5 cm, 15°C, 1 cm/min (0.0009 MPa/s) calculates to a stiffness value of 180 kPa and the cracking limit or point beyond which cracking will occur of 3 cm, 15°C, 1 cm/min (0.003 MPa/s) calculates to a stiffness of 600 kPa. The cracking warning value of 180 kPa has since the publication of the 2011 paper become known in the industry as the G-R parameter.

STUDIES OF MIX AND BINDER AGING RELATED TO PERFORMANCE

The preceding information is a necessary background to understand the motivation for the work that follows. We all know that as pavements age they become brittle and ultimately crack leading to further aging and moisture damage. Knowing this isn't the same as understanding what is going on at a fundamental level. Additionally if data can be obtained that supports the binder is moving towards a critical point remediation efforts can be implemented to retard that aging. Anderson, et al suggested this approach their 2011 paper for remediation of airfield pavements and clearly the approach is amenable to any bituminous pavement.

As binders aged they lose their ability to relax stresses both mechanical and thermal. This embrittlement manifests as decreases in ductility, increase in the Glover stiffness parameter (or the "march to death" as he so colorfully puts it), an increase in the spread between BBR S and m critical temperature value (ΔT_c) because the m critical temperature increases far faster than the *S* critical temperature, an increase in the *R*-value, decrease in the crossover frequency, and increases in the G-R parameter. There is no shortage of metrics by which to identify the degrading character of binders in our pavements, but we need to invest the effort to obtain the data that will give us the answers. What follows are discussions of two projects in which the authors' company was involved either directly or indirectly over a period of 10 years or more. The original goals of these studies were not to identify factors associated with pavement deterioration or to employ the analysis technics previously discussed.

Comparative Crude Source Study

In August 2006, the Minnesota DOT's contractor, under the direction of WRI, built five test sections as part of a general paving project on Olmsted County Trunk Highway (CTH) 112 north of Rochester, Minnesota. Originally the contractor was directed to build three virgin binder test sections using PG 58-28 binders from three different crude sources. Because the actual paving project was to use a PG 58-34 plus 20% RAP, the contractor was also asked to construct a virgin test section using just the PG 58-34 and a designated test section using the actual project mix containing PG 58-34 and 20% RAP. The test section identity codes and crude sources are presented in Table 2. The identifying codes were assigned by WRI and have been used in numerous reports to evaluate this project.

TABLE 2 Code Identification of Binder Test Sections and Crude Sources

Identification Code	PG Grade	Crude Source
MN1-1	PG 58-34 + 20% local RAP	PMA-modified Western Canadian PG 52-34 + RAP
MN1-2	PG 58-34	PMA-modified Western Canadian crude
MN1-3	PG 58-28	Western Canadian crude, sourced at refinery in Minnesota
MN1-4	PG 58-28	Mideast Kirkuk crude, sourced at refinery in south Texas
MN1-5	PG 58-28	Venezuelan crude, sourced at refinery in New Jersey

These pavement test sections had been monitored yearly through 2012 by WRI. WRI had identified an increase in total cracking (reported in meters for transverse and longitudinal cracking and m^2 for fatigue cracking) between 2010 (year 4) and 2011 (year 5). Those results are plotted in Figures 3 and 4. The data showed a substantial increase in overall pavement distress between years 4 and 5 for sections MN1-3 and MN1-4, however in that same time period section MN1-5 showed no real increase in distress and MN1-1(the 20% RAP) and MN1-2 showed very little increase. The performance of MN1-1 and MN1-2 could well be attributed to the presence of PG 58-34 binder.

In 2014 the authors' company was made aware that the PG 58-28 used to construct MN1-4 had been blended with re-refined engine oil bottoms (REOB) also referred to as vacuum tower asphalt extender. As the impact of REOB on binder aging and pavement performance was a contentious issue at that point the authors' company decided to further examine the test sections on Olmsted CTH-112. There had not been a pavement distress survey conducted in 2013 and therefore in 2014 the authors' company commissioned the former WRI evaluator of the test project to perform one more distress survey of the monitoring sections. The authors' company had also retained 5-gal samples of the virgin binders used in those four virgin binder test sections. The binders were subjected to PAV aging through 20 and 40 h and x-ray fluorescence testing was performed on the three PG 58-28 binders and verified the presence of zinc (a marker element for REOB) in MN1-4 PG 58-28 at a level indicating the use of 8% to 9% REOB in that binder.

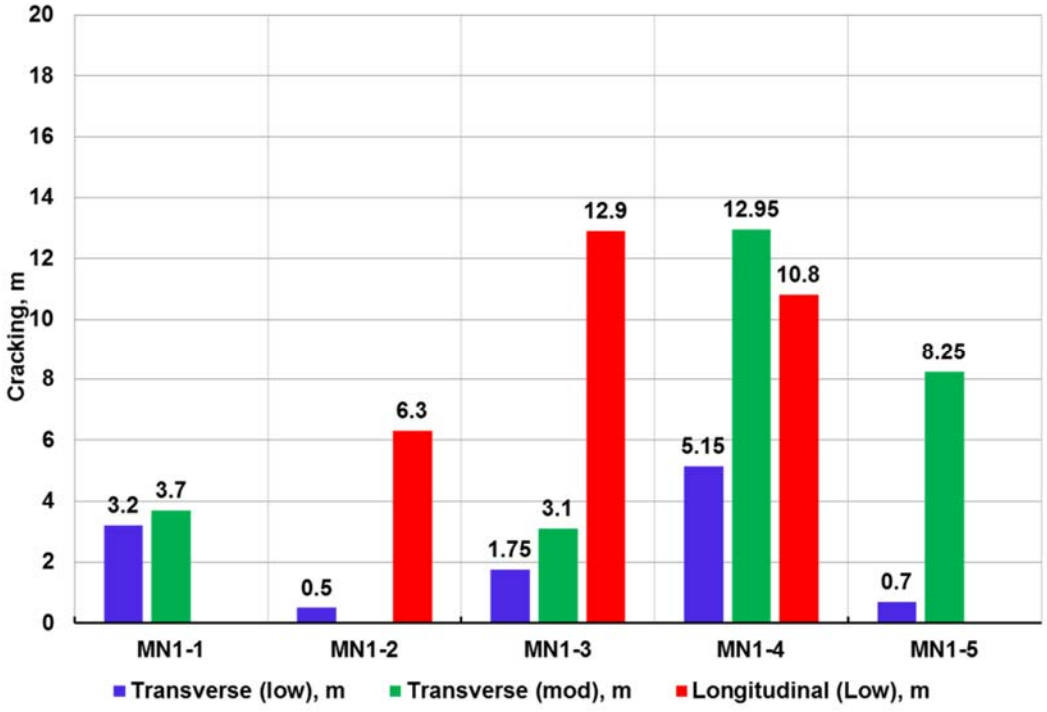

FIGURE 3 Cracking results from 2010 pavement survey.

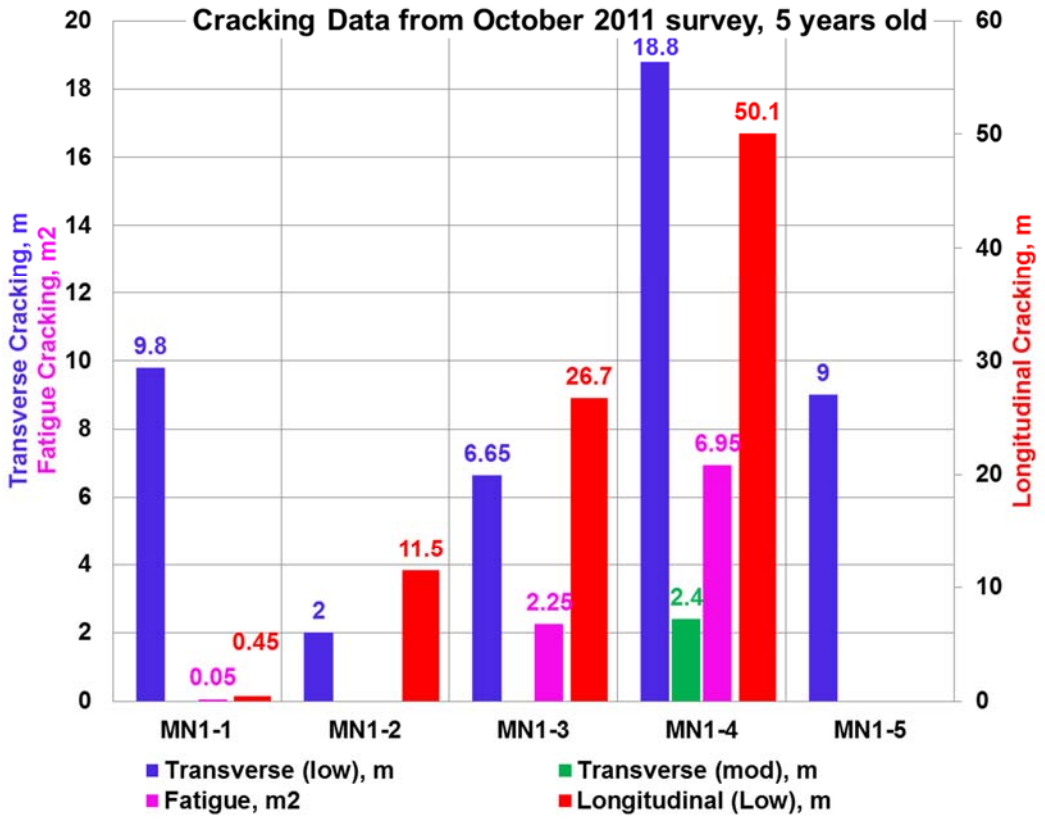

FIGURE 4 Results from 2011 pavement survey.

While this paper is focused on the aging of binders and the impact that has on pavement performance, REOB turned out to be the motivating factor initiating further investigation of the performance of the test sections on Olmsted CTH-112. As a result of initiating this investigation important information regarding poor and exceptional performance of binders and mixtures was developed and that is within the scope and goals of this paper.

The testing performed on the four virgin binders from the Olmsted CTH-112 project consisted of determining the ΔT_c parameter on unaged, RTFO residue, 20- and 40-h PAV residues. It would normally be difficult and time consuming to obtain those data for unaged and RTFO binders, but is actually quite easy using the 4-mm DSR test procedure. From these data the low-temperature *S*-critical and *m*-value critical values were determined, ΔT_c and the rheological index (*R*-value). The Asphalt Institute performed the DENT test on the 20- and 40-h PAV residues and generated the CTOD values reported below. Other data were also generated which is available in several sources (Reinke 2016; G. Reinke 2015; Reinke 2014). Table 3 shows the 4-mm DSR-derived data for the four virgin binders used on Olmsted CTH-112 as well as the CTOD data.

The results of the pavement distress survey conducted in 2014 are summarized in Table 4. The CTOD of the 20-h PAV residue as expounded by Hesp does show a reasonable relationship total between pavement distresses after 8 years in service (see Figure 5).

TABLE 3 *S*-Critical, *m*-Critical, ΔT_c, *R*-value, and CTOD for Olmsted CTH-112 Binders

Bitumen Source	Aging	*S*-Critical	*m*-Critical	ΔT_c	*R*-Value	CTOD results (mm)
MN1-2	unaged	–38.7	–41.5	2.8	1.933	
MN1-3	unaged	–35.3	–38.5	3.2	1.626	
MN1-4	unaged	–38.5	–37	–1.5	2.037	
MN1-5	unaged	–34.2	–37.7	3.5	1.370	
MN1-2	RTFO	–37.7	–39.6	1.9	2.255	
MN1-3	RTFO	–34.4	–36.7	2.3	1.909	
MN1-4	RTFO	–38.3	–36.4	–1.9	2.465	
MN1-5	RTFO	–32	–34.8	2.8	1.606	
MN1-2	PAV 20	–35.5	–36.3	0.8	2.687	9.2
MN1-3	PAV 20	–31.9	–31.8	–0.2	2.416	6.2
MN1-4	PAV 20	–35.5	–30.7	–4.2	2.967	5.4
MN1-5	PAV 20	–30.5	–32.2	1.7	1.877	10.7
MN1-2	PAV 40	–33.9	–31.3	–2.6	3.061	4.9
MN1-3	PAV 40	–31.8	–28.1	–4.2	2.872	4.3
MN1-4	PAV 40	–35.2	–27.6	–7.6	3.281	4.3
MN1-5	PAV 40	–29.3	–30.1	0.8	2.162	7.1

TABLE 4 Summary of Distress Survey Conducted in 2014

Bitumen Source	Total Distress	Transverse Cracks	Total Fatigue (Total Distress-Transverse)	Centerline	Non-Centerline_ Fatigue
MN1-2	205.9	13.5	192.4	78.8	113.6
MN1-3	363.4	19.5	343.9	73.3	270.6
MN1-4	472.6	51.2	421.4	82.2	339.2
MN1-5	44.1	19.5	24.6	12.3	12.3

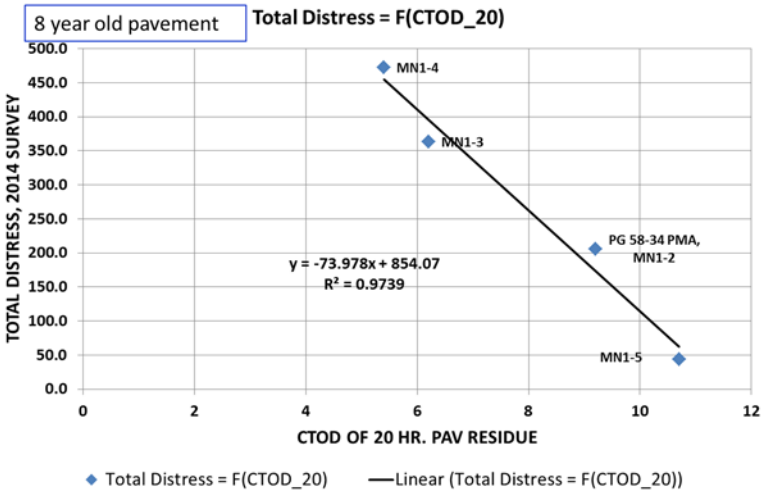

FIGURE 5 Relationship between CTOD of 20-h PAV residue and total distress of CTH-112 pavement after 8 years of service.

However the relationship between CTOD of the 40-h PAV residue and the total distress after 8 years in service is not a linear relationship and for the poorest performing binders there is not substantial variation in the CTOD parameter (see Figure 6). Whereas the relationship for the 20-h PAV was linear the relationship for the 40-h PAV is decidedly not linear, suggesting that perhaps the CTOD parameter has a lower limiting value based on binder aging.

As the binders age their ductility value as determined by the DENT test asymptote towards a minimal level of approximately 4 mm based on the present data. The ΔT_c data for these samples however do not trend towards a minimal value as shown in Figure 7.

A plot of CTOD as a function of the ΔT_c of 20- and 40-h PAV residues yields the relationship shown in Figure 7. The four binders with CTOD values between 5.4 and 4.3 cover a range of ΔT_c values of –2.6°C to –7.6°C. These data indicate that CTOD may be a directionally useful parameter, but it is not a reliably quantitative predictor of binder performance.

At the time of the 2014 Olmsted CTH-112 survey cores of each test section were also taken. Binder from the top ½ in. of cores from each test section was extracted, recovered and tested using the 4-mm DSR procedure. The distress data from the 2014 survey were plotted as functions of the ΔT_c results of the binder recovered from the top ½ in. of the 2014 cores. Those results are plotted in Figure 8. Three relationships are shown in Figure 8. The most robust relationship plots total distress as a function of the binder recovered from the top ½ in. of the pavement. Total distress includes longitudinal cracking, centerline cracking, fatigue cracking, and non-centerline longitudinal cracking. The poorest relationship plots just transverse cracking as a function of ΔT_c of the binder recovered from the top ½ in. of the pavement. It would seem reasonable to that a parameter such as ΔT_c which is derived from the low-temperature binder properties would correlate the best with transverse cracking which is believed to be a single

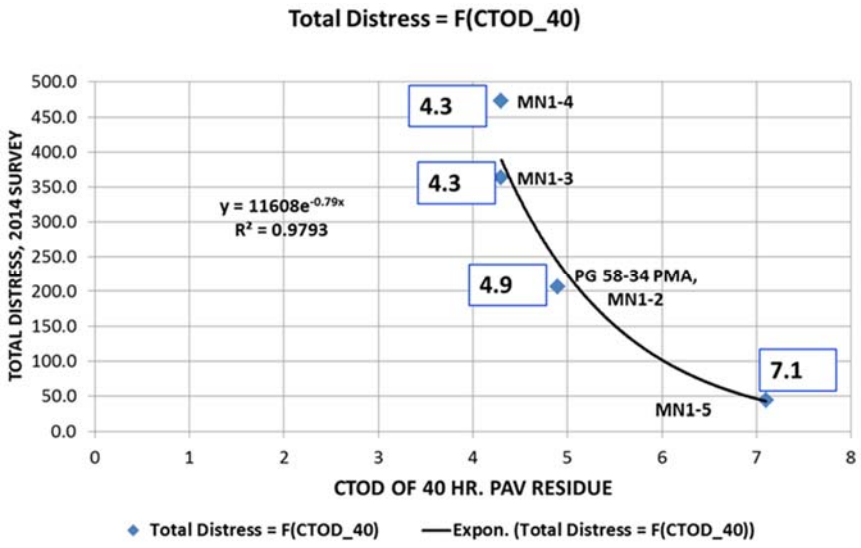

FIGURE 6 CTOD of 40-h PAV residue and total distress of CTH-112 pavement.

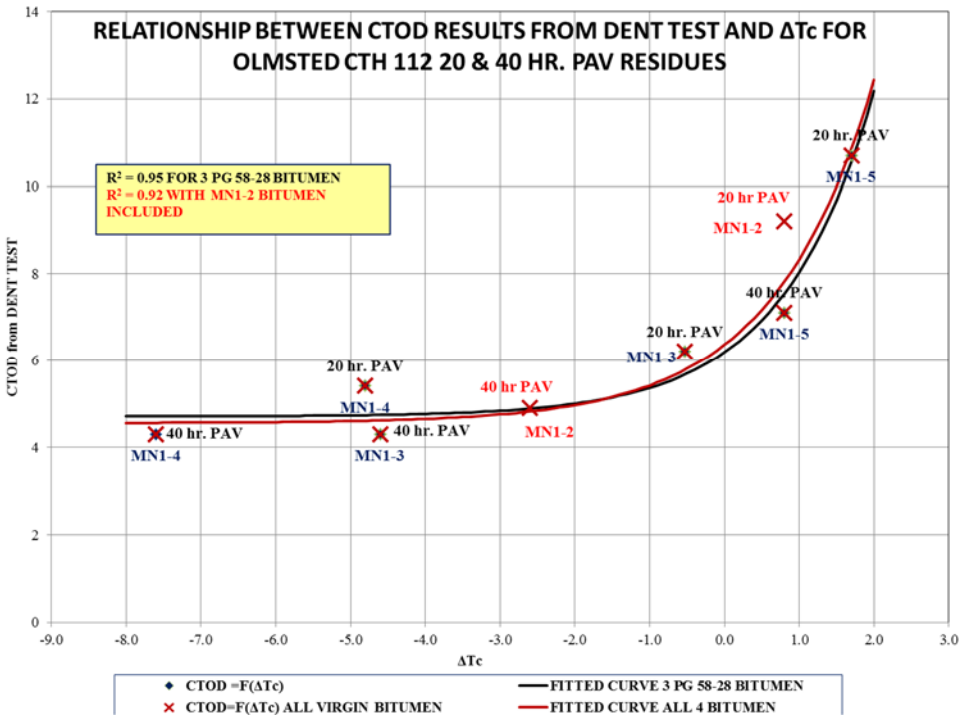

FIGURE 7 Relationship between CTOD results from DENT test and ΔT_c.

event low temperature caused phenomenon. This data suggests this assumption is incorrect. The significance of ΔT_c is that it is a measure of the increasing inability of a binder to relax stresses as it ages and stresses are not only thermal; they are mechanical and they are also due to thermal cycling at temperatures above the critical cracking temperature. The low-temperature stiffness critical temperature is much better correlated to single event thermal cracking and as the data shows the *S*-critical temperatures in some instances are 6°C or 7°C colder than the *m*-critical temperature. The relationships in Figure 8 show that when transverse cracking is removed from the total distress calculation the correlation between ΔT_c and the remaining cracking distress is still very good at an R^2 value 0.93. Transverse cracking is part of total pavement distress, but the loss of binder relaxation has significance beyond single event thermal cracking.

The following pictures (Figures 9 through 13) were taken in 2014 and are representative of the relative distress on the pavement test sections. In all cases the test section is to the right side of the picture except for Figure 11 where the test section is in the foreground. MN1-1 and MN1-2 show little distress; MN1-2 shows some cracking the outside wheelpath. MN1-3 shows randomized longitudinal cracking and the patterns shown are indicative of the pavement at that point in 2014. MN1-4 which has the most severe cracking shows wheelpath cracking and shows cracking in the shoulder area which is a non-loaded portion of the pavement. The shoulder cracking was evident throughout the test section. If you examine MN1-4 (Figure 12) closely you will see there are three sealed transverse cracks at the top of the picture. MN1-5 shows virtually none of the randomized cracking evident in MN1-3 and MN1-4. There were some locations of transverse cracking one of which is shown as a sealed crack in Figure 13.

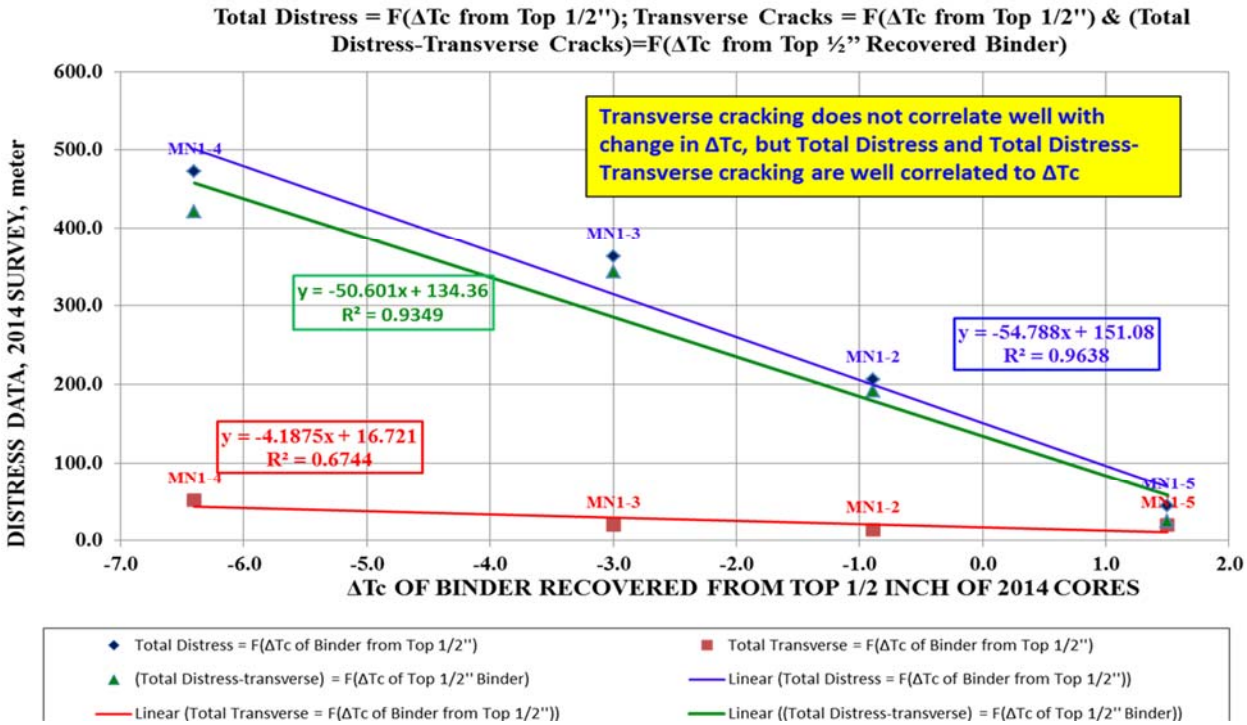

FIGURE 8 Total distress = $F(\Delta T_c$ of binder from top ½ in.); transverse cracks = $F(\Delta T_c$ of binder from top ½ in.) and (total distress – transverse cracks) = $F(\Delta T_c$ of binder from top ½ in.).

FIGURE 9 Test section MN1-1.

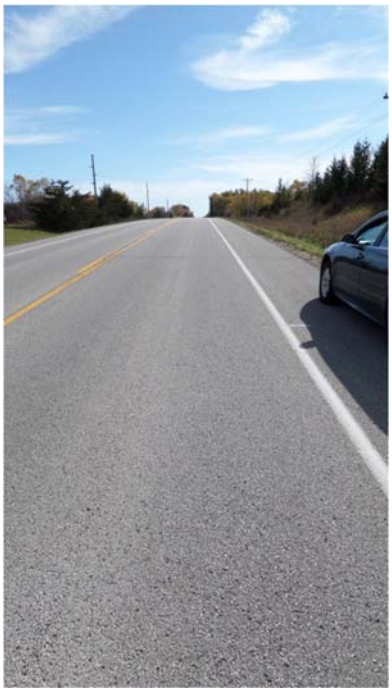

FIGURE 10 Test section MN1-2.

FIGURE 11 Test section MN1-3.

FIGURE 12 Test section MN1-4.

FIGURE 13 Test section MN1-5.

Two additional analyses were undertaken on the Olmsted CTH-112 binders. The ΔT_c properties of the 20- and 40-h PAV residues of the four virgin binders were correlated against the ΔT_c properties of the binders recovered from the top ½ in. of the test sections constructed with those binders. The results of the analysis are shown in Figure 14. The data plotted in Figure 14 show that after 8 years in service the binder in the surface of the test sections has aged more severely than the 20-h PAV would predict but not as severely as the 40-h PAV would predict. These test sections were virgin binder test sections and therefore the potential impact of RAP or RAS is not a factor. The use of reclaimed materials would likely have accelerated the overall aging the of the binder.

This pavement is located in Minnesota and the aging conditions are not nearly as severe as a pavement in more southerly latitude. It might well be that in midcontinental United States the 40-h PAV data would match the data after 8 years in service. In addition, the binder from the top ½ in. of MN1-3 after 8 years had a ΔT_c value of –3.0°C and it was already showing a fair amount of distress. This is consistent with Anderson's data from their 2011 paper where he postulated the onset of cracking as occurring in the range of ΔT_c equal to –2.5°C. This test section by 2014 had gone beyond the onset of cracking and therefore this test section provides support for both Glover's and Anderson's work.

The final analysis performed was to age the loose mix from MN1-3, MN1-4, and MN1-5 at 135°C for 12 and 24 h, extract the binder and determine the ΔT_c properties of the recovered binders. Unfortunately we did not have any samples of the MN1-2 mix at our lab. The relationship between the ΔT_c properties of binder recovered from the top ½ in. of the 8-year

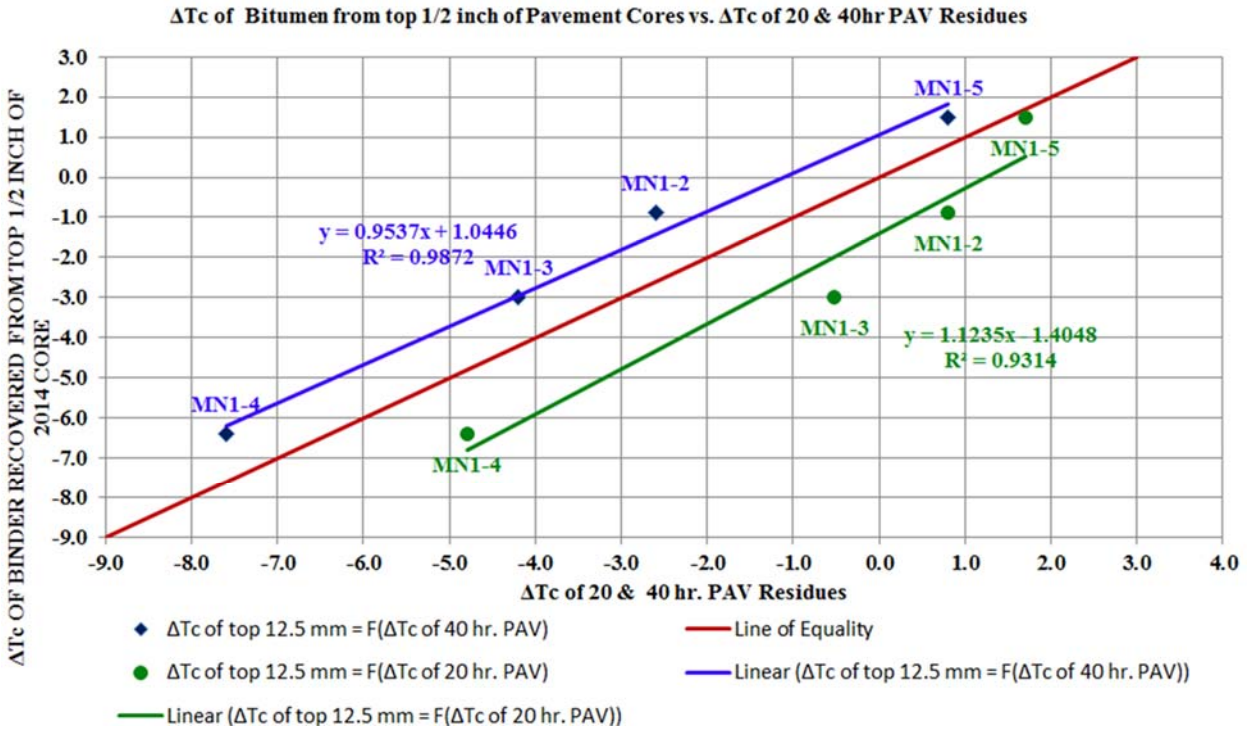

FIGURE 14 ΔT_c of binder from top ½ in. of pavement plotted as a function of ΔT_c for 20-h PAV and 40-h PAV residue. The line of equality is for the ΔT_c of the binder from the top ½ in. of pavement.

-old pavement and the ΔT_c properties of the binder recovered from the 12- and 24-h 135°C loose mix is shown in Figure 15. The data in Figure 15 shows that 12 h of loose mix aging at 135°C is not sufficient to match the aging of 8 years in the field. The 12-h loose mix aged MN1-5 binder did match the field result but then so did the 24-h loose mix aged sample of MN1-5. The MN1-5 binder is resistant to aging unlike binders used in MN1-3 and MN1-4 which aged substantially after 24 h of loose mix conditioning. The MN1-3 binder aged to a point after 24-h equivalent to the MN1-4 binder after only 20 h. This accelerated loose mix aging at 135°C demonstrates that binders from different crude sources have markedly different responses to aging.

MnROAD Performance Evaluation of Three Binder Grades

In 1999 three test sections were constructed on MnROAD to evaluate the relative performance of three test binders. The binders were PG 58-28, PG 58-34, and PG 58-40 all produced from the same crude source. PG 58-34 and PG 58-40 were polymer modified and the PG 58-40 had been softened with REOB to meet the low-temperature PG grade, although that fact was not generally known until much later. The authors' company was contracted to evaluate the low-temperature cracking potential of the mixes in 2000 with the result that the Low-Temperature Indirect Tensile Test as specified by SHRP researchers indicated that the PG 58-40 should have the best

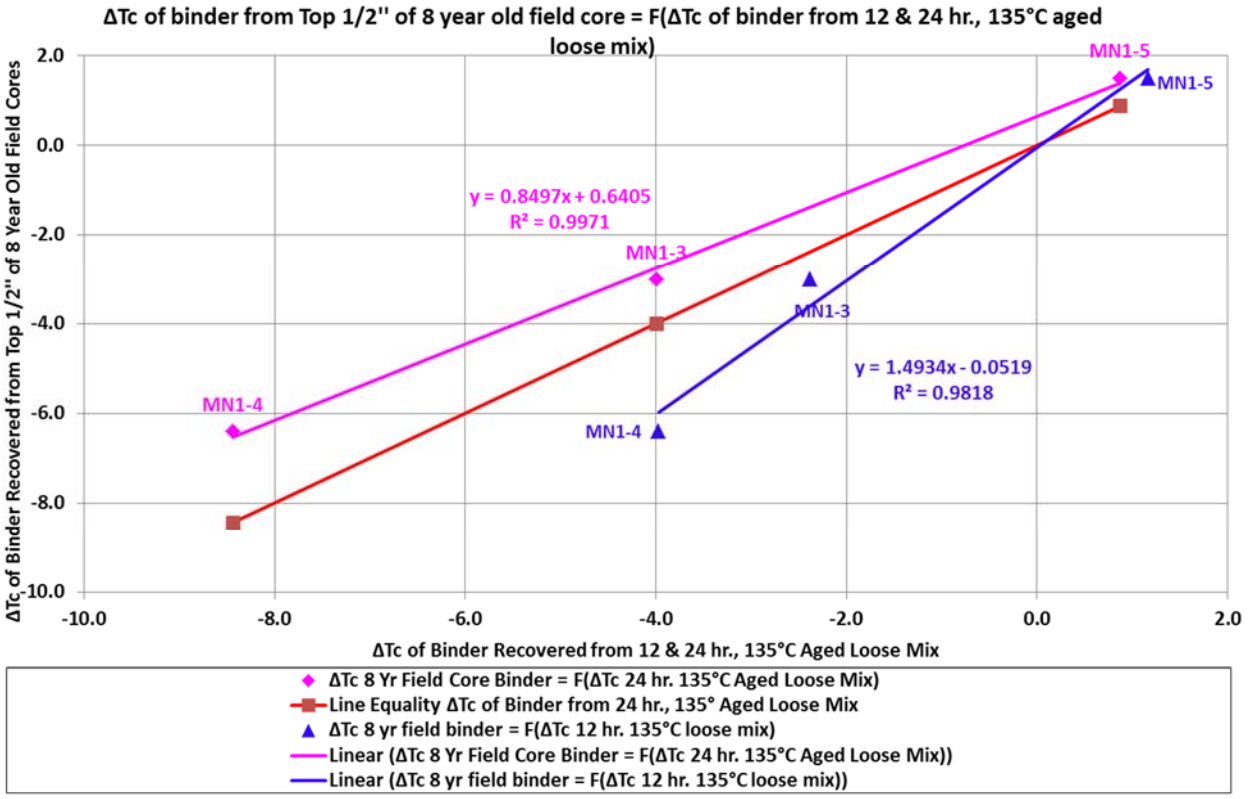

FIGURE 15 ΔT_c from the top ½ in. of pavement plotted as a function of ΔT_c of binder recovered from loose mix aged for 12 and 24 h at 135°C. The line of equality is for the ΔT_c of the binder from the top ½ in. of pavement.

performance. Based on an evaluation of the binders, aged mixtures and recovered binder properties from those mixtures a paper was presented at the 2001 Canadian Technical Asphalt Association meeting (Reinke and Dai 2001). Based on extensive testing and aging of the mixtures for up to 10 days at 85°C all results showed that the PG 58-40 binder would outperform the other two mixtures for low temperature cracking, rutting and fatigue performance. The MnROAD test sections were reconstructed at the end of the contract in 2007. At that point the PG 58-40 mixture had performed the worst of the three binders in terms of overall pavement cracking. In 2015 in the midst of discussions at the Binder and Mixture ETG meetings the question was raised by Minnesota DOT as to whether the PG 58-40 binder contained REOB. The authors' company still had retained samples of the three binders from the investigations performed in 2000. A check for zinc identified the presence of approximately 9% to 10% REOB in the binder. As with the Olmsted CTH-112 analysis the binders were aged and tested for low-temperature properties using the 4-mm DSR test procedures. More in-depth information on this investigation can be found in Reinke (2016). The results of aging the binders through 60 h in the PAV are shown in Table 5.

Because this binder had undergone preliminary testing in 2000 there was BBR data for 20-h PAV-aged binder which is shown for comparison to the 4-mm DSR data for the 20-h PAV aged sample from 2015. The data shows that after 20 h of PAV aging there would have been little reason to suspect the PG 58-40 binder would be a poor performer. The alarming result for this particular binder is the substantial jump in ΔT_c that occurs between the 20- and 40-h PAV aging cycles. Note from the data that most of problem is the substantial increase in the *m*-critical temperature for the PG 58-40.

Cracking data was available from MnROAD on a periodic basis. Table 6 summarizes the distress results from year 3 through year 7.5 at which time the cells were reconstructed. Prior to year 3 very little cracking had been observed on any cell.

Figure 16 shows the trend for total linear crack length at years 4, 5.5, and 7.5 versus ΔT_c of the 40-h PAV residue for each binder. A linear regression value for these plots was not applied because there is no way to know what the actual ΔT_c values were for the field-aged binders in those years. This plot merely demonstrates that at any time the cracking was determined the trend with ΔT_c of the 40-h PAV residues for these binders were the same. An important point to note is the substantial increase in cracking between years 4 and 5.5. The PG 58-34 did not show much cracking in year 5.5, but it had shown no cracking in year 4.

TABLE 5 *S*-Critical, *m*-Critical, and ΔT_c for 20-, 40-, and 60-h PAV (Residues of MnROAD Binders from 1999 Study)

	20-h PAV, 2000			20-h PAV, 2015			40-h PAV			60-h PAV		
Bitumen Grade	BBR, S, 2000	BBR, m, 2000	**ΔTc, 2000**	4-mm, S, 2015	4-mm, m, 2015	**ΔTc, 2015**	4-mm, S, 2015	4-mm, m, 2015	**ΔTc, 2015**	4-mm, S, 2015	4-mm, m, 2015	**ΔTc, 2015**
58-28	–30.9	–30.3	**–0.5**	–31.3	–30.5	**–0.8**	–29.5	–26.7	**–2.8**	–28.5	–22.7	**-5.8**
58-34	–34.8	–35.4	**0.6**	–35.6	–35.4	**–0.2**	–34.9	–32.4	**–2.5**	–33.1	–27.6	**-5.5**
58-40	–44.2	–42.9	**–1.3**	–44.4	–42.0	**–2.4**	–42.9	–34.6	**–8.3**	–42.9	–30.5	**-12.4**

TABLE 6 Summary of Cracking on MnROAD Cells 33, 34, and 35 for 2004 Through 2007

PG 58-28, Cell 33				
Year	Transverse	Fatigue, ft^2	Center Line	Total Linear Cracks (with CL)
3	0	0	0	0
4	20	0	0	20
5.5	125	0	171	297
7.5	149	24	223	375
PG 58-34, Cell 34				
Year	Transverse	Fatigue, ft^2	Center Line	Total Linear Cracks (with CL)
3	0	0	0	0
4	0	0	0	0
5.5	10	0	0	13
7.5	20	0	0	26
PG 58-40, Cell 35				
Year	Transverse	Fatigue, ft^2	Center Line	Total Linear Cracks (with CL)
3	0	17	0	60
4	41	17	476	553
5.5	555	106	492	1416
7.5	1050	281	492	2205

NOTE: CL = center line.

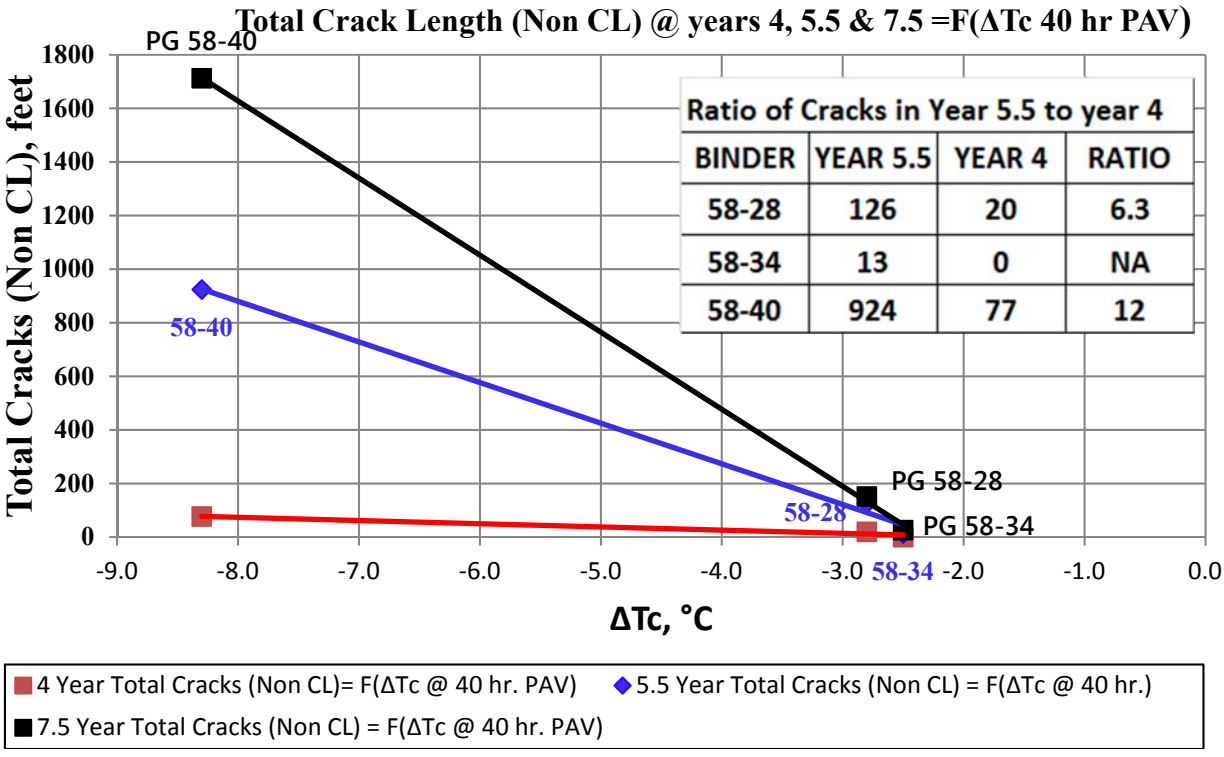

FIGURE 16 Trend of total linear cracks for years 4 through 7.5 versus ΔT_c at 40-h PAV for PG 58-34 and PG 58-28.

As part of the mixture analysis performed in 2000 IDT at low-temperature tests were conducted on 5- and 10-day compacted mixtures aged at 85°C. Binder from the 5- and 10-day aged mixtures were extracted, recovered, and BBR-graded for precise low-temperature grade. Those test results are shown in Table 7 along with the original BBR results for the 20-h PAV residue and the 4-mm DSR results conducted in 2015 for the 40-h PAV residue. ΔT_c was not a concept anyone considered in 2000, but had there been awareness of the significance of ΔT_c at that time a value of –4.5°C for the PG 58-40 binder recovered from the 10-day aged mix would have flagged concern before any pavement distress had developed. Table 7 shows what some researchers have been saying for a couple years, compacted mix aging even for 10 days is not sufficiently aging the binders in these mixtures to provide meaningful information about LTPP. Ten days of aging did not produce ΔT_c values that matched the 40-h PAV data for any of the mixtures. Five days of aging resulted in data that matched the 20-h PAV for the PG 58-40.

Figure 17 shows trend relationships between ΔT_c of the binder from compacted mixtures aged for 10 days at 85°C and the cracking levels of the MnROAD test cells at different point in time. As a result of those trends, the recovered binder data from 2000 had potential for additional insight. The plots for pavement cracking at years 5.5 and 7.5 plot an exponential relationship with the recovered ΔT_c data. Relative to the ΔT_c results for the PG 58-28 and PG 58-34 binders recovered from the 10-day aged mixtures the change in ΔT_c represented an exponential increase.

TABLE 7 ΔT_c Summary of 20- and 40-h PAV Results and of Binder Recovered from 5- and 10-Day Compacted Mix Aging at 85°C (Note: 40-h Results Were Obtained from 4-mm DSR, Other Data from BBR)

Sample	Aging Condition	BBR *S*-Critical	BBR *m*-Critical	ΔT_c
PG 58-28	20-h PAV	–30.87	–30.34	–0.53
	40-h PAV	–29.5	–26.7	–2.8
	5-day aged IDT specimens	–31.72	–32.17	0.45
	10-day aged IDT specimens	–30.85	–29.08	–1.77
PG 58-34	20-h PAV	–34.77	–35.36	0.59
	40-h PAV	–34.9	–32.4	–2.5
	5 -day aged IDT specimens	–35.15	–36.2	1.05
	10-day aged IDT specimens	–35.45	–35.98	0.53
PG 58-40	20-h PAV	–44.18	–42.92	–1.26
	40-h PAV	–42.9	–34.6	–8.3
	5-day aged IDT specimens	–44.93	–43.27	–1.66
	10-day aged IDT specimens	–43.73	–39.22	–4.51

The last project to be discussed is one that has not exhibited major cracking issues. In 2007 Wisconsin STH-33 La Crosse County was reconstructed with a typical Wisconsin 3 million ESAL mix using a PG 58-28 and 15% RAP. Periodically cores have been taken and tested to follow the aging of the pavement. Data from cores taken in year 4 and year 8 are shown in Table 8 and pictures of the pavement from those two time periods are shown in Figures 18 and 19. There are two important properties to discuss in Table 8. After 8 years in service the binder in the top ½ in. of the pavement has become warmer than the target PG grade of –28. Actually the La Crosse County climate is a PG –34°C climate although that temperature is rarely achieved; however –28°C is not uncommon. Therefore, some thermal cracking would likely have occurred by year 8. The second property is the fact that at year 8 the ΔT_c of the recovered binder was –2.3°C.

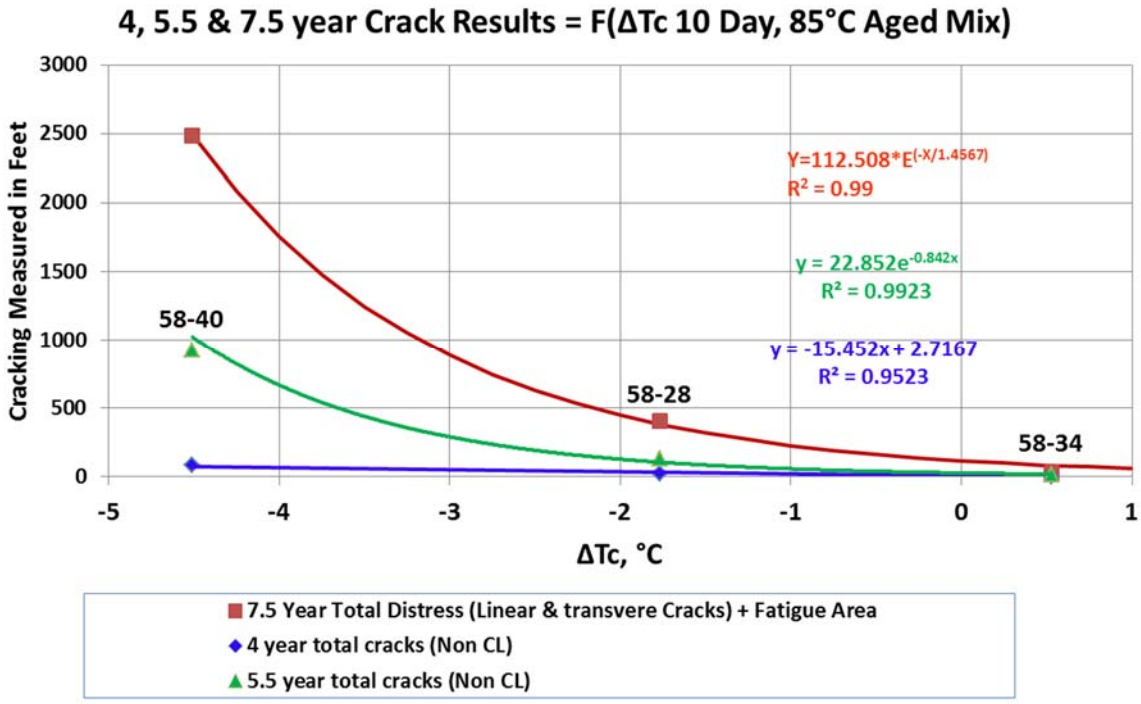

FIGURE 17 Relationship between pavement cracking at years 4, 5.5, and 7.5 expressed as a function of ΔT_c of binder recovered from compacted mixtures aged for 10 days at 85°C.

TABLE 8 Low-Temperature Properties of Binder Recovered from Top ½ in. of Pavement

Core Time Post Construction	*S*-Critical Temperature, °C	*m*-Critical Temperature, °C	ΔT_c, °C
4 years	–30.2	–30.9	0.7
8 years	–28.9	–26.7	–2.3

Final Comments

As stated previously, Anderson et al. (2011) identified a point of cracking onset associated with a ΔT_c value of –2.5°C, which had been calculated from Glover's work and further associated with a low temperature ductility value of 5 cm. After 8 years in service there is cracking on STH-33, some of it transverse, some wheelpath, and some random cracks all of which are visible in the pictures by the use of crack filler. The pavement does not have the more abundant randomized cracking shown by MN1-3 after 8 years in service with a ΔT_c of –3 (see Figure 11), but distress is beginning to develop. It is therefore necessary to consider whether a recovered binder ΔT_c value of –2.5 or –3 represents a condition at which some form of remediation should be considered to protect our investment in the pavement. However, if the long-term performance of our roads is considered in jeopardy, then we should to obtain cores and test the binders in the top ½ in. of those cores to find out how they are aging. Then and only then can we make an informed decision about pavement preservation alternatives. The cost of such testing is trivial compared to the user costs associated with deteriorating pavements and the costs of in-depth rehabilitation.

As previously mentioned, not all binders are created equal. The variation in binder properties and performance are evident in the results discussed for Olmsted CTH-112. Not all binders are processed equally either as evident by the much different performance of the binders on the MnROAD test project. In both of those instances an additive contributed to the performance issues. However both of the problem binders met PG specifications and currently there are no AASHTO or ASTM prohibitions regarding how one meets a given PG grade. Assuming that such prohibitions existed, consider that the binder used on test section MN1-3 was likely not altered beyond the typical refining process yet the binder exhibits performance issues as based on observed distresses in the field.

FIGURE 18 Wisconsin STH-33 at 4 years of age.

FIGURE 19 Wisconsin STH-33 at 8 years of age.

There are binders that age more severely than others in a given time period. A case in point is a PG 64-22 obtained from an unknown crude and refinery source and detailed in Table 9.

There is no evidence of a deleterious additive such as REOB or that the binder was oxidized; it just happens to not age well although it meets the PG specification for PG 64-22. A ΔT_c value of –3.3°C after 20-h of PAV aging however is cause for concern and the doubling of that value after 40-h of PAV aging is more confirming. This binder was provided for evaluation as a commercially available product and therefore is likely in use at someplace on a regular basis. Some questions that should be considered are as follows:

- How do the roads paved with this binder perform?
- Is anyone following the behavior of pavements produced with this binder, is recovered binder data being collected over time?

TABLE 9 Change in Properties of PG 64-22 Binder with Aging

22 (no Zn, P, Mo), Source Unknown	Aging	*S*-critical from 4-mm DSR, °C	*m*-Critical from 4-mm DSR, °C	ΔT_c
64-22	Unaged	–30.9	–31.7	0.8
64-22	RTFO	–29.9	–30.4	0.5
64-22	20-h PAV	–26.9	–23.6	–3.3
64-22	40-h PAV	–25.6	–19.4	–6.2
64-22	60-h PAV	–25.0	–14.0	–11.0

- Is a contractor being blamed for poor quality work when with this binder it would seem impossible to produce a well-performing long-life pavement?
- What motivation would any supplier, contractor ,or agency have to randomly select a project paved with a typical PG graded binder to in-depth scrutiny?

In response to aforementioned question, there would likely be no motivation because current specifications do not specify potentially problematic materials. Specifically, binders are not aged long enough to find out if they age poorly, and mixes are not subjected to meaningful accelerated aging to identify potential problems. Time is often a limiting factor as completing test results quickly has taken priority over gaining insight into how a mix might perform and figuring ways to mitigate problems that arise.

As Kandhal (1977) said, "After the penetration of asphalt drops below 30 due to hardening, the pavements containing asphalt with low ductilities are likely to show poorer service than pavements containing asphalts of the same penetration but with high ductilities." This quote emphasizes not that some people do good quality work and others do not; rather, it emphasizes that all are responsible for quality and performance. Thus, one question to be considered is as follows: "What do I really know about the long-term aging properties of the binder I am about to certify for this project?" A final question to be considered is "Why should testing, collecting data, and gaining insight be done if it will not be used to improve the product to which we have devoted our careers and to which we owe our livelihood?

REFERENCES

Anderson, R. M., G. N. King, D. I. Hanson, and P. B. Blankenship. Evaluation of the Relationship between Asphalt Binder Properties and Non-Load Related Cracking. *Proc., Association of Asphalt Paving Technologists*, Vol. 80, pp. 615–663, 2011.

Clark, R. Asphalt Volatility and Weathering Tests. *Proc., Association of Asphalt Paving Technologists*, Vol. 25, 1956, pp. 417–431.

Clark, R. G. Practical Results of Asphalt Hardening on Pavement Life. *Proceedings of Association of Asphalt Paving Technologists*, Vol. 27, 1958, pp. 196–208.

Farrar, M., R. W. Grimes, C. Sui, J. P. Planche, S. C. Huang, T. F. Turner, and R. Glaser. Thin Film Oxidative Aging and Low Temperature Performance Grading Using Small Plate Dynamic Shear Rheometry: An Alternative to Standard RTFO, PAV and BBR. Presemted at Eurasphalt and Eurobitume 5th E&E Congress, Foundation Euraspalt, Istanbul, Turkey, 2012.

Farrar, M., S. Salmans, C. Sui, J. P. Planche, and F. Turner. Status: 4 mm Dynamic Shear Rheometry. Verbal Report, FHWA Asphalt Binder ETG Meeting, Baton Rouge, La., 2012.

Glover, C. J., R. R. Davison, C. H. Domke, Y. Ruan, P. Juristyarini, D. B. Knorr, and S. H. Jung. Development of a New Method for Assessing Asphalt Binder Durability with Field Validation. FHWA/TX-05/1872-2, 2005.

Halstead, W. J. The Relation of Asphalt Ductility to Pavement Performance. *Proc., Association of Asphalt Paving Technologists*, Vol. 32, 1963, pp. 247–270.

Hesp, S. A. M., S. N. Genin, D. Scafe, and H. F. Shurvell and Subramani. Five year performance review of a northern Ontario pavement trial. *Proc., Canadian Technical Asphalt Association*, Moncton, NB, 2009, pp. 99–126.

Hesp, S. Development of an Improved Asphalt Binder Specification Testing Approach HIIFP-034. Ontario Ministry of Transportation Provincial Highways Management Division Report, 2006.

Kandhal, P. S. Low Temperature Ductility in Relation to Pavement Performance. ASTM STP 628.

Marek, E. Low Temperature Properties of Bituminous Materials and Compacted Bituminmouis Paving Mixtures. ASTM STP 628. ASTM, 1977.

Reinke, G., A. Hanz, M. Ryan, S. Engber, and D. Herlitzka. A Discussion of Some Factors Impacting Performance of Binders Blended with Additives for Reducing Low-Temperature Properties of Asphalt Binders and Their Impact on Mix Performance. FHWA Mixture and Binder Expert Task Group Meeting, Baton Rouge, La., September 17, 2014. www.asphaltetgs.org.

Reinke, G., and S. Dai. Performance Properties of Three Mixes Constructed at the MnROAD Test Site. *Proc., Canadian Technical Asphalt Association 46th Annual Meeting*. Toronto, Ontario, 2001, pp. 213–248.

Reinke, G., et al. Binder ETG Meeting, 2015. www.asphaltetgs.org.

Reinke, G., R. Anderson, R. Michael, and A. Hanz. Impact of re-refined engine oil bottoms on binder properties and mix performance on two pavements in Minnesota. Presented at 6th Eurasphalt and Eurobitume Conference, Czech Technical University in Prague, 2016. dx.doi.org/10.14311/EE.2016.284.

Sui, C., M. J. Farrar, P. M. Harnsberger, W. H. Tuminello, and T. F. Turner. New Low-Temperature Performance-Grading Method: Using 4-mm Parallel Plates on a Dynamic Shear Rheometer. *Transportation Research Record: Journal of the Transportation Research Board, No. 2207*, 2011, pp. 43–48.

Sui, C., M. J. Farrar, W. H. Tuminello, and T. F. Turner. New Technique for Measuring Low-Temperature Properties of Asphalt Binders with Small Amounts of Material. *Transportation Research Record: Journal of the Transportation Research Board*, *No. 2179*, 2010, pp. 23–28.

The National Academies of
SCIENCES • ENGINEERING • MEDICINE

The **National Academy of Sciences** was established in 1863 by an Act of Congress, signed by President Lincoln, as a private, non-governmental institution to advise the nation on issues related to science and technology. Members are elected by their peers for outstanding contributions to research. Dr. Marcia McNutt is president.

The **National Academy of Engineering** was established in 1964 under the charter of the National Academy of Sciences to bring the practices of engineering to advising the nation. Members are elected by their peers for extraordinary contributions to engineering. Dr. C. D. Mote, Jr., is president.

The **National Academy of Medicine** (formerly the Institute of Medicine) was established in 1970 under the charter of the National Academy of Sciences to advise the nation on medical and health issues. Members are elected by their peers for distinguished contributions to medicine and health. Dr. Victor J. Dzau is president.

The three Academies work together as the **National Academies of Sciences, Engineering, and Medicine** to provide independent, objective analysis and advice to the nation and conduct other activities to solve complex problems and inform public policy decisions. The National Academies also encourage education and research, recognize outstanding contributions to knowledge, and increase public understanding in matters of science, engineering, and medicine.

Learn more about the National Academies of Sciences, Engineering, and Medicine at **www.national-academies.org**.

The **Transportation Research Board** is one of seven major programs of the National Academies of Sciences, Engineering, and Medicine. The mission of the Transportation Research Board is to increase the benefits that transportation contributes to society by providing leadership in transportation innovation and progress through research and information exchange, conducted within a setting that is objective, interdisciplinary, and multimodal. The Board's varied committees, task forces, and panels annually engage about 7,000 engineers, scientists, and other transportation researchers and practitioners from the public and private sectors and academia, all of whom contribute their expertise in the public interest. The program is supported by state transportation departments, federal agencies including the component administrations of the U.S. Department of Transportation, and other organizations and individuals interested in the development of transportation.

Learn more about the Transportation Research Board at **www.TRB.org**.

TRB

TRANSPORTATION RESEARCH BOARD
500 Fifth Street, NW
Washington, DC 20001